

PLACE IN RETURN BOX to remove this checkout from your record.
TO AVOID FINES return on or before date due.
MAY BE RECALLED with earlier due date if requested.

DATE DUE	DATE DUE	DATE DUE

**A COMPUTER-CONTROLLED SPECTROPHOMETER
FOR RAPID REACTION RATE MEASUREMENTS**

By

Timothy Gregory Kelly

A DISSERTATION

**Submitted to
Michigan State University
in partial fulfillment of the requirements
for the degree of**

DOCTOR OF PHILOSOPHY

Department of Chemistry

2004

ABSTRACT

A COMPUTER-CONTROLLED SPECTROPHOMETER FOR RAPID REACTION RATE MEASUREMENTS

By

Timothy Gregory Kelly

A computer-controlled transient EPR spectrometer was developed to follow rapid radical reaction rates. The EPR system consists of a commercial 2 MHz magnetic field modulator, a microwave cavity with an internal modulation loop, a modified Varian Fieldial for external control of the magnetic field and a PDP 8/E computer for data acquisition and instrument control. A flash-lamp source was used to create the radicals to be studied in situ in the EPR cavity.

Modifications were made to the electronics of the 2MHz modulator and phase-sensitive detector to increase the S/N ratio of the system. Additionally, high modulation frequency cavity problems led to the development of a second EPR cavity with an internal modulation loop, which was used for low temperature experiments.

The flash-lamp trigger was interfaced to the computer to give the computer control over the repetition rate of the flash. Remote optical sensors at the flash lamp provided feedback information to the computer. The technique of Actinometry was used to help characterize the flash lamp, optics and light gathering capability of the EPR cavity by providing a determination of the number of light quanta/pulse available inside of the EPR cavity.

The computer-controlled EPR spectrometer is capable of recording a standard EPR spectrum or recording signal intensity as a function of time or a

time-resolved spectrum of a radical in a transient state. This system was applied to the study of a Na-THF-Cryptate solution. A solvated electron, $e^-_{(solv)}$, signal was observed that increased upon intermittent sample illumination and subsequently decayed to a steady state. The kinetics of the decay of the $e^-_{(solv)}$ was recorded both as a time-resolved spectrum and as $e^-_{(solv)}$ signal intensity as a function of time at a constant magnetic field. The decay time observed is anomalously long and is explained in terms of the rate of release of the sodium cation from the cryptate complex.

To Carol, a.k.a. C. Dors, and Mom and Dad

ACKNOWLEDGMENTS

I wish to express my deepest gratitude to Professor Chris Enke for his help, guidance, encouragement and friendship during the course of my research at Michigan State University.

I thank the faculty and staff of the MSU Chemistry Department for the excellent support they offered. I especially thank Professor J. L. Dye for his many interesting discussions, Dr. T. V. Atkinson for his assistance and moral support, and W. Burkhart for his valuable assistance.

I thank my wife Carol and my parents for their interest in my studies and their unfailing encouragement and moral support.

Finally, I thank the Nuclear Beer Group and the POETS Club for making my life a bit more exciting.

TABLE OF CONTENTS

LIST OF TABLES	viii
LIST OF FIGURES	ix
CHAPTER 1	
Introduction	1
CHAPTER 2	
The EPR System	9
Introduction.....	9
Basic Elements.....	9
The Cavity System.....	10
The Source System	16
The Magnet System.....	17
The Modulation System.....	18
The MSU 2 MHz EPR Instrument.....	20
The Source System	21
The Cavity System.....	22
The Modulation System.....	26
The Fieldial.....	30
The Flash Lamp.....	34
The Computer.....	35
CHAPTER 3	
Experimental Techniques	38
Introduction.....	38
The EPR Spectrum	39
System Tuning.....	50
Time-Varying Data	51
Time-Resolved Spectra.....	57
CHAPTER 4	
Applications	63
Introduction.....	63
The Sodium-THF Sample	65
Discussion	78
Recommendations	82
CHAPTER 5	
Characterization of the Flash Lamp	84
Introduction.....	84
The Flash Lamp.....	85
Characterization of the Flash Lamp	91

Preparation of the Working Curve	95
Photolysis Experimental Setup	96
Photolysis of the Actinometer Solution	100
CHAPTER 6	
System Modifications	104
Introduction.....	104
The Fieldial.....	105
Fieldial Error Signal.....	112
The Flash Lamp.....	118
The 2 Mhz Modulator.....	118
The Modulator/Demodulator.....	124
The Microwave Cavity	131
APPENDIX A	
Program Listings	137
BIBLIOGRAPHY	159

LIST OF TABLES

5-1 Measured Quanta of Light per Pulse Available in the Micro-Now and Varian Cavities	102
--	------------

LIST OF FIGURES

2-1	Block diagram of a typical EPR spectrometer with 100 kHz magnetic field modulation and phase-sensitive detection	11
2-2	A rectangular TE ₁₀₂ microwave cavity.....	13
2-3	Block diagram of the Micro-Now 509 2Mhz modulator and phase-sensitive detector.....	27
2-4	Simplified schematic of a Varian Fieldial magnetic field regulator	32
3-1	Flow chart for the field-step method employed by EPRSCN.....	41
3-2	A spectrum of the perylene positive ion in sulfuric acid recorded with 2 MHz field modulation. The spectrum is the result of 1024 averages at field increments of 0.024 G.....	45
3-3	The narrow-line spectrum of e-(solv) in THF recorded with 100 kHz (a) and 2 MHz (b, c) field modulation	47
3-4	A spectrum of a Varian standard weak pitch sample	49
3-5	Flow chart for the timed data acquisition program TIMEDA.....	52
3-6	Computer-acquired data testing the response time of the Micro-Now spectrometer. The nominal time constants setting are 10, 1, 0.1 microseconds.....	56
3-7	Flow chart for recording a time-resolved spectrum with TIME12	58
3-8	A time-resolved spectrum of e-(solv)	62
4-1	A spectrum of Na-THF-Crypt recorded with 2 MHz field modulation	70
4-2	The e-(solv) signal as a function of time after a perturbing illumination pulse recorded with 2 MHz modulation and a 1 ms filter time constant.....	71
4-3	A spectrum of Na-THF-Crypt recorded with 100 kHz field modulation.....	73
4-4	A time-resolved spectrum of e-(solv) employing 100 kHz field modulation .	74
4-5	Spectra extracted from the time-resolved data set in Figure 4-4 showing the spectrum at 0.1 ms after the flash and continuing at 10-second intervals...	76

4-6	The decay of the e-(solv) signal as a function of time recorded with 100 kHz field modulation and a 20 ms filter time constant	77
5-1	Circuit diagram showing the flash lamp and associated trigger circuitry	86
5-2	The flash-lamp trigger interface to the PDP 8/E computer	88
5-3	The lamp-flashed detector and light integrator	90
5-4	A digital capacitance meter	92
5-5	The flash-lamp pulse shape with a 10 kV lamp supply voltage. The abscissa is 2 μ s/div	94
5-6	A calibration curve of absorbance of 1,10-phenanthroline Fe(II) complex as a function of Fe(II) molar concentration	97
5-7	Diagram of the focused light beam of the flash lamp	99
6-1	The simplified schematic of the externally controlled Fieldial magnetic field regulator	107
6-2	Circuit diagram of the modulator enabling external control of the magnetic field	109
6-3	The magnetic field as a function of the external sweep voltage at a sweep width of 100 Gauss	111
6-4	The computer interface to the Fieldial internal error signal	114
6-5	Computer-recorded error-signal data as a function of time after a magnetic field increment. (a) A 500 G increment at a 1kG sweep range. (b) A 250 G increment at a 500 G sweep range. (c) A 5 G increment at a 500 G sweep range	116
6-6	The 2 MHz power amplifier and cavity modulation loop with its associated impedance matching capacitors	117
6-7	The Micro-Now internal 2 MHz modulation loop. (a) A side view showing the dimensions of the loop. (b) A top view showing the addition of the magnetic field from the individual wires	121
6-8	A plot of calculated Hm(p-p) as a function of the power amplifier supply current	123
6-9	The circuit diagram of the EPR output amplifier capable of driving a 50-ohm load	126

6-10 The response-time test circuit used to determine the true response time of the EPR spectrometer electronics	127
---	------------

CHAPTER 1

Introduction

Electron Paramagnetic Resonance spectroscopy was born in 1945 when Zavoisky [ZA45] and later Cummerow and Halliday [CU46] detected electron spin resonance absorption in solids. The fact that the discovery occurred shortly after World War II is easily understood since a great deal of war-related research was directed toward the development of radar. The development of high power microwave generators, sensitive diode detectors, perfection of narrow-band amplifiers, and lock-in detectors to increase the sensitivity of radar systems advanced the state of the art sufficiently to supply the components necessary for the magnetic resonance spectroscopy.

Early EPR spectrometers relied on DC detection of the absorption signal. For a strongly paramagnet sample (Cummerow and Halliday [CU46] used 173 grams of $\text{MnSO}_4 \cdot 4\text{H}_2\text{O}$), a change in resonance absorption results in a variation of incident microwave power at the detector. The detector can be either a bolometer or a diode coupled to a milliammeter. As techniques and instruments improved, sensitivity was limited by the ability to maintain the klystron output power at a constant value. Feher [FE57] explained in a classic paper on EPR sensitivity considerations that the power of the klystron must be kept constant to a greater degree than the smallest change in power detectable due to sample absorptions. The minimum detectable sample size produces a current change of approximately 10^{-14} amps. Unfortunately, it is not feasible to maintain the klystron power constant to the degree required by such small current variations.

To overcome the stringent requirement on controlling the absolute klystron power, modulation and phase detection techniques were introduced. Modulation also helps reduce the contributions to low frequency noise by the diode detector. These sources of noise, which show up as instabilities at the output, are classified as $1/f$ noise. At the time of Feher's experiments, the modulation frequencies used were in the audio range, 20 to 6000 Hertz (Hz). Higher modulation frequencies were introduced when it was discovered that the signal-to-noise ratio improved proportionally to the square root of the modulation frequency. Piette and Landgraf [PI60] reported a 16-fold improvement in sensitivity when they changed their modulation frequency from 400 Hz to 100 kHz. They used this increased sensitivity to measure steady-state concentrations of unstable intermediates photolytically produced in situ in the EPR cavity. Rate studies of the decay processes of three radicals were conducted by setting the EPR spectrometer to on resonance line of the radical and then extinguishing the light. Decay curves were plotted on a recorder. The results of the experiment prompted Piette and Landgraf to claim that EPR would be an extremely useful research tool for photochemists who were relying on product analysis, quantum yields, and trapping and flashing techniques to determine mechanisms for free-radical formation and decay in the photolysis of organic compounds. The use of EPR to detect radical reaction intermediates has an obvious advantage over the use of optical methods since optical methods merely ascertain the presence of the intermediates but only in a few cases where the band spectra can be interpreted is it possible to identify the intermediate as a free radical. EPR, on the other hand, only responds to systems containing

unpaired electrons, such as free radicals, and thus presents a highly sensitive was to determine if the reaction intermediate is really a free radical. Quite often, the free radical can be identified by its hyperfine pattern. The main disadvantage of using EPR rather than optical techniques when Piette and Landgraf published their results was the time response of the EPR instrument.

The first comprehensive and elegant demonstration of EPR studies of transient radicals was conducted by Fessenden [FE63] in a study of transient alkyl radicals created by continuous irradiation with fast electrons. However, due to the relatively short radical lifetimes involved (about 5 ms), it was not possible to directly observe the decay of the EPR signals when the electron beam was interrupted. In 1964, Fessenden [FE64] reported using a modified 100 kHz field modulation system and a pulsed radiolysis source to determine short radical lifetimes (7.3 ms for the ethyl radical). The basic change in experimental setup was the use of the 100 kHz output signal normally used for the oscilloscope display as the EPR absorption signal. In 1968, Atkins et al. [AT68a] used Piette's technique to study radicals created in flash photolysis. Using a Decca X-band spectrometer and 100 kHz modulation, reaction-rate data were taken at 640 μ s intervals with a pulse-height analyzer. The analyzer was capable of triggering a xenon flash tube. Decay curves obtained from several flashes could then be averaged. This process, repeated at several magnetic field values, allowed a full time-resolution EPR spectrum to be manually reconstructed from the individual averaged decay curves. Using this technique, Atkins et al. [AY68b] recorded what is believed to be the first high-resolution EPR spectrum of a radical intermediate taken under conditions other than steady state. He recorded the

hyperfine spectrum of a benzophenone radical at intervals of 0.1 Gauss.

Effort to develop EPR as a true kinetic research tool intensified in the late 60's. Glarum and Marshall [GL70] modified the receiver/detector electronics of a Varian 100 kHz spectrometer to obtain a net response time of 200 μ s. Bennet and coworkers [BE67] modified their spectrometer by changing the field modulation frequency to 500 kHz, which resulted in a wide instrumental bandwidth (50 kHz) and a short response time (6.5 μ s). In later work they used the slightly smaller modulation frequency of 465 kHz [BE69].

In what is believed to be the first use of 2 MHz as a field modulation frequency, Smaller et al. [SM68] inserted a hairpin loop inside a microwave cavity and reported a system response time corresponding to a time constant of 1.6 μ s. Subsequently, Atkins et al. [FAT70a] modified their Decca X-band spectrometer and modulated the 100 kHz coils with 2 MHz. Due to the high impedance presented by the modulation coils at 2 MHz, the maximum amplitude of the field modulation was limited to one Gauss peak-to-peak. Atkins reported a response time on the order of 1 μ s. This response time approaches the limit for obtaining useful information from EPR determined by the response time of a microwave cavity. The time required to change the microwave field in the cavity by 1/e is approximately 2Q oscillations [SM77]. For the X-Band cavity with a Q of 5000, the time constant is about 1 μ s.

Atkins et al. were able to use their transient response EPR system to obtain important new magnetic relaxation data pertinent to the mechanism of reactions in solution [AT70a, b]. They reported that immediately after the flash, they saw emission from 2-chlorobenzaldehyde in liquid paraffin decaying with a

time constant of 14 μs into an absorption signal. As a consequence of chemical reaction, the absorption signal then decayed with a half-life of about 2.4 ms. This is believed to be the first well-documented report of Chemically Induced Dynamic Electron Polarization (CIDEP).

A commercial 2 MHz field modulation EPR spectrometer built by Micro-Now Instrument Company of Chicago became available in the early 1970's [HO77]. The EPR cavity contained an internal modulation coil similar in design to the modulation loop described by Smaller et al. [SM68]. Thus, a true transient EPR spectrometer was commercially available to the scientific community. J.K.S. Wan used a Micro-Now system for his published CIDEP studies [WA75].

Huisjen and Hyde [HU74] have taken a unique approach toward developing a transient EPR spectrometer. A saturating microwave pulse of short duration (100 ns) was applied to the sample followed immediately by a monitoring low-power microwave, which allowed observation of radicals as soon as 0.2 μs after the pumping microwave pulse. The system is used with magnetic field modulation, thereby eliminating side bands caused by the field modulation frequency. To decrease $1/f$ noise, the pumping pulse is repeated at 6-50 kHz. The range of lifetimes accessible with this instrument is 250-0.2 μs .

With the availability of instrumentation, which allowed data to be taken 0.2 μs after the perturbation pulse, the problem of handling the potentially tremendous volume of data needed to be considered. Researchers who used the original technique of Piette and Landgraf [PI60] (which was to hold the magnetic field constant and record kinetic data as a function of time) acquired data with devices such as a standard recorder for long lived radicals [PI60], a

storage oscilloscope [GL70], and transient recorders that eventually sent their output to an X-Y recorder [FI67, WI68, AT68a]. Atkins et al. [AT68b] used a 'Biomac 500' pulse-height analyzer to record and average data at several magnetic field values. After the experiment, they had to manually reconstruct a time-resolved spectrum of the radical. The volume of data that could be acquired using the new, fast instruments posed a serious problem for data storage and analysis.

In an effort to eliminate the need for manually reconstruction a time-resolved spectrum from multiple decay curves, Bennett et al. [BE67] designed a six channel sampler system which was triggered by the flash lamp and which acquired data at fixed time intervals along the decay curve. The output of each channel was connected to a recorder. The magnetic field was linearly varied and data were recorded during the magnetic field sweep. At the end of the field sweep, six spectra had been constructed, each spectrum corresponding to one of six time intervals after the flash. Holbrook et al. [HO72] built a 16-channel sampler that wrote data on a 16-channel tape recorder. The spectra were later plotted on an X-Y recorder. Again, each channel corresponded to a spectrum at a specific time after the flash.

Another approach for obtaining a spectrum of a transient radical is to add auxiliary field sweep coils [SO68, HI68, HS73] and synchronize the field sweep with both a signal-averaging device and a pulsed excitation source. There are several problems, however, associated with this technique [BO37] including nonlinearity of sweep fields, limited sweep range and decreased field homogeneity as sweep amplitudes are increased. There is also a problem using

a CAT (Computer of Average Transients) to store the entire spectrum since most signal averaging devices have limited memory, typically 4096 words.

For data acquisition and analysis both small [KL72, GR73] and large [GO72, SE73] computers have been used to greatly simplify data analysis compared to previous methods. However, to allow optimization of experimental conditions and to eliminate problems associated with other techniques, interactive control between the computer and spectrometer is necessary. In 1975, Goldberg and coworkers [GO75] designed a computer-controlled EPR spectrometer, which had the magnetic field under computer control. The software for their system, enabled data to be acquired either in field-step or field-sweep mode. In the field-step mode, the computer increments the magnetic field and waits for it to stabilize before accumulating data, while in the field-sweep mode, the field is continually changed while data are taken. Results of several studies using this computerized system have been published by Goldberg [GO76a, GO76b, GO76c, GO78].

The purpose of this thesis is to describe the computer interface and the necessary modifications, which were made to an EPR system to create a computer-controlled EPR spectrometer for rapid reaction rate measurements.

Chapter 2 contains an introductory discussion which first familiarizes the reader with EPR instrumentation and then describes the interfacing, modifications, and programming that are necessary to construct a functioning computer-controlled spectrometer. This chapter includes only brief statements of problems and modifications made to the purchased Micro-Now 2 MHz spectrometer. The detailed circuit descriptions are left until Chapter 6 for readers

who desire a more complete knowledge of the electronics.

The various modes of operation of the computer-controlled spectrometer are described in Chapter 3 and Chapter 4 discusses applications of the techniques to chemical problems.

The properties of the flash lamp and design of its computer interface for kinetic studies are discussed and characterized in Chapter 5.

Finally, the appendix to this thesis contains listings of the computer programs that were essential for completion of this project.

CHAPTER 2

The EPR System

Introduction

In this chapter, a description of a standard EPR spectrometer is presented. The reader will be familiarized with the components and their functions in a typical instrument. Then, modifications necessary to change the modulation frequency to 2 MHz and allow computer control and data acquisition are described. A detailed discussion of the system modifications is presented in Chapter 6.

Basic Elements

All absorption spectrometers, regardless of frequency range, have four basic components:

1. Source of electromagnetic radiation
2. Dispersing element
3. Absorption cell containing the sample to be studied
4. Detector

Various spectroscopy techniques differ in the properties of these four elements. The main characteristic of the radiation source is its frequency, e.g. UV, visible, infrared and microwave. EPR instruments, which use microwave sources, operate at one of two common frequencies: nominally 35 GHz (referred to as Q-band) or 10 GHz (referred to as X-band). The wavelengths for Q and X bands are 0.85 and 3.0 cm, respectively. The dispersive element in EPR is the

magnetic field. However, its action is much different than the dispersive element in other forms of spectroscopy because it disperses the response of the sample (Zeeman splitting) instead of the frequency of the source. The absorption cell is the microwave cavity, which contains the sample. An EPR detector is usually a silicon diode biased to operate in its linear region with a voltage output proportional to the square root of the incident power [HY63].

Figure 2-1 is a block diagram of a typical 100 kHz EPR spectrometer [WE72a]. The block diagram is divided into five functional groups. The region labeled source contains all the components, which control and measure the microwave frequency and intensity. The cavity system is composed of the resonant microwave cavity that holds the sample and the components that direct the microwave to and from the cavity. The modulation and detection region contains the components that encode and phase detect the absorption signal. The magnet system provides the homogeneous, linearly variable magnetic field that surrounds the sample. Each of these functional blocks will be discussed briefly starting with what is generally considered the central component of the instrument – the cavity system.

The Cavity System

The heart of an EPR spectrometer is the resonant cavity containing the sample. The cavity (1) establishes the spectrometer frequency by its internal dimensions, (2) contributes substantially to the sensitivity, and (3) may be an important factor in resolution [AL68c]. A cavity can be characterized by the

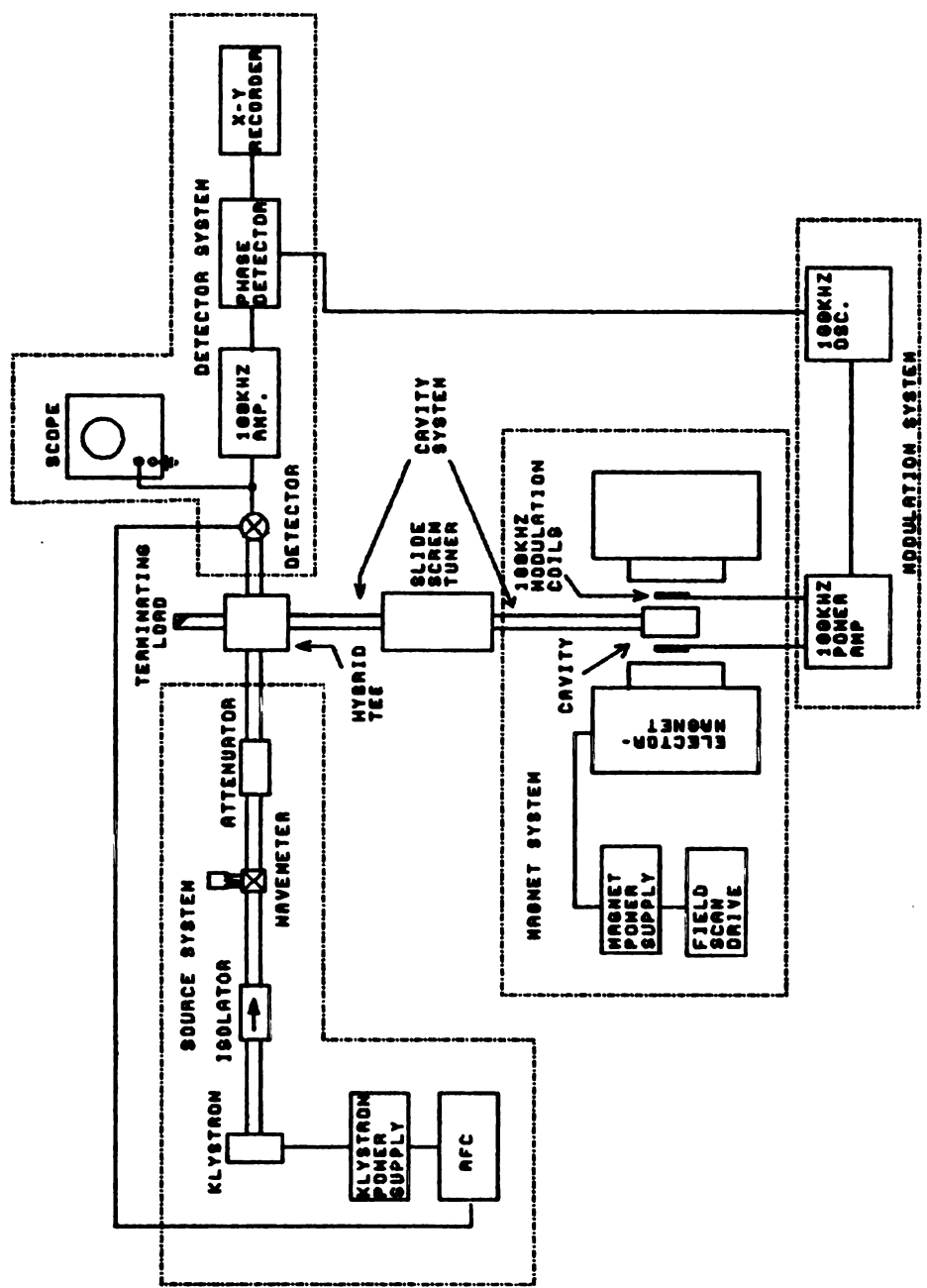


Figure 2-1: Block diagram of a typical EPR spectrometer with 100 kHz magnetic field modulation and phase-sensitive detection.

following parameters [AL68c]:

1. Mode or standing wave pattern of the microwaves
2. Resonant wavelength
3. Selectivity factor (commonly called Q factor)

Electromagnetic waves traveling in free space or in an ideal waveguide propagate with the magnetic (H) and electric (E) fields in phase. In a resonant cavity however, the H and E fields form standing wave patterns with the H and E nodes separated. This allows a sample to be placed in a region where the magnetic field is at maximum amplitude while encountering a minimum in the electric field strength. Cavities are classified by the internal field patterns that result from the separated E and H fields as either transverse electric mode, $TE_{l,m,n}$, where the electric field has no Z component or transverse magnetic mode, $TM_{l,m,n}$, where the magnetic field has no Z component. The subscripts l, m, n, refer to the number of half-period variations of the E and H fields along the X, Y, Z, dimensions of the cavity. Figure 2-2 shows the X, Y, Z axes as defined for a TE_{102} cavity. As one can see from the internal field patterns, a sample would be in an area of maximum H field and a minimum E field if inserted along the X axis at the center of the Z axis. TE_{102} is the mode of the cavity used in this research. This mode cavity is commonly used because its width is not important as long as it is less than one half-wavelength. This allows the construction of narrow cavities that fit very easily between the pole tips of all magnets. The field patterns in the cavity allow one to cut large holes in the sides of the cavity, e.g. to let in light, without affecting the quality of the cavity. The narrow cavity shape also provides flat sidewalls on which to mount field modulation coils. The

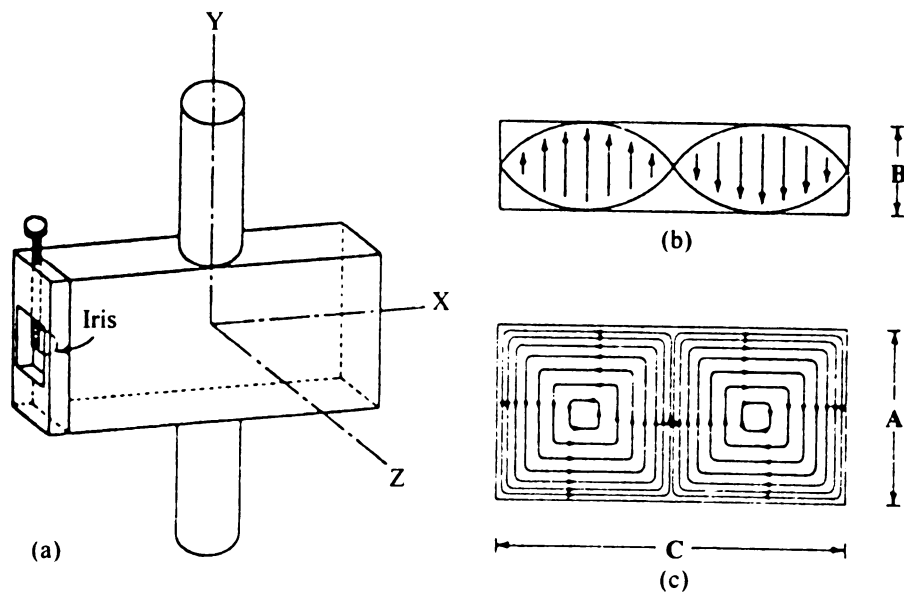


Figure 2-2: A rectangular TE_{102} microwave cavity.

fundamental resonant frequency of a cavity is the frequency at which one half-wavelength of the microwave corresponds to a cavity dimension. The internal dimensions of a TE₁₀₂ cavity at a resonant frequency of 10 GHz are 1.5x1.5x3.0 cm.

The selectivity factor or quality factor, Q, of a cavity is usually defined by Equation 2-1 [PO67a].

$$Q = \frac{2\pi(\text{energy stored})}{(\text{energy dissipated per cycle})} \quad (2-1)$$

In an ideal unloaded cavity (loss due only to ohmic losses in the cavity walls), the “energy stored” can be expressed as an integral of the power density over the volume of the cavity. The “energy dissipated” is power released as heat when the current induced in the walls of the cavity by the varying magnetic field flows through the resistance in the cavity walls. Cavity Q can be approximated by Equation 2-2 [AL678]

$$Q_0 \cong \frac{\text{Volume of the cavity}}{\delta \times (\text{surface area of the cavity})} \quad (2-2)$$

where δ is the skin depth (depth at which the current density has decreased to 1/e of the surface value) of the current at the cavity resonant frequency. For a given cavity mode, i.e. a fixed cavity volume, cavity Q depends inversely on the skin depth which in turn inversely depends on the conductance of the surface metal. Therefore, to minimize resistive losses and maximize Q, the internal surfaces of the cavity are usually plated with a highly conductive metal such as silver or gold.

In early EPR literature, expressions were developed showing the relationship of various parameters to the signal. Signal power was expressed as [AL67a]

$$P_s = \frac{P_0 (4\pi\chi''\eta Q_0)^2}{16} \quad (2-3)$$

where P_0 is the incident microwave power, Q_0 is the unloaded cavity Q, χ'' is the imaginary part of the susceptibility, and η is the filling factor. It should be noted from this equation that signal power is proportional to the square of the unloaded cavity Q, but only proportional to the first power of the incident microwave source power. A figure of merit for cavity Q in a TE₁₀₂ cavity is about 7000.

The microwave energy traveling through the waveguide is coupled to the cavity through a small hole called an iris. This hole provides the function of matching the impedance of the cavity to the impedance of the waveguide. Since the reflected signal observed at the detector should be due only to the sample in the cavity, reflected power due to a mismatch of waveguide and cavity impedances must be avoided. When the impedances of the waveguide and cavity are matched, this source of reflected power is at a minimum. An adjustment screw in the iris permits optimum impedance matching.

The final component of the cavity system is the hybrid Tee. This is a "magic" device, which will not permit microwave power to pass in a straight line from one arm of the Tee to the other. The power coming from the source is equally divided between the cavity arm and an arm that contains a terminating load and a slide screw tuner. If all the power is absorbed in the two arms of the Tee, no power reaches the detector arm. Anything done in either arm to change

the terminating impedance, e.g. a microwave-absorbing sample, will cause a reflected signal to reach the detector. The slide screw tuner in the terminating arm of the Tee is used to reflect the proper phase and amount of microwave to destructively interfere with any unwanted reflections arising from discontinuities in the waveguide or imperfect matching of microwave components.

The Source System

The predominant source of microwave power used in EPR is a klystron. A klystron is a vacuum tube, which produces microwave radiation by causing electrons to oscillate in a resonant cavity by applying an accelerating and a reflecting voltage. The microwave radiation is tunable over a small frequency range by varying the applied reflector voltage. A coarse adjustment of the frequency can be made by physically changing the resonator cavity dimensions using a mechanical tuning stub on the klystron. To prevent the frequency of the klystron from drifting, a small modulation (typically 10 kHz), which is placed on the reflector voltage, results in a modulated microwave frequency at the cavity. The reflected signal from the cavity due to a mismatch of the microwave frequency and the cavity resonant frequency is phase detected and used as an error voltage to the klystron power supply to “lock” the klystron frequency to the resonant frequency of the cavity. This frequency “locking” process describes the function of the AFC circuit.

An isolator is a device similar to the hybrid Tee in that it will only pass microwave radiation in one direction. It is used in the EPR source system to

prevent reflected radiation from the cavity from interfering with the operation of the klystron.

The wavemeter is a variable length resonant cavity, which can be adjusted to an integral number of half-wavelengths by a micrometer. It is used in a typical EPR instrument as a measurement device to determine the actual frequency of the microwave being used.

The amount of microwave power reaching the sample cavity is controlled by a variable attenuator. The attenuator is a resistive element, such as a nickel-chromium film on glass that absorbs energy when inserted into the microwave through an opening in the waveguide. The depth of penetration, and therefore the amount of energy absorbed, is controlled by a calibrated dial on the front panel of the instrument.

The Magnet System

The large, constant magnetic field (H_0) used to produce the resonant absorption is provided by an electromagnet and a highly regulated power supply. Assuming a g-factor of 2 (g for a free electron is 2.00229), at the X-band microwave frequency; this field must be approximately 3400 Gauss. At Q-band frequencies, it must be about 12,500 Gauss. The field must be homogeneous over the entire sample volume, and should be very stable. Total field variations should be less than 10 mG over the entire sample volume [PO67b]. Modern magnet systems utilize a Hall-effect device in the field as a magnetic field-to-voltage transducer. An error signal applied to the magnet power supply is

obtained by comparing the voltage signal from the Hall probe to a reference signal. A scanning system is created by linearly varying the reference voltage and allowing the resulting error signal to change the magnet current. Therefore, the actual magnetic field at the sample tracks the reference voltage.

The Modulation System

In general, when making a measurement requiring high sensitivity in a noisy environment, modulation techniques are used. A physical property is modulated, amplified by a narrow band amplifier tuned to the modulation frequency, and phase detected. Only noise near the modulation frequency can interfere with the measured signal. By looking at the resonance equation for EPR,

$$h\nu = gbH \quad (2-4)$$

one can see two variables that might be modulated, microwave frequency (ν) or magnetic field (H). James Hyde [HY63] has shown that due to the narrow bandwidth of microwave components, it is impractical to modulate the absorption resonance by modulating the microwave frequency. Therefore, spectrometers keep the microwave constant, "locked" to the resonant frequency of the cavity by the AFC, and modulate instead the applied magnetic field.

The magnet field is modulated by placing a pair of small Helmholtz coils on the sides of the cavity and applying a modulation signal to the coils. The most common modulation frequency used today is 100 kHz.

Detection of the signal is accomplished through the use of a silicon diode that rectifies the reflected microwave signal. Because of the high frequency of microwaves, capacitance in the detector and cables filter out the microwave carrier so that the only signal passed to the detector electronics is the 100 kHz modulation. This 100 kHz is amplified by a narrow band amplifier, phase detected, filtered and displayed on an X-Y recorder with the X axis of the recorder synchronized to the magnetic field sweep. The transient response which one sees from an EPR instrument depends upon the modulation frequency, the bandwidth of the narrow band amplifier, the amount of electronic filtering used to remove noise and the response of the recording mechanism.

A discussion of an EPR spectrometer would not be complete without considering the parameters affecting the sensitivity of the instrument. The minimum detectable number of paramagnetic centers, N_{\min} , in an EPR cavity at a signal-to-noise (S/N) of unity is [WE72b].

$$N_{\min} = \frac{3V_c k T_s \Gamma}{2\pi g^2 \beta^2 s(s+1) H_r Q_u'} \left(\frac{Fk T_d b}{P_0} \right)^{1/2} \quad (2-5)$$

Here V_c is the volume of the cavity, k is Boltzmann's constant, T_s is the temperature of the sample, Γ is half of the half-width of the absorption line in Gauss, H_r is the magnetic field at resonance, Q_u' is the unloaded cavity Q, T_d is the temperature of the detector, b is the bandwidth of the entire detector and amplifying system, P_0 is the microwave power incident on the cavity, and F is a noise figure (>1) used to describe noise other than thermal noise. Ideally, F would be 1. The terms of particular importance for this research are the

bandwidth of the system b , the cavity Q , and the noise figure F . Assuming a resonance line quarter-width of 1 Gauss, room temperature and a TE_{102} cavity, $N_{\min} = 10^{11}$ spins.

It is generally accepted that the three components, which limit the S/N, are the klystron, the detector diode and microphonics (mechanical vibrations or spurious electrical transients) [AL68b]. Any of these three may be the noise-limiting component under certain experimental conditions. For example, at low power levels, $1/f$ crystal detector noise dominates while at high power levels, klystron noise predominates.

The MSU 2 MHz EPR Instrument

Since the first reported use of 2 MHz field modulation by Smaller et al. in 1968 [SM68], researchers who had no desire to design and develop the instrumentation for 2 MHz EPR have been interested in applying this new kinetic tool to their particular research. In the early 1970's, a small company named Micro-Now instruments started marketing a Model 509 2 MHz EPR spectrometer. The sales brochure advertises, "The Model 509 is an EPR spectrometer which uses a 2 MHz field modulation frequency, which makes it ideal for pulsed type systems such as those used in flash photolysis and pulse radiolysis. Its very fast recovery time permits the Model 509 to be used for the study of paramagnetic species which have half lives as short as one microsecond" [MNOW]. The Model 509 is made up of three subassemblies:

1. 509-1 microwave source system

2. 509-2 microwave cavity system
3. 509-3 2 MHz modulation and detection system.

It is sold without magnet or power supply, and thus it is meant be used with an existing EPR spectrometer.

Since many applications for a fast-response EPR spectrometer existed within the MSU chemistry department, a system was purchased. The commercial EPR spectrometer designated to receive the Micro-Now modification was a Varian 4502 Q-band spectrometer. Since the microwave plumbing for Q-band is not compatible with X-band, an entire 509 system was ordered. The resultant instrument, the M.S.U. 2MHz EPR spectrometer (Micro-Now Serial Number 5) will be discussed briefly.

The Source System

The Model 509-1 consists of the complete source system described above minus the klystron power supply and AFC. These functions are supplied by the Varian host spectrometer.

The microwave source is a V153 klystron with a power output of 300 mW at a maximum power supply voltage of 350 volts. At this voltage, the klystron must be water-cooled. Fortunately, the klystron could be safely operated at the stated maximum 350-volt limit since that value corresponded to the absolute minimum output of the klystron power supply in the host Varian console. Varian incorporates a higher voltage, quieter klystron than the V153 in their systems. Varian literature states that the V153 was initially designed for radar applications

and has molded leads and base to allow operation at high altitudes without pressurization. The NMR-EPR service group here at MSU had several V153 klystrons that came as military surplus. It is unfortunate that Micro-Now saw fit to skimp on a component that is generally accepted as a S/N limiting component; but to manufacture an inexpensive spectrometer, priced so that researchers would be willing to gamble on it, manufacturers cut corners wherever possible. This philosophy bodes ill for the MSU 2 MHz EPR.

The slide screw tuner used to null unwanted microwave reflections arriving at the detector was replaced in the Micro-Now instrument by an RF phase shifter-bias attenuator to fulfill the same function. It was found that the phase shifter was not capable of shifting the phase quite far enough for proper nulling of the unwanted reflected signal from the cavity arm. However, no modifications were made to this unit.

The Cavity System

The Micro-Now 509-2 EPR cavity is an X-band, rectangular, TE₁₀₂ cavity designed specifically for 2 MHz field modulation. The cavity is machined from a solid block of brass and then is silver plated to decrease the surface electrical resistance. This procedure is necessary since the cavity Q is inversely dependent on the surface resistance. Only the resistance of the internal surface of the cavity is important for cavity Q because high frequency electric current is carried in the skin or surface of a conductor. The "skin depth" for silver (i.e. the depth at which the current has decreased to 1/e of the surface current) is 0.64

μm at 10 GHz [AM72]. Since better than 99.9% of the current flows within 5 skin depths of the surface, only the resistance of the top 3.2 μm is important.

The cavity has a small rectangular opening on one side to allow in situ irradiation of a sample. This opening was quite small and proved to be difficult to use with a flash lamp. This light intensity problem is discussed in detail in Chapter 5.

The 2 MHz modulation coil is similar in design to one published by Smaller [SM68]. The coil was a single loop of wire shaped like a hairpin positioned inside the EPR cavity. At high modulation frequencies, an internal modulation coil is preferable because it would be difficult to pass a high frequency magnetic field through metal. The oscillating field induces eddy currents in metallic cavity walls such that the direction of the induced electron flow produces a reverse magnetic field in opposition to the original flux [ST74]. The magnetic field decreases to $1/e$ of its incident value in one skin depth. The skin depth in silver at 2 MHz is 45 μm [AM72]. To pass an appreciable amount of the magnet field modulation, the walls must be one skin depth or less thick at the modulation frequency. However, to keep the microwave radiation inside the cavity, the walls must be five skin depths thick at the microwave frequency. This corresponds to 3.2 μm at 10 GHz. At a modulation frequency of 2 MHz, the dimension of the walls is critical and becomes too thin to properly support the modulation coils. Therefore, internal modulation coils are commonly used.

The Micro-Now cavity had several drawbacks. First, the sample irradiation opening in the cavity wall was smaller than it should have been, unduly restricting the amount of light available in the EPR cavity. Second, the

magnetic resonance peak drifted in the Micro-Now cavity. This effect was noticed when a quartz dewar, necessary for low temperature studies, was inserted in the cavity. The problem was thought to be caused by the bottom of the modulation coil loop. The coil is bent to go around the quartz dewar, but the arc of the bend is not quite large enough. When the dewar is inserted in the cavity, the coil is pushed out into the microwave field destroying the cavity Q by drastically increasing the losses in the cavity. The AFC does not work well on a cavity with low cavity Q because a low Q cavity will support a wide range of frequencies. Therefore, the AFC modulation will not modulate the cavity out of resonance and will not receive an error signal back from the system and the klystron is free to drift. The shape of the bottom bend in the modulation coil is undesirable because it will produce a component of magnetic field perpendicular to the desired magnetic field.

Several modification ideas were tried to create a more stable cavity. Unfortunately time did not permit starting from scratch to build a new cavity so the modifications were made to an existing Varian TE₁₀₂ cavity, which then could be operated at 2 MHz without the drifting problem inherent in the Micro-Now cavity.

For room temperature work, the Micro-Now cavity was satisfactory. The cavity Q measured by Professor J. Cowen [COWN] was about 4000, a respectable value for Q. It was because of this moderately high Q that the drifting problem was not seen until low temperature experiments were attempted. Therefore, for much of the work done and spectra recorded, the Micro-Now

cavity was used. The maximum modulation amplitude was measured at 3 Gauss peak-to-peak.

A Varian cavity (Q about 7000) was modified for the low temperature studies. Several attempts were made to introduce a 2 MHz field modulation into the cavity but with the restriction that the Varian cavity coil not be permanently altered. The selected method of introducing modulation into the cavity was to install a quartz dewar which had a single strand of 28 gauge magnet wire glued down its front and back. This piece of wire is used as the modulation loop. The resulting cavity was better than the Micro-Now cavity in two ways. First, the resonance did not drift during low temperature work and second, the sample irradiation opening was larger than that of the Micro-Now cavity allowing a greater fraction of the flash lamp output to be collected in the cavity. The major drawback is that not as much field modulation can be produced in the cavity (less than 1 Gauss peak-to-peak). This is not a problem for narrow resonance lines studied in this research because a modulation amplitude greater than 0.2 times the peak width will distort the line shape [WE72c]. The optimum S/N occurs with a modulation amplitude 1.6 to 3.5 times the peak width, depending on the line shape [WA61, SM64].

An unexpected benefit of installing a quartz dewar in the cavity was an increase in the S/N. The presence of a low-loss dielectric, such as quartz, in the cavity has the effect of decreasing the apparent cavity size and increasing the apparent fill factor, n , of the sample [AL68e]. According to Equation 2-3 above, this will increase the signal power. For example, Depireqx [AL68f] observed that

signal amplitudes were increased by a factor of 2 to 3 when the samples were encased in quartz tubing.

The Modulation System

A block diagram of the modulator/demodulator electronics is shown in Figure 2-3. This unit contains the 2 MHz crystal oscillator/preamplifier used to drive the power amplifier connected to the modulation coil, plus all of the electronics to amplify and phase detect the resulting signal. The signal preamp has a selectable gain of 25 or 35 dB and is battery operated for low noise. The preamp output is used both as the klystron AFC signal and also as the EPR signal to be amplified and phase detected. The signal is routed through a 0-41 dB attenuator to a detector/video amplifier circuit built around an integrated circuit balanced demodulator detector (Motorola part number MC15961). The final output passes through an offset and time-constant-select amplifier. The range of time constant selections is 0.001 – 100 μ m plus a position marked NONE.

The modulator/demodulator system had several problems that led to a need for eventually replacing all of the electronics in the system except for the 2 MHz crystal oscillator and phase shifter. The details of the modification will be discussed in Chapter 6 on system modifications.

After the system had been taken apart and set up a few times, the EPR would not even produce a spectrum of strong pitch, which is one of the strongest samples ever used in EPR. The problem was tracked to the lack of 2 MHz

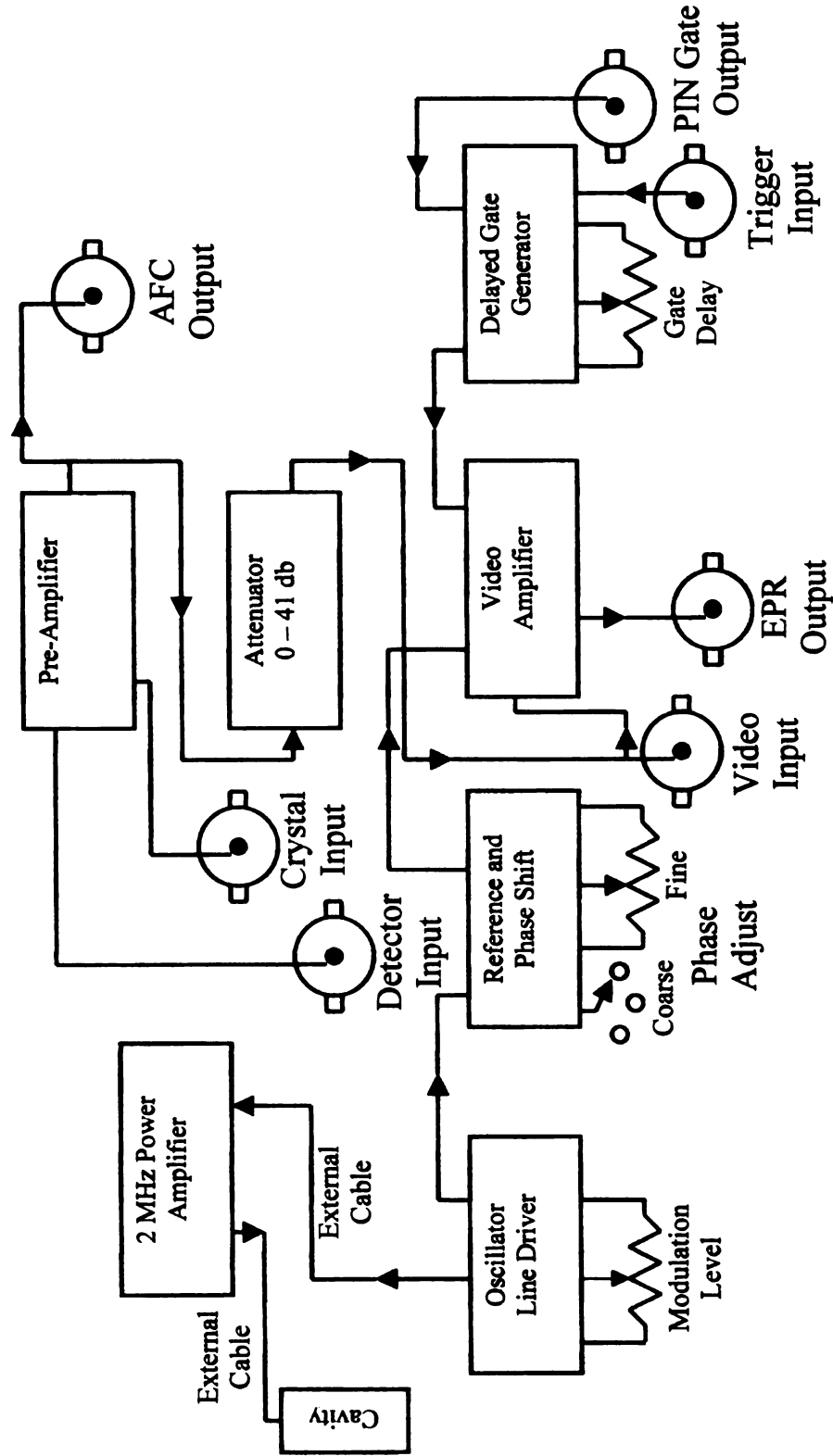


Figure 2-3: Block diagram of the Micro-Now 509 2 MHz modulator and phase-sensitive detector.

modulation in the cavity. The Micro-Now 2 MHz power amplifier required a specific cable to be used between the power amplifier and the cavity for the modulation to work. Also, disconnecting the cable while the power was on would cause the output transistor in the power amplifier to burn out. The basic philosophy used in the design of the power amplifier was at fault. The modulation loop in the cavity is a zero-ohm load at the end of a 50-ohm cable. This impedance mismatch was probably causing a total reflection of the 2 MHz modulation at the end of the 50 ohm cable. To eliminate this problem, the 2 MHz power amplifier was redesigned such that it would not self-destruct if the cable was disconnected while the power was on. To terminate the cable properly, the cavity modulation loop was used as the inductor in the tuned LC circuit with an input impedance of 50 ohms and thus the coaxial cable was terminated at its characteristic impedance. The measured Q of the LC circuit containing the modulation loop was 20, giving a 20-fold increase in the circulation current in the modulation loop over the current from the power amplifier. The circuit for the power amplifier and tuned LC circuit is show in Figure 6-6. A tuned LC circuit was also built for the Varian cavity, again using the modulation loop as the inductor. The measured Q for the LC circuit including the modulation loop for the Varian cavity was 2. This low Q was probably the result of capacitive coupling between the wire carrying the 2 MHz current into the cavity and the metal neck of the cavity. To increase the Q of the tuned circuit, it would be necessary to decrease the capacitive coupling between the wire and cavity which could be accomplished by drilling holes in the top of the cavity to pass the wires through as little metal as possible. Without drilling holes in the cavity, a Q of 2 was the

best that could be achieved. The resulting maximum peak-to-peak modulation amplitude, $H_{m(p-p)}$, for the Micro-Now cavity was 3 Gauss. For the modified Varian cavity, the maximum $H_{m(p-p)}$ was 0.5 Gauss..

The EPR output of the Micro-Now spectrometer drives a 20-foot length of 50-ohm coaxial cable terminated at the computer ADC with an input impedance of 1 M Ω . This is not a problem with the slowly varying signal levels observed when recording a standard spectrum; however, when transmitting a transient, it is important to match all impedances to prevent reflections of the electrical signals at the interfaces. A 50-ohm terminator was inserted at the interface between the cable and the ADC. It was also discovered that the output impedance of the EPR output amplifier was about 10 k Ω . An operational amplifier circuit based on a National Semiconductor LH0032C and LH0063C, capable of driving a 50-ohm load was built. The bandwidth of the buffer amplifier is 3.5 MHz, sufficient for the pulse response of this system.

At this point it was thought that the system was ready to use; however, the first attempt to study a transient reaction proved otherwise. The reaction rate observed was much slower than could be explained by the chemistry involved. It was discovered through pulse response tests described in Chapter 6, that the EPR output filter time constant was longer by a factor of 10000 than indicated on the front panel of the instrument. When the filter was modified to correct this problem, system noise rose to a level that totally swamped the detector electronics. The noise problem led to an immediate need for a study of the electronics of the EPR amplifier-phase detector circuits, after which everything except the 2MHz oscillator was rebuilt. Details are discussed in Chapter 6. The

amplifiers were replaced with home built low noise amplifiers and the phase detector was replaced by a Mini-Circuits Laboratory, ZAD-1, double-balanced mixer. In building the circuitry, a trade-off between S/N and amplifier bandwidth had to be made which thereby eliminated the possibility of studying reaction rates shorter than 5 μs .

Total instrumental time constants were measured by switching the 2MHz modulation to the cavity modulation loop on and off while the EPR was at the maximum of a strong pitch resonance peak and recording the corresponding decay of the EPR output signal. Actual time constants of 3, 10, 100, and 2500 μs were determined and the labels on the front panel output filter switch were changed to these measured numbers.

The Fieldial

The magnetic field to be applied to the sample is selected by using digital controls on a Varian Fieldial™ Mark II magnetic field regulator. The selector controls indicate field density directly in kilogauss. The Fieldial senses the magnetic field through a temperature-controlled Hall-effect transducer located on one of the magnet pole tips and drives the magnet power supply to maintain the selected field value. A field-sweep range selector on the Fieldial in conjunction with a field-sweep potentiometer driven by an AC motor provides a repetitive saw tooth sweep of the magnet field over the selected field range. The field-stability and sweep-linearity specifications of the unit are excellent; however, there is no

direct was to control the field sweep externally. There is a potentiometer connected to the field-sweep motor which gives a reference voltage proportional to the position of the field-sweep potentiometer, but this will not allow control of the field; it only lets one follow the position of the Fieldial. One approach to external control could be to switch the field-drive motor ON while the computer follows the field reference voltage and switch the motor OFF when the appropriate voltage is present. However, this approach is unacceptable for several reasons. When the motor is switched off, it continues to turn for a short period of time after the power is off making it difficult, if not impossible, to stop at the exact field desired. To minimize this overshoot, an extremely slow scan rate would have to be selected, which would mean that it would take an unacceptably long time to move from one field setting to another setting.

The interfacing approach, which was selected as the best means for external control allows the computer to randomly select the percentage of field sweep desired. A detailed discussion of the interface is presented in Chapter 6. An overview will be presented here.

A block diagram illustrating the function of the Fieldial is shown in Figure 2-4. The Hall-effect transducer is positioned in the magnetic field by attaching it to a magnet pole tip. A 1290-Hz reference signal is applied to the Hall-effect transducer, the field-set controls, and the sweep-range controls. The signal from the sweep-range control is applied to the field-sweep potentiometer. The signal from the field-sweep potentiometer is then combined with voltages from the field-set controls and the Hall-effect voltage at the input of an error amplifier. Any change in the field or sweep control settings results in an error signal that is

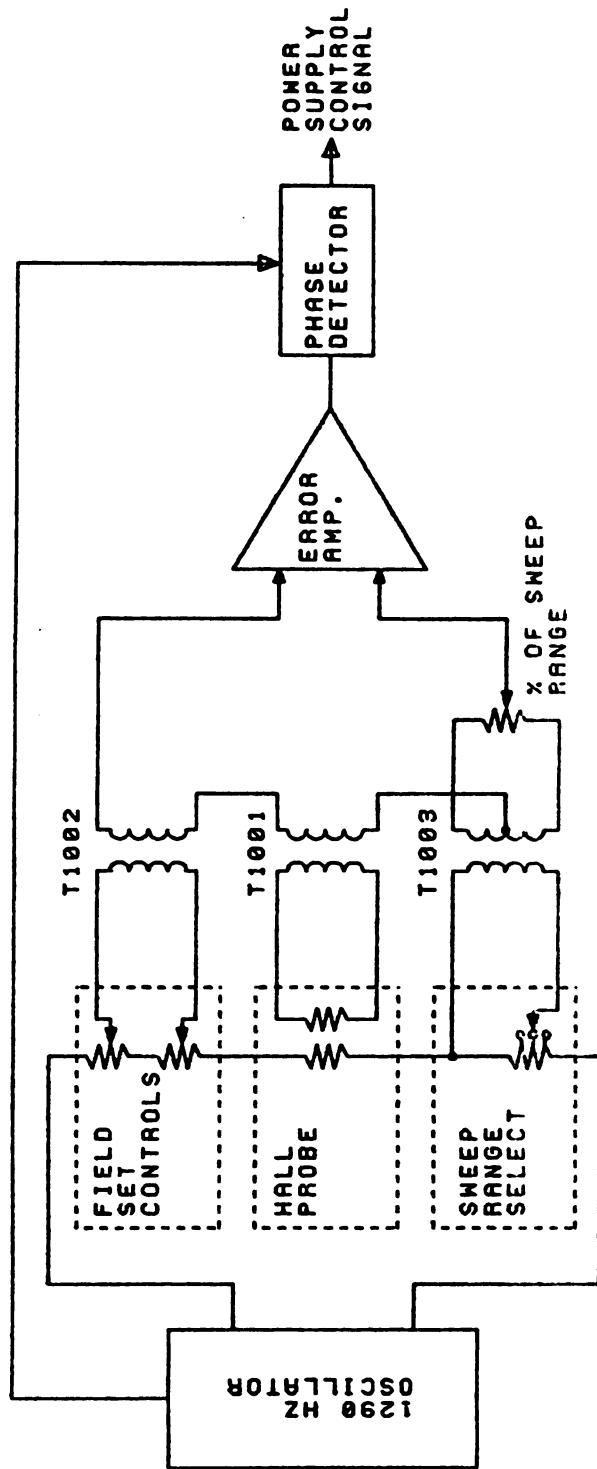


Figure 2-4: Simplified schematic of a Varian Fieldial magnetic field regulator.

phase detected and applied as a control signal to the magnet power supply. The magnetic field changes as a result of the error signal and the Hall voltage increases or decreases accordingly. As the magnet field attains the correct value, the error signal approaches zero.

By replacing the field-sweep potentiometer with a four-quadrant analog multiplier, the computer can control the field by applying a DC voltage from a digital-to-analog converter to one input of the analog multiplier. The output of the multiplier ($X*Y$) is connected to the error-sense board of the Fieldial.

The DC analog voltage is derived from a 10-bit DAC within the computer giving a resolution of slightly better than 0.1% of the field-sweep range selected. This resolution is adequate for the small field-sweep ranges selected in this research but at a sweep range of 1 kG, the resolution is only 1 G, which is wider than many EPR lines. The DAC should be replaced with a 12-bit DAC (resolution of 1 part in 4096) for general use.

The linearity of the field sweep was determined by applying a DC voltage to the analog multiplier and measuring the resultant magnetic field with a home-built gauss meter utilizing the NMR resonance of the proton. The plotted results are shown in Chapter 6, Figure 6-3. A linearity test at sweep-width settings of 10, 100, 500 and 1000 G resulted in linearity within $\pm 0.25\%$ of the sweep width. These values are better than the linearity specifications claimed by Varian in their Fieldial literature (0.5% of sweep width).

The short-term stability of the field was difficult to measure with the home-built gauss meter used in this analysis since it was not a tracking gauss meter. It had to be manually adjusted. The frequency to establish proton resonance was

selected using a variable capacitor. During the entire integration period of the frequency meter one's hand had to be kept on the adjustment knob to prevent the frequency from changing, which prevented continuous monitoring of the magnetic field. The short-term stability results are based on five readings made over about one minute. At sweep-range settings of 50 and 100 G, with zero volts applied to the sweep input, the maximum field deviation seen was 25 mG. This change corresponds to 7 parts per million in the measured frequency.

Considering the manual method of adjusting the frequency of the gauss meter, this error may not be significant. The error value is about 25 larger than the value reported by Glarum [GL73]. With a voltage input of +5 volts, the maximum field excursion detected was 35 mG.

An error-signal monitoring circuit was built and is described in Chapter 6. The monitoring circuit produces an analog signal proportional to the error signal in the Fieldial. The output voltage is connected to one channel of the multiplexed analog-to-digital converter in the PDP 8/E computer. The main EPR computer program calls a subroutine called ERRSUB every time a new magnetic field is selected. ERRSUB monitors the error voltage and returns to the calling program when the error signal reaches a steady state.

The Flash Lamp

The excitation source selected for this research was a low repetition rate (4 Hz at 10 kV supply voltage) Xenon flash lamp. The lamp electronics, optics and housing were built by Photochemical Research Associated in London,

Ontario, Canada [PHOT]. The high voltage power supply used for the lamp was a Hipotronics Model 820-50 variable voltage supply.

Characterization of the flash lamp system is the topic of Chapter 5. Only the results will be presented here.

The duration of the light pulse was measured using a monochromator and a photomultiplier. The photomultiplier output was recorded on a storage oscilloscope. The full-width at half-maximum of the light pulse from the flash lamp is 2 μs with the entire pulse over in an absolute maximum of 10 μs at all supply voltages used (8, 9, 10 kV). Actinometry, a chemical photon counting technique, was employed to estimate the number of quanta of light available inside of the cavity at three lamp supply voltages (8, 9, 10 kV). The quanta/pulse for wavelengths below 450 nm at 10 kV in the Micro-Now cavity was 2×10^{15} .

The Computer

Because of the high-speed data acquisition, instrument control, and event synchronization necessary to perform the desired EPR experiments, the system is placed entirely under computer control during data acquisition. During system tuning prior to an experiment, the computer assists the operator by acquiring, averaging and displaying results as the operator varies the many parameters necessary to tune the system. In addition to the control and acquisition function, the computer performs all the data reduction and analysis necessary to interpret the results. A number of peripherals are available for displaying and storing the results. The computer used for control and data acquisition is a Digital

Equipment Corporation [DEC] PDP Lab 8/E with 12k words of memory, an analog and a digital laboratory-peripherals option comprised of a four-channel multiplexed, 10-bit analog-to-digital converter (ADC), two 10-bit digital-to-analog converters (DAC), a 12-bit parallel digital input-and output port and three Schmitt triggers with selectable slope and variable trigger threshold. The Schmitt triggers can be used to synchronize the computer with external events. This option also includes a programmable real-time clock used for time synchronization of events. Additional standard peripherals on the PDP 8/E were an Extended Arithmetic Element (hardware multiply and divide circuit), an ASR 33 Teletype, a high-speed paper tape reader, and a single DECTape drive with a TD8E controller.

The computer system, affectionately called the Rolling 8/E, has been enhanced by several custom and nonstandard peripherals. The addition of a dual Sykes floppy-disk drive eliminated the dependence on a single DECTape unit and was a giant step forward in reducing input-output (I/O) time for compiling and data storage. Data display was on a Tektronix storage oscilloscope [LAST] that was modified to include an ASCII character generator enabling the scope to be used for high-speed alphanumeric output. The scope was configured to emulate a line printer so that standard DEC software could be used to support the device.

The computer uses DEC's OS/8 operating system, which includes a FORTRAN II compiler. This FORTRAN compiler permits in-line inclusion of machine assembly language (SABR) statements in the FORTRAN code yielding an extremely flexible programming tool. One can use the power and ease of FORTRAN programming when timing is not crucial, but one can also include

direct in-line assembly language instructions when timing is critical or when handling nonstandard peripherals.

All of the programs for the EPR system were written in FORTRAN-SABR code. Listings of the main programs and subroutines used with this system are included in Appendix A. Each program will be discussed in the appropriate experimental sections of the thesis.

In addition to the Rolling 8/E, a second computer was used for some data reduction and plotting of the results. This second computer is a Digital Equipment Corporation PDP 11/40 with a Floating-point Instruction Set (FIS), 28 k words of memory, an RK05 disk drive, a Tektronix T4010 graphics-alphanumeric terminal, a dual Sykes floppy disk, a surplus 900 line-per-minute line printer from an old RCA 301 computer [HAHN], and a home-built incremental plotter [HO76].

Data were transferred between the PDP 8/E and the PDP 11/40 using floppy disks as the transfer medium. The transfer is accomplished by PIP8 [PIP8], a program running on the PDP 11/40, which is capable of interpreting the data structure written by OS/8. A general purpose plotting routine, MULPLT [MULP] was used to produce the hardcopy output.

CHAPTER 3

Experimental Techniques

Introduction

The current research project was spawned by the desire to integrate a fast EPR spectrometer with a data-logger so that the combined system could be used to study transients EPR data. The interface was designed to incorporate an intelligent controller since the use of a computer as a controller provides flexibility not possible with a hardware controller or data-logger. Data-taking and experimental monitoring capabilities provided by the system software created for the interfaced EPR spectrometer are described in this chapter.

The computer interface, discussed briefly in Chapter 2, was designed and built to allow computer control over the elements of the total system that are essential for the interactive data acquisition. The interfaced components include the Varian Mark II Fieldial magnetic field controller with a transducer circuit to monitor field stability, the flash-lamp trigger and the lamp monitoring circuits. The flash-lamp interface is discussed in Chapter 5. Many aspects of EPR system tune-up, such as adjusting optimum microwave power and the magnet field modulation amplitude, were not placed under computer control, but instead were left to the experimenter. Having such functions interfaced would be a luxury, not a necessity, since they add nothing to the capabilities of the instrument.

A computer-controlled EPR spectrometer capable of measuring transient data is a very versatile instrument. Once the computer interface is built, the

flexibility of the instrument depends entirely on the computer programs written for instrument control, data acquisition, and data analysis. To accommodate a different experiment it is necessary only to modify or add to existing software, not redesign the hardware.

The software written to fulfill the current research demands allows the experimenter to acquire an EPR spectrum or to monitor signal amplitude as a function of time for the kinetic data studies. The functions are combined to obtain a time-resolved spectrum of a transient radical. Since the hardware is the same for all three data acquisition methods, each method will be discussed from the standpoint of its software implementation.

The EPR Spectrum

An EPR spectrum is a plot of the first derivative of the absorption signal of an unpaired electron as a function of magnetic field strength. A first derivative signal is obtained rather than a normal absorption signal as a consequence of the magnetic field modulation, which is used for signal enhancement. The spectrum is obtained by linearly varying the main magnetic field, H_0 , and recording the EPR signal output on an X-Y recorder. The X-axis of the recorder is linked to the magnetic field sweep by some electrical method (for example, Varian uses a follower potentiometer that is ganged on the field-sweep potentiometer to provide an output voltage proportional to the magnetic field). The rate at which the magnetic field can be linearly swept depends on several factors. The magnetic field must be capable of tracking the reference signal

used to sweep the field. This tracking requirement is not usually the limiting factor for sweep-rate. Sweep rates of 100 Gauss/minute, linear to better than 0.02% have been reported [GO75]. The sweep-rate limiting factor is usually the response time of the spectrometer detector electronics coupled to the X-recorder. The magnetic field must be swept slowly enough to allow the electronics and X-Y recorder to respond to the true line shape and amplitude of the sample. The only method of averaging a signal to improve S/N ratio when using either an X-Y recorder or a data-logger as a readout device is to increase the time constant of response of the instrument. This prevents the output signal from following the noise signals that are faster than the desired EPR signal. In an experiment where the signal-to-noise ratio is small, the output filter time constant must be large, possibly as much as 10 seconds, to remove random noise and allow the average signal to pass to the recorder. Such long time constants require the magnetic field scan to be very slow to prevent distortion of the output signal since it takes five time constants for the signal to reach 99.9% of the new true value after a step-function change.

With the MSU computer-controlled spectrometer, an EPR spectrum is recorded by using a field-step method. The computer, using a 10-bit DAC is capable of dividing the selected field-sweep range of the Fieldial into 1024 discrete steps. (Due to the nature of the interface to the Fieldial, the computer is capable of randomly selecting for its starting point any one of the 1024 discrete magnetic field values.) The field-step method of recording an EPR spectrum is best described by following the flow chart in Figure 3-1.

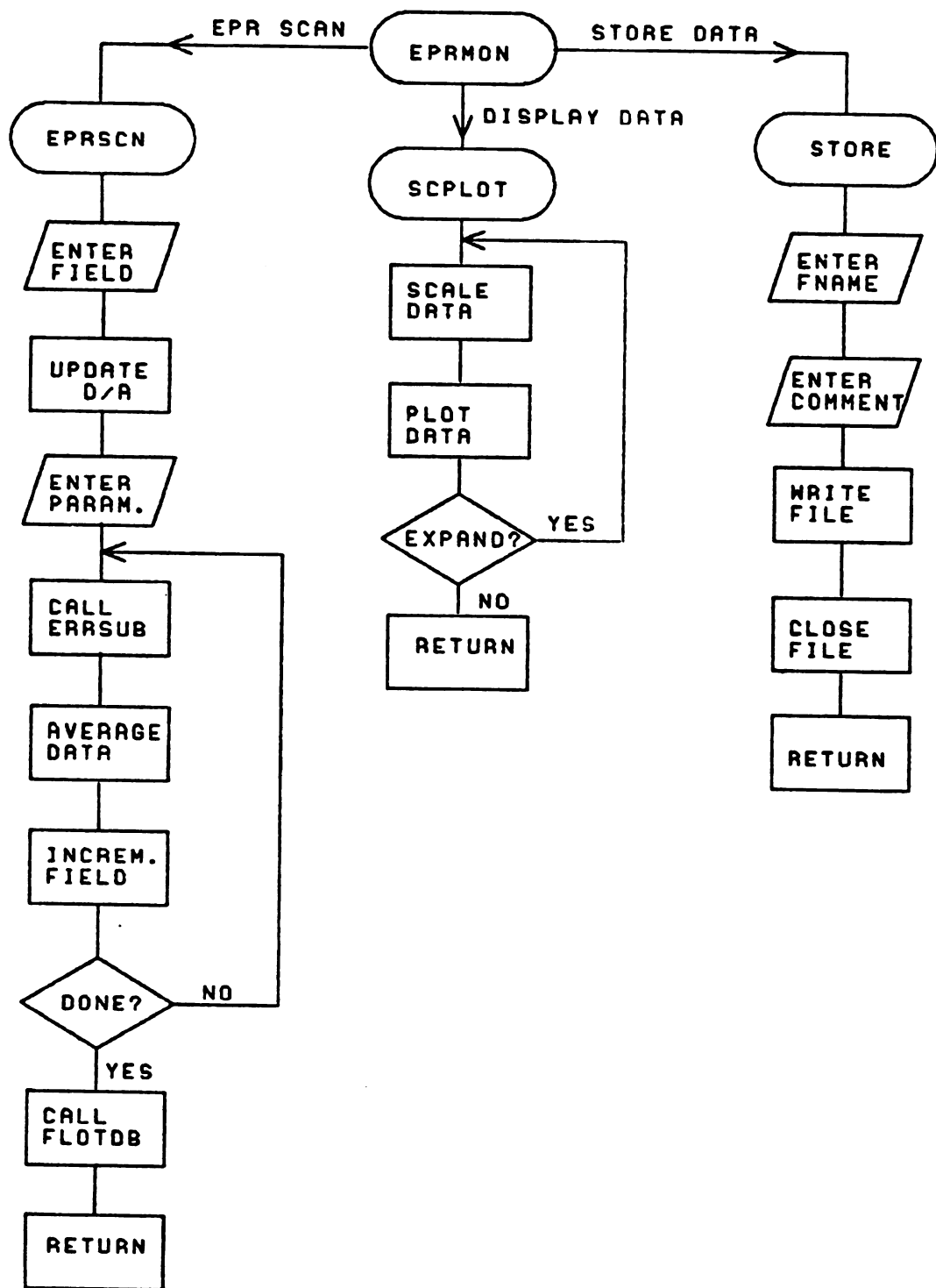


Figure 3-1: Flow chart for the field-step method employed by EPRSCN.

An EPR spectrum is one of the options that can be selected by the experimenter while the computer is in the monitor routine, EPRMON. A program listing of EPRMON along with a list of other options available to the experimenter appears in Appendix A.

When the EPR spectrum option is selected, EPRMON chains to a program called EPRSCN. Through initial dialogue, the experimenter first selects a starting field value for the scan. The default starting field value corresponds to 50% of the sweep range below the magnetic field value selected on the field-set dials of the Fieldial. However, the sweep may be started at some other value. Since it may take several seconds for the Fieldial to stabilize if the starting field value is much different than the value currently selected, the computer updates the magnetic field first and then continues the remaining dialogue to allow time for the magnetic field to stabilize. The remaining parameters to be specified are the resolution and the number of data points to be averaged at each field setting. The resolution is the magnetic field sweep-width divided by the number of points to be taken across the spectrum. The maximum value that the resolution may take on is $1/1024^{\text{th}}$ of the field-sweep width. The number of data points averaged affects the signal-to-noise ratio. For truly random noise, the S/N improvement in the averaged signal is proportional to the square root of the number of averages. Signal averaging is an alternative to instrument response-time filtering used by conventional EPR spectrometers.

Once the scan parameters have been selected, the computer enters the data collection loop. The first task in the data collection loop is to see if the magnetic field has stabilized. The subroutine ERRSUB, called by the main

program, monitors the error signal generated by the error-signal interface in the Fieldial. The voltage signal produced by the error electronics appears at one input of the computer's multiplexed ADC. When the error signal reaches a constant value (which indicates that the magnetic field has reached the desired value), ERRSUB returns to the calling program. When ERRSUB returns control to EPRSCN, the requested number of data points are acquired at time intervals equal to the filter time constant and then averaged. Next, the field is incremented and the process continues until the scan is complete.

The averaged data are stored as double precision integers during data collection and are converted to floating point format by a subroutine called FLOTDB. ERPSCN then returns to EPRMON where the data are auto scaled and displayed on the computer storage oscilloscope using a program called SCPLOT. SCPLOT also reports the X and Y-coordinates of the maximum and minimum points in the spectrum. The spectrum can be expanded for observation of the certain portions of the spectrum so that the operator can make decisions about parameter changes before taking additional spectra. If the operator is satisfied with the spectrum, it can be saved on an output device, such as floppy disk. Subroutine PUT writes the data file onto the specified output device. The operator is queried for a standard OS/8 "device-filename" which is used to open the output file. The name of the file, the current date, and all of the scan parameters are written into the output file for a permanent record of the scanning conditions. In addition, the operator can enter a comment that will be written into the data file identifying the sample and explaining any special conditions that were used to acquire the data. The comment may be any length and is

terminated by typing a control G. The data are written in a standard file format used widely within the Department of Chemistry, i.e. a two character tag to describe the data on the current line, such as ';' for a comment, 'RD' for real data format or 'ED' for end of data. The data, the scan parameters and the comment can be later recalled by subroutine GET for plotting or data manipulation using the data retrieval and manipulation monitor DATMON. The computer is left in EPRMON after the scan.

Since this project was developmental in nature, the scanning technique was mainly utilized in characterizing the instrument. Standard samples such as pitch and perylene were used in the characterization experiments.

Figure 3-2 is a spectrum of the perylene positive ion in sulfuric acid recorded at magnetic field increments of 0.024 G and modulation amplitude of approximately 0.1 G. Each datum is an average of 1024 samples with an instrumental time constant of 100 μ s. The hyperfine splitting constants determined from this spectrum are 4.11, 3.09 and 0.46 G. These values are in good agreement with the literature values reported by Carrington and coworkers [CA59].

A normal EPR spectrum should be symmetrical with respect to the central peak; this perylene spectrum, however, is asymmetric. The cause for the asymmetry is the presence of strong 2 MHz sidebands in the spectrum. Since the diode detector is a nonlinear device, its output will contain the sum and difference of the microwave frequency and the modulation frequency. These sum and difference frequencies result in sidebands, which are associated with each resonance line and are spaced at intervals of the modulation frequency,

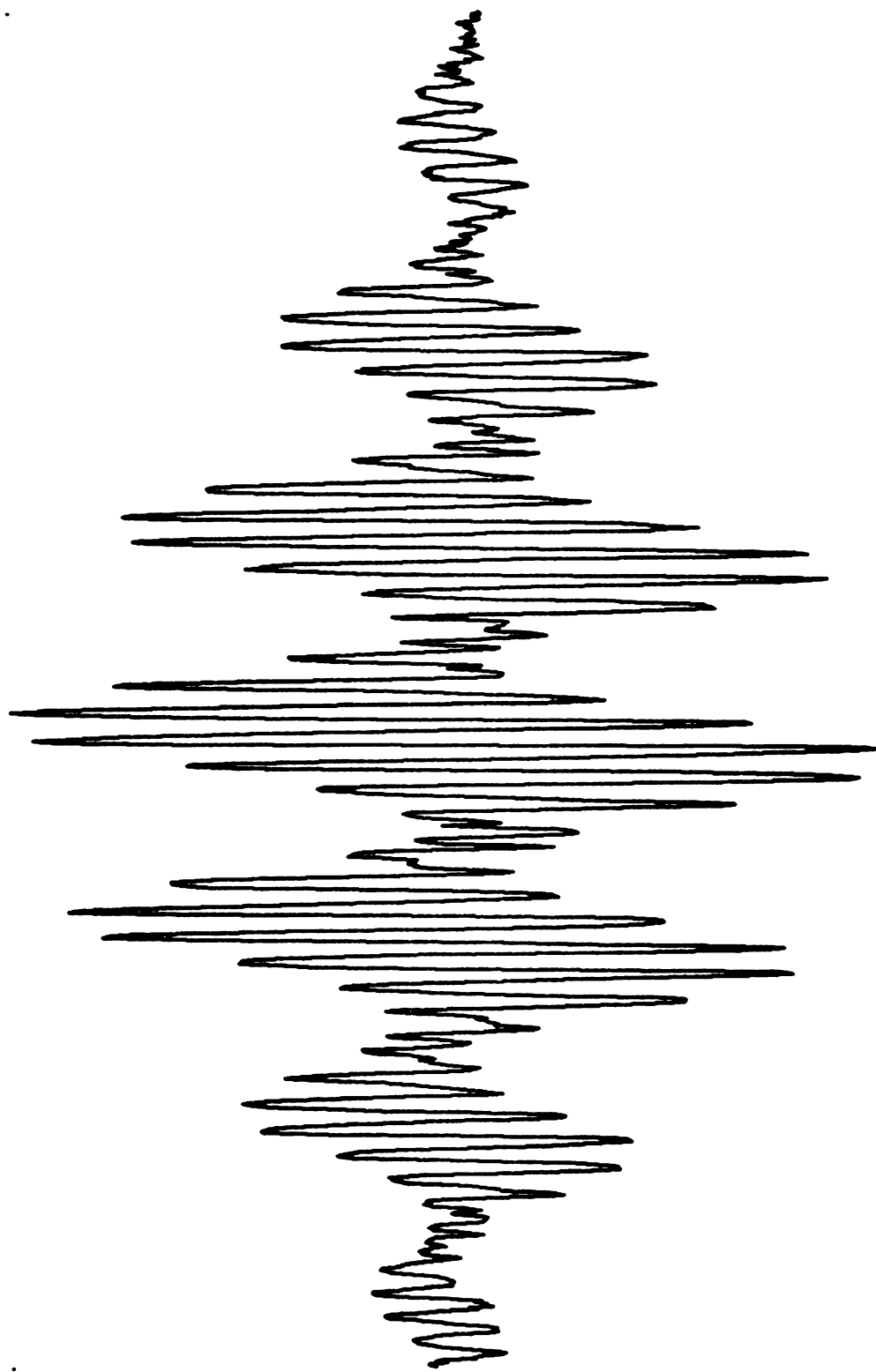


Figure 3-2: A spectrum of the perylene positive ion in sulfuric acid recorded with 2 MHz field modulation. The spectrum is the result of 1024 averages at field increments of 0.024 Gauss.

Wm. Conversion from frequency to observed magnetic field splitting values is obtained by direct substitution into the EPR resonance equation

$$h\nu = g\beta H \quad (3-1)$$

or

$$W_m = g\beta H$$

or

$$W_m = \gamma H$$

When the modulation frequency, W_m , exceeds the line width being observed ($\gamma\Delta H$), sidebands develop at intervals of W_m/γ , in units of Gauss, from the resonant magnet field, H_0 . Assuming a g of approximately 2 for the free electron, the sideband interval is 720 mG at 2 MHz. The 720 mG interval for sidebands is approximately twice the smallest coupling constant of perylene. Therefore, the first harmonic of the sideband, which is 180 degrees out of phase with the parent peak, will cause peak broadening and amplitude reinforcement or reduction of the second peak away from it in the spectrum. The number of prominent sidebands, n , on each side of H_0 is given by

$$n = \gamma H_m / 2W_m \quad (3-2)$$

The number n must be rounded to the nearest integer.

The spectrum of perylene is too complex to use for demonstrating the influence of sidebands. Figure 3-3 shows a spectrum comprised of a single very narrow resonance line attributed to the solvated electron and recorded with 100 kHz and 2 MHz magnetic field modulation. The top spectrum, recorded with 100 kHz modulation (sidebands at intervals of 36 mG), is a standard first-derivative

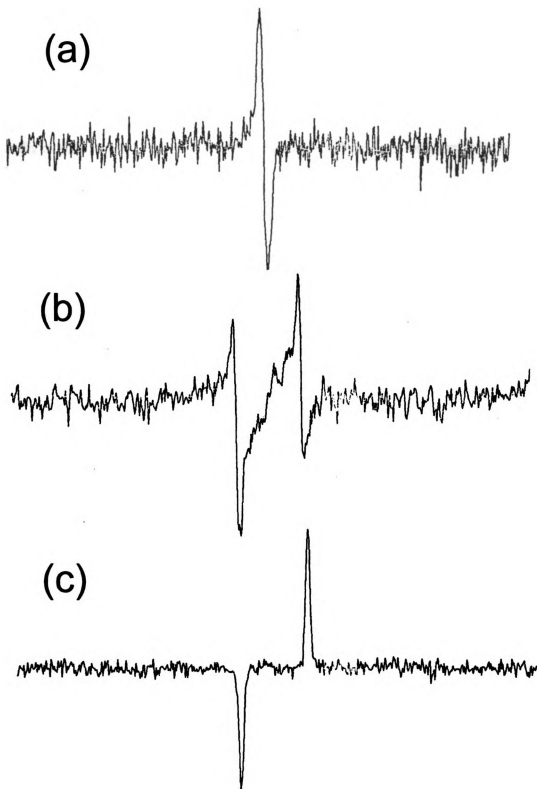


Figure 3-3: The narrow-line spectrum of $e^-_{(\text{solv})}$ in THF recorded with 100 kHz (a) and 2 MHz (b, c) field modulation.

curve with possible broadening due to the 100 KHz modulation. The middle spectrum, recorded at 2 MHz, shows a pair of prominent sidebands while the original resonance line almost disappears. By adjusting the reference signal phase to 0 degrees instead of the normal 90 degrees, the spectrum that would normally appear as a central line with sidebands will appear only as sidebands [PO67c]. This phenomenon, shown in the bottom spectrum, was demonstrated by Burgess and Brown [BU52] in a study of the NMR of protons in water.

The spectrum showing the separated sidebands is easier to use for observation than the more complex spectrum of resonance lines plus sidebands; therefore, all narrow-line spectra and kinetic data were taken with the reference phase set to 0 degrees.

In Figure 3-3, the two peaks, one positive and one negative, are 1.4 G apart or twice the modulation frequency expressed in Gauss. Information concerning the original resonance peak shape is lost by using 2 MHz modulation but then for line-shape analysis of extremely narrow lines, audio range modulation frequencies should be used rather than 2 MHz modulation.

Figure 3-4 is a spectrum of a Varian weak pitch (coal diluted with KCl) sample. A Varian standard weak pitch sample is 0.00033% coal, which corresponds to 10^{13} spins/cm in the active region of the microwave cavity. The active region of the Micro-Now cavity is 3.8 centimeters, which corresponds to approximately 3.8×10^{13} spins. The spectrum was recorded with a 1 ms time constant and is the result of 128 averages. Weak pitch has a measured line width of approximately 1.2 G; thus the sensitivity of the system at a time constant of 1 ms is about 3×10^{13} spins/Gauss. Therefore, to use the 2 MHz EPR system

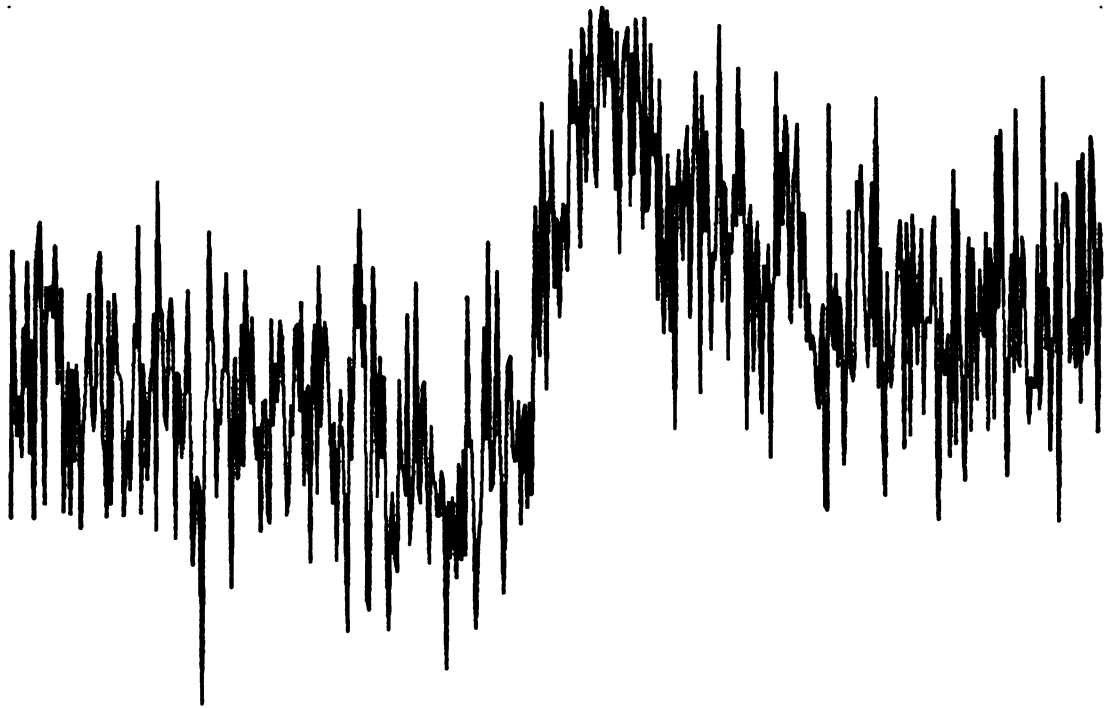


Figure 3-4: A spectrum of Varian standard weak pitch sample.

successfully, either the number of spins must be very large, or the line width must be very small. Varian advertises a sensitivity of 5×10^{10} spins/Gauss with its 100 kHz system at a time constant of 1 s. At a time constant of 1 ms, the sensitivity of the 2 MHz spectrometer is about three orders of magnitude less.

System Tuning

System tune-up involves optimizing several instrumental parameters in order to obtain the maximum signal amplitude of the true line shape for the sample being observed. Since each of the parameters involved in tuning the instrument affects the peak amplitude or line width, system tuning can be considered a special case of recording a spectrum. The normal tune-up procedure involves recording a section of a sample spectrum and then changing a parameter such as the amount of microwave power. The same section of the spectrum is again recorded and compared to the previous one. The process is repeated until the optimum setting is obtained for each parameter. Some of the parameters involved in the optimization process are the amount of microwave power, the amplitude of the magnetic field modulation, and the phase of the modulation reference signal, which is sent to the phase-sensitive detector. The controls for these parameters have not been interfaced to the computer and therefore, must be manually adjusted by the experimenter. SETUP, a specialized version of EPRSCN, was written as an aid for optimizing these parameters. SETUP allows the operator to select the section of the spectrum used for observation, the resolution desired, and the number of points to average

at each field setting. SETUP then displays on the oscilloscope an automatically scaled spectrum and reports the peak amplitude and width. SETUP waits for the operator to change any one of the tune-up parameters, e.g. the field modulation amplitude, and press the carriage-return key on the terminal. It then displays, without going through the dialogue again, another partial spectrum so that the results of the change can be observed. This process continues until the operator is satisfied with the setup and elects to return to the monitor program, EPRMON.

Time-Varying Data

The time-varying data acquisition method developed for use on the MSU EPR system is similar to the method of Piette and Landgraf [PI60]. In the experiment performed by Piette and Landgraf, the EPR spectrometer was adjusted to one of the lines of the sample and a shutter was closed to stop illumination for the sample while the EPR output was observed with an X-Y recorder. Instead of using a continuously operated lamp to build up a steady-state population of the radical being studied, the MSU system uses a xenon flash lamp to produce a transient radical population. Data are then collected using an ADC connected to a PDP 8/E computer. The ADC is triggered by a crystal clock for precise timed-data collection.

To record time varying data at a constant magnetic field strength, the operator selects the timed data acquisition program, TIMEDA, from the list of options in the monitor, EPRMON. The experiment can be followed in the flow char in Figure 3-5. It is assumed that the operator has already chosen the

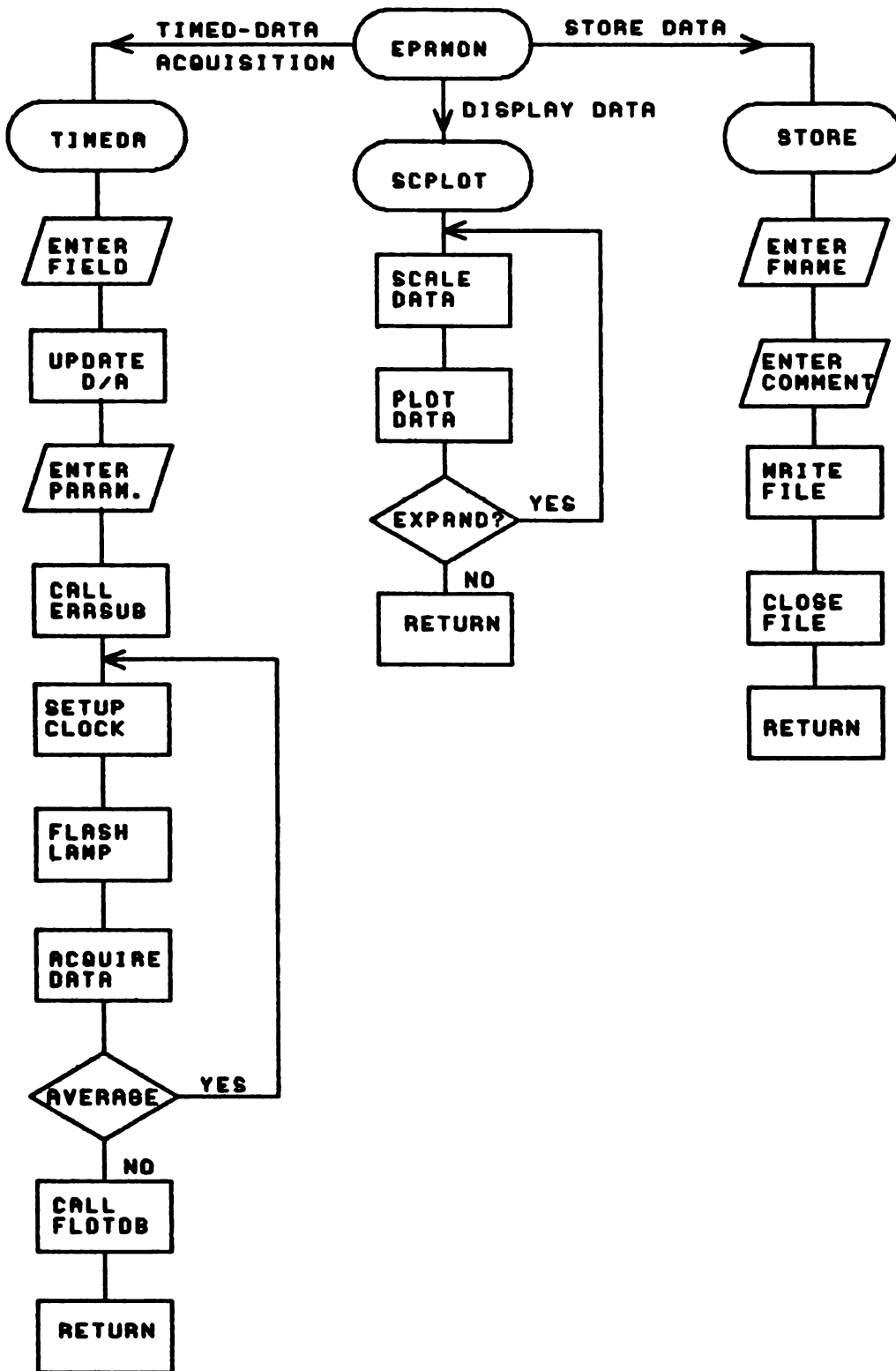


Figure 3-5: Flow chart for the timed data acquisition program TIMEDA.

magnetic field setting appropriate for observing the desired transient response.

During initial dialogue in TIMEDA, the operator selects the magnetic field appropriate for the sample being observed. As is the case with the field-step method initialization, the computer selects the magnetic field immediately to allow time for the magnetic field to stabilize. Additional parameters that must be entered are the time between data points, the number of data points, and the number of transient responses to average. The computer initializes the programmable clock used to trigger the ADC and waits for the operator to press any key on the terminal to indicate READY.

The computer triggers the flash lamp and then waits for data from the ADC. A "lamp-flashed" signal is generated at the flash lamp at the time that the lamp flashes by an ultra-fast photodiode circuit described in Chapter 5. This pulse is received by a Schmitt trigger input at the computer, which starts both the ADC for a time zero point and the programmable clock. From this point on, the crystal clock starts the ADC at the data rate selected during the initial dialogue until the requested number of points has been acquired. The nominal conversion time for a successive approximations converter is 20 μs with a sample acquisition time of 3 μs ; however, in practice, the shortest time interval that does not yield an ADC timing error from too-fast sampling is 25 μs . This is sufficient time to average the collected data as the data are taken. The computer averages the requested number of transient responses, and pauses long enough between flashing the lamp to maintain the maximum duty cycle recommended for the lamp.

When the averaging process is complete, the data, which are stored as double precision integers, are converted to floating-point format by subroutine FLOTDB before returning to the monitor routine, EPRMON. The data are subsequently scaled and displayed on the storage oscilloscope to allow the experimenter to decide if the data set should be kept. If desired, the data can be written onto a storage device, such as a floppy disk for later retrieval, plotting and analysis.

Acquiring kinetic data at a constant field value is not possible for all radical studies since the exact field position of the resonance peak must be known before the experiment starts. If a sample does not have a dark spectrum, i.e. a detectable concentration of the radical of interest already existing in the solution before irradiation, the probability of choosing the correct field setting for the resonance peak is very small. Radicals with a dark spectrum allow prior selection of an appropriate magnetic field by the use of the field-step method discussed previously. For example, alkali metals dissolved either in ethers or amines dissociate to produce a cation and a metal anion [TE74]. Experimental evidence also indicates the presence of the solvated electron and monomer radical in these solutions [DY71]. In fact, Friedenber and Levanon [FR77] reported observing a dark spectrum attributed to the solvated electron in a solution of potassium metal dissolved in THF at room temperature. Thus, the kinetics of the formation and disappearance of the solvated electron peak under intermittent illumination is a possible application for the time-varying data acquisition method discussed here.

The time-varying data acquisition method was used to characterize the time response of the MSU EPR spectrometer. In Chapter 2, it was mentioned that the instrumental response time of the Micro-Now spectrometer was incorrectly labeled on the front panel. To determine the actual instrumental time constants, the response-time test circuit shown in Figure 6-10, was devised. The double-balanced mixer was used to switch the 2 MHz field modulation which drives the modulation coils. The signal generated by the computer which normally triggers the flash lamp, was used to turn off the 2 MHz modulation and was also used as the "lamp-flashed" signal at the computer. First, the spectrometer was tuned up on a standard strong pitch sample and an appropriate magnetic field was selected to observe the maximum amplitude of the resonance line. Then, the 2 MHz modulation was switched off and the decay of the EPR signal was recorded as a function of time. This procedure was repeated for each time constant setting on the Micro-Now spectrometer. Computer-acquired data for three time-constant settings of the Micro-Now EPR are shown in Figure 3-6. The nominal time-constant values of 10, 1, 0.1 μs yielded calculated time constants of 120, 31 and 7 ms respectively. These values differ by more than four orders of magnitude from the labeled values. As the selected time constant is decreased, the noise level becomes a major component of the signal. In the 0.1 μs plot (actually 7 ms time constant), the noise level is already at an unacceptable level.

The computer could not be used to determine the time constants of the rebuilt EPR spectrometer due to the limited data acquisition rate of the ADC in the PDP 8/E (40 kHz). If necessary, the ADC data rate could be increased by

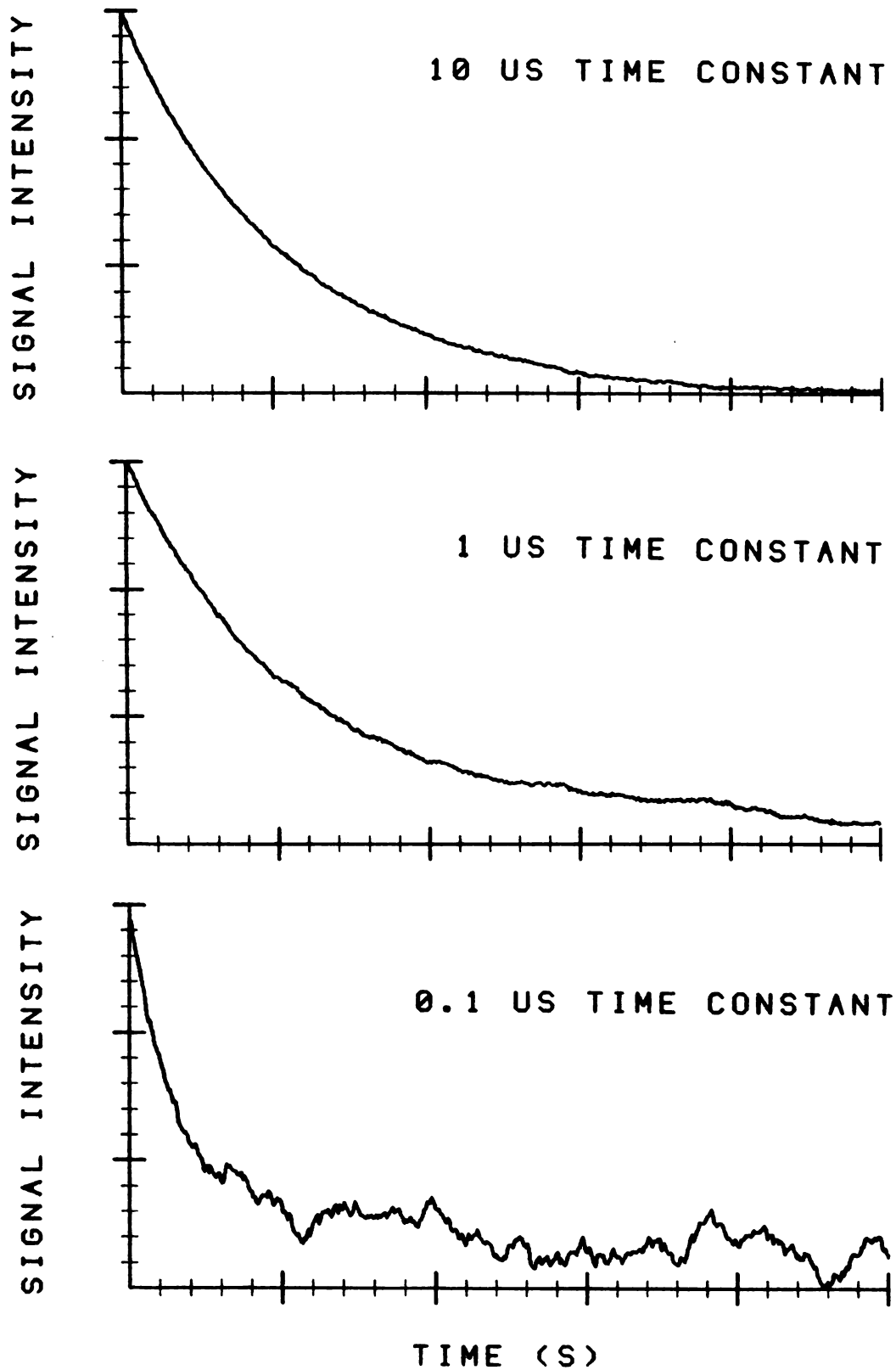


Figure 3-6: Computer-acquired data testing the response time of the Micro-Now spectrometer. The nominal time constant settings are 10, 1, and 0.1 μ s.

purchasing a high-speed converter. An 8-bit A/D converter with 50 ns conversion time is currently commercially available. However, the computer is not fast enough to handle such high data rates. The solution to the data-rate problem is to use an analog shift register such as the one developed by Last [LA77]. The analog shift register is capable of being clocked at data rates of 10 MHz for a total of 100 samples. The sampled data may then be clocked to the output of the device at a data rate that the computer can handle i.e. 40 kHz. Only 100 data points can be taken at the maximum data rate, but additional data can be acquired while data are output to the computer, at the output rate.

Time-Resolved Spectra

The time-varying data acquisition method described above is of limited usefulness in the study of transient radicals that do not have a dark spectrum. However, when this method of timed-data acquisition is combined with the field-step method, the instrument has the capability of obtaining a full time-resolved spectrum of a transient radical by taking three parameter data (signal amplitude as a function of time and magnetic field). The time-resolved experiment is best described by following the flow chart in Figure 3-7. The control program, called TIME12, can be selected as one of the options in the monitor routine or it can be run as a stand-alone program without going through ERPMON. The initial dialogue to set up the experiment is necessarily the combination of the two previously discussed techniques. The experimenter selects the starting magnetic field value, which is immediately issued to the Fieldial to allow plenty of time for

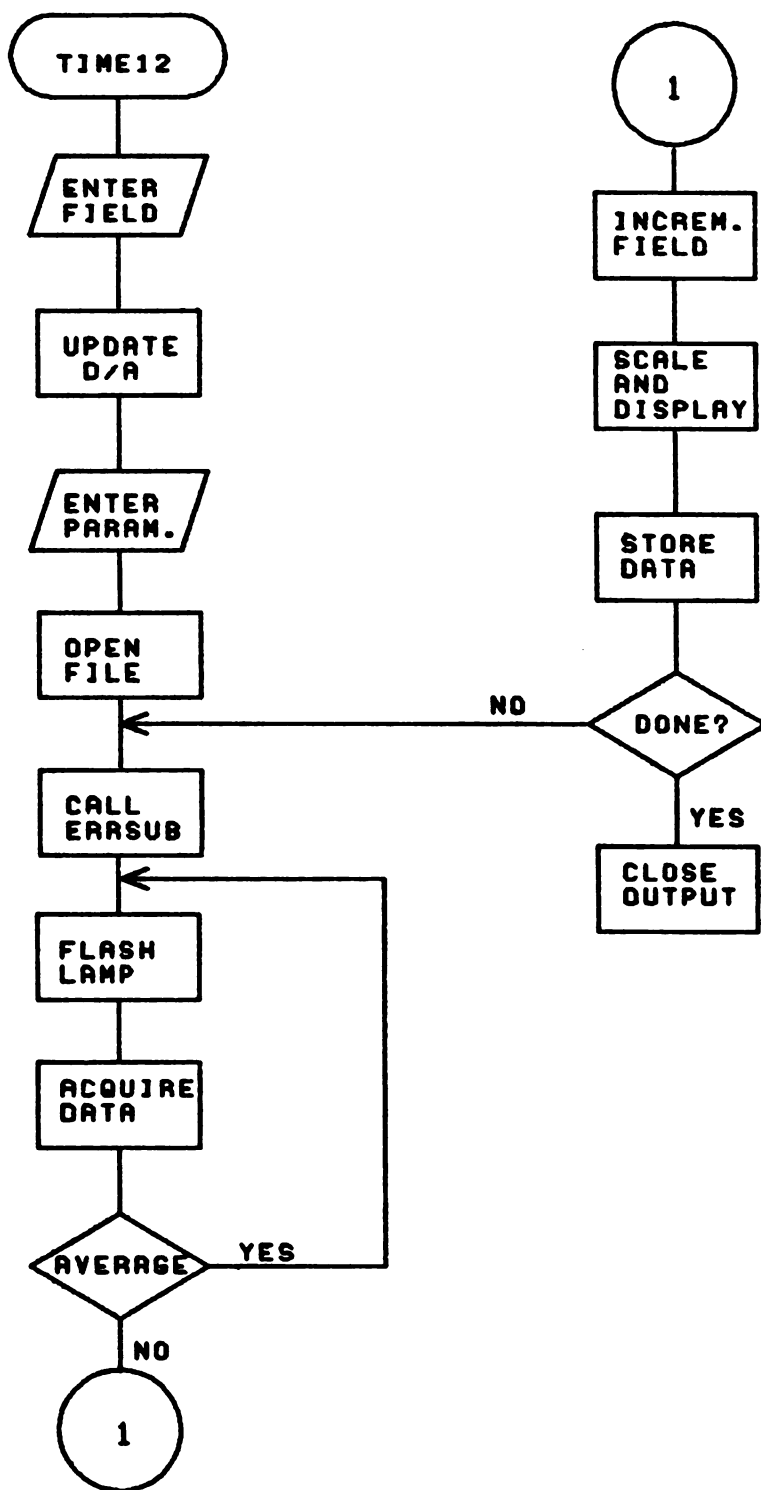


Figure 3-7: Flow chart for recording a time-resolved spectrum with TIME12.

the field to stabilize. Other parameters that are specified by the experimenter are the magnetic field resolution, the number of data points to be taken at each magnetic field value, the time interval between these points, and the number of transient responses to average at each magnetic field value.

Since the total number of data points collected during a time-resolved EPR experiment can be vary large, in-memory storage of the data is not possible. Therefore, the data for each magnetic field value are averaged in memory, displayed on the oscilloscope and then written into a data file that is opened during part of the initial dialogue. All of the parameters specified by the experimenter are written into the data file along with the name given to the data file, the current date, and a comment entered by the experimenter to help identify the experiment at a later date. Typing a control G terminates the comment.

When all of the parameters have been selected and the experimenter is ready, the experiment is started by typing any character on the terminal. First, the magnetic field stability is checked by a call to ERRSUB. When ERRSUB returns control to the main program, an average baseline value is obtained and then the flash lamp is triggered. Data collection proceeds in an analogous fashion to that used in the time-varying method described above. After the requested number of averages at a magnetic field value is complete, the data are automatically scaled and plotted along with a baseline on the storage scope. The data are then written into the output file. The magnetic field is incremented if the scan is not complete and the process is repeated. After the entire experiment is complete, the output file is closed. The data acquisition can be

halted gracefully at any time during the experiment by typing an "S" on the terminal.

After the data file has been closed, the data can be displayed on the storage oscilloscope on the PDP 8/E computer; however, this computer has no hardcopy facilities. Therefore, the data file must be transferred to the PDP 11/40 computer for plotting. A translator program, PIP8 (Peripheral Interchange Program) [PIP8], translates the OS/8 data file into a file that is compatible with the PDP 11 computer operating under DOS/BATCH. The DSTRIP (see Appendix A) interprets the OS/8 data and creates secondary data files that are compatible with the plotting routine MULPLT [MULP]. Data are written in the original OS/8 file as a series of decay curves, one for each magnetic field value. DSTRIP will extract a series of EPR spectra from the data starting at any point along the time axis and continuing at the time interval selected by the experimenter. The maximum number of spectra extracted each time the program is run is 99. The file created by SDTRIP can then be plotted, 10 spectra at a time, by MULPLT. DSTRIP will also write each individual decay curve from the original data file into separated data files to be used for plotting or for data processing in order to obtain information concerning the decay mechanism. DSTRIP also has an option allowing digital smoothing of the data by calling subroutine SMOOTH. This subroutine is a Savitzky and Golay [SA64] Quadratic-Cubic smoothing routine capable of a 5-to-25 point smooth. However, care must be exercised when smoothing data because smoothing will distort the information contained in the data. Smoothing should be used for cosmetic purposes only, since the process will not yield more information than that contained in the original data

[EN76]. DSTRIP has one other function: it will create a data file that can be transmitted to the MSU CDC 6500 computer for three-dimensional perspective plotting using GEOSYS [GEOS]. Figure 3-8 is a 3-D perspective plot of the decay of the solvated electron as a function of both time after the flash and magnetic field.

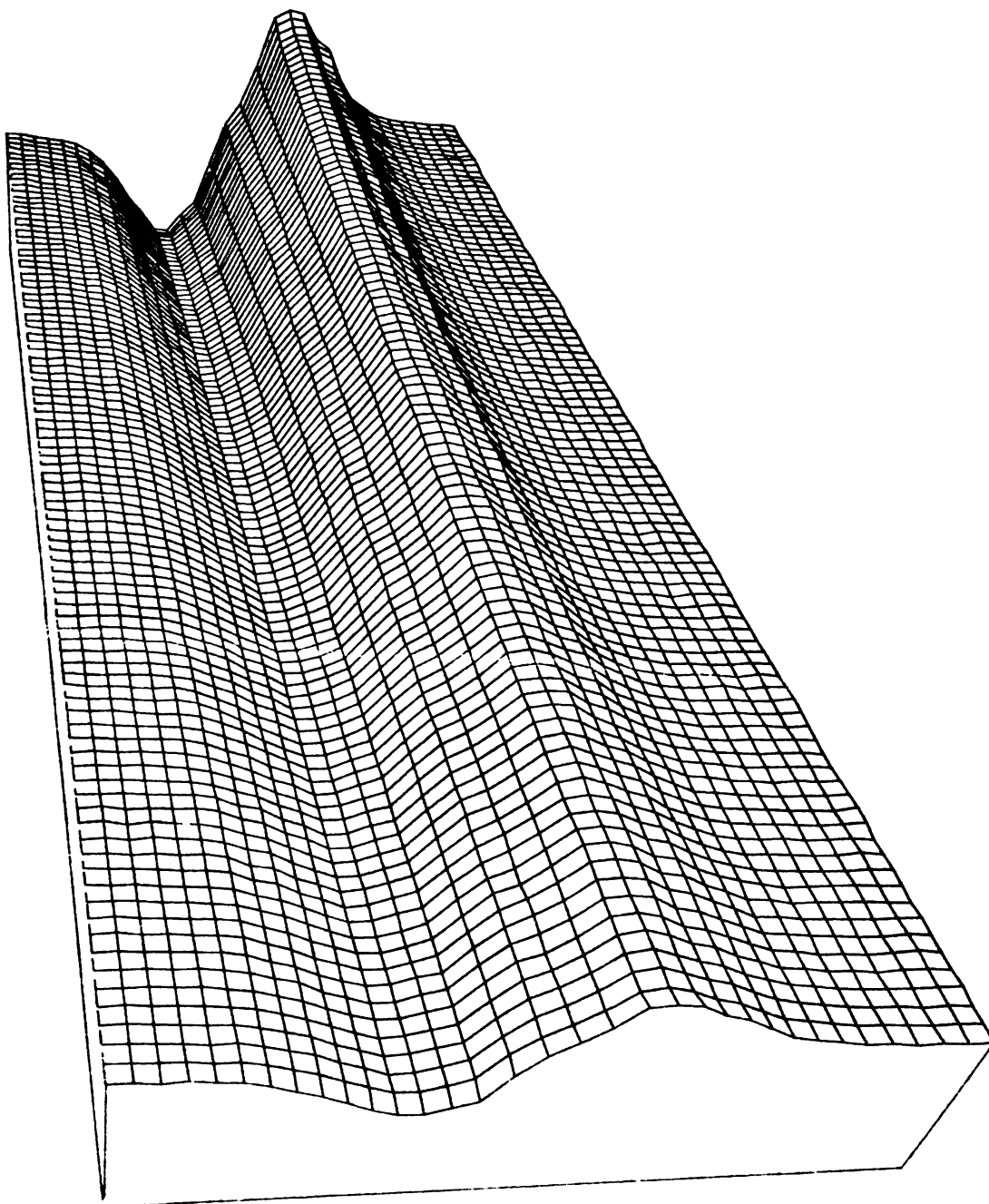


Figure 3-8: A time-resolved spectrum of $e^-_{(solv)}$.

CHAPTER 4

Applications

Introduction

The observation of blue solutions consisting of alkali metals dissolved in liquid ammonia was first reported in 1863 [WE63]. Since that time, it has been shown that alkali metals also dissolve in amines and ethers [QI27, DO57, DO59]. However, unlike the metal-ammonia solutions that are lacking in specific optical bands or EPR patterns, which could be used to characterize the various species in solution, metal solutions in amines and ether provide abundant information about distinguishable species. Optical and EPR spectra indicate the presence of at least three reducing species in these solutions.

Alkali metal-amine solutions have been studied extensively with the aid of optical and magnetic resonance techniques [DY73, CA75, GA70]. Information about metals dissolved in ethers has been obtained mainly by optical [LO72, EL63, KL71, SE77] and, to a lesser extent, magnetic resonance experiments [GL70, FR77].

These solutions appear blue in color since they possess an absorption band between 600-1000 nm. The exact position of the band depends on the metal-solvent combination [LO72, DE64]. However, it wasn't until the work of Hurley, Tuttle and Golden [HU68] that the information contained in the optical spectra was interpreted. They were able to demonstrate that the alkali metal in solution was exchanging with the sodium present in the Pyrex glassware used during preparation, thus giving rise to a third, extraneous, absorption band in the

spectra of the alkali metals. Therefore, only the remaining two absorption bands needed to be considered for any given metal-solvent combination [DY73]. These absorption bands have been attributed to the species M^- and $e^-_{(solv)}$ [MA69, GI70, KL71]. The frequency of one of the two absorption bands, the IR band, is independent of the type of metal in solution, hence, is attributed to the presence of the solvated electron species. In addition to the species identified by optical methods, EPR evidence indicates, by the observation of hyperfine splitting in the metal-amine solutions, the existence of low concentrations of a species with stoichiometry, M [VO63, BA64, Ga70]. Dye [DY71] has proposed an equilibrium mechanism to describe the experimental observations.



Even though EPR evidence indicates the presence of a monomer species in solution, the concentration is too low to observe its optical spectrum under static conditions. However, using flash photolysis coupled with optical absorption techniques, researchers have observed a third absorption band associated with a transient intermediate produced in the solution [GA71, KL71]. They proposed that the intermediate species was a monomer radical, $M\cdot$.

Alkali-metal ether solutions present an excellent application for a transient EPR study. The original species in solution, M^- , is diamagnetic and will not be observed with EPR techniques. After the flash, a single resonance line for the e^-

(solv) and multiple lines for the monomer, $M\cdot$, if present as suggested [MA69, GL70, KL71], should be detected and will show the same lifetime as was seen in the optical studies. The EPR spectrum of the monomer should contain $2I+1$ lines where I is the nuclear spin of the alkali metal. The nuclear spin of sodium is $3/2$, producing a quartet of lines.

The Sodium-THF Sample

In order to obtain a better understanding of the species present in alkali-metal solutions in ethers, a study of Na-THF (tetrahydrofuran) using EPR techniques was proposed. Sodium was chosen as the alkali metal in order to complement previous studies which deal exclusively with potassium and higher alkali metals.

In related work that has been reported, Glarum and Marshall [GA70], using a modified Varian EPR spectrometer (response time of $200 \mu\text{s}$), observed an increase and subsequent second-order decay of the solvated electron signal for potassium, rubidium, and cesium in dimethoxyethane (DME). They concluded that the recombination kinetics of the solvated electron indicated the probable presence of an M radical, but they could not explain the absence of a signal from the monomer in the EPR spectra.

The optical spectrum of $\text{Na}^{\cdot-}$ in THF shows the presence of $\text{Na}^{\cdot-}$ and $e^{\cdot-}(\text{solv})$ absorption peaks [LO72]. The Na-THF solution should give rise to a strong EPR singlet due to $e^{\cdot-}(\text{solv})$ but contrary to the results obtained optically, EPR, being much more sensitive than optical techniques, might observe hyperfine splitting

from the monomer. Irradiation of the sample with light containing wavelengths above 600 nm, the region of the Na^- absorption band, should produce an increase in the concentration of the $e^-_{(\text{solv})}$ and either a sodium monomer or a sodium cation. Using flash photolysis and optical absorption techniques, Kloosterboer [KL71] observed an immediate decrease of Na- absorption after the flash coupled with the appearance of a strong $e^-_{(\text{solv})}$ absorption at its IR band. As the $e^-_{(\text{solv})}$ absorption decreased, a third band, interpreted by Kloosterboer as Na (monomer radical), appeared and subsequently decayed leaving only the original absorption band. The second-order decay kinetics of the $e^-_{(\text{solv})}$ suggests that the intermediate is composed of one sodium cation and one $e^-_{(\text{solv})}$. However, it has been suggested that the transient absorption band observed in this research was actually due to the presence of a potassium contaminant in the solution, not sodium monomer as reported by Kloosterboer [CA77].

A similar kinetic study experiment yielded results, which are in apparent conflict with the reaction mechanism proposed by Kloosterboer. Huppert and Bar-Eli [HU70], studying Na-amine solutions optically, interpreted their findings by the mechanism:



and a subsequent second-order recombination of M^- :



The addition of NaI did not change the kinetics to pseudo-first-order and therefore, it was assumed that $\text{Na}\bullet$, not Na^+ , was formed upon sample irradiation. However, they did not observe a Na absorption peak. Similar results

were reported by Gaathon and Ottolenghi [GA70] studying Na-amine solutions and again the monomer was not detected. They reported that the mechanism for sodium appeared to be different than that generally accepted for potassium. Potassium solutions decay to their original state through a transient intermediate, which is thought to be a monomer radical.

The introduction of organic macrocyclic complexing agents for alkali-metal cations, increases the stability and the solubility of metals in solution and opens many interesting possibilities in the study of alkali-metal solutions [LO72]. Friedenbergs and Levanon [FR77] reported an EPR study of potassium, rubidium, and cesium in THF with and without the presence of crown ether. Without the addition of crown, CR, the only paramagnetic species, which was observed, was the solvated electron. With the addition of a small amount of CR, a weak signal corresponding to the monomer was detected. Due to poor S/N ratio of the monomer signal, the kinetic study was based on the observation of the decay of the $e^-_{(solv)}$ resonance line. They reported pseudo-first-order rate constants for potassium, rubidium, and cesium in THF at different CR concentrations and found them to be CR concentration dependant.

For the present study of the Na-THF system, the cation-complexing bicyclic diamine ether (2,2,2-crypt), a more powerful complexing agent than crown, was added. The complexing agent, C222, is expected to enhance the concentration of Na^+ and solvated electrons according to the equilibria suggested by Dye [DY73]:





Additionally, there may be a small increase in the concentration of monomer, which might yield a detectable monomer dark spectrum. By this effect, Friedenber^g and Levanon [FR77] were able to observe a dark spectrum of potassium monomer with K-THF solutions when a small amount of crown ether was added as a cation-complexing agent to their solutions. However, adding large amounts of complexing agent may produce other reactions, such as ion-pair formation, which cause the monomer to be undetectable [FR77]. Care must be taken in sample preparation since, only as long as cryptand, C, is in excess, is it certain that both Na⁻ and e⁻ will be observed. For a saturated solution of sodium and C222, the e⁻_(solv) concentration depends upon the equilibrium:



Experimental evidence indicates that the equilibrium constant for this reaction heavily favors the formation of Na⁻. Dye [DY71] reported observing the disappearance of infrared absorption band of e⁻_(solv) in a saturated solution while observing an off-scale absorbance at the Na⁻ absorption band. Lacoste [LA76] has estimated the equilibrium constant for the equilibrium in Equation 10 as approximately 10⁻¹⁰. However, it is difficult to totally saturate the Na-THF-C222 solution because of the time required to complete the saturation process.

Therefore, there will be both an excess of C222 in the solution and an $e^-_{(solv)}$ concentration above the $e^-_{(sat)}$ concentration.

The details of the preparation of reagents, glassware and the samples used in this study are discussed elsewhere [DA79, LO72]. To retard sample decomposition, after preparation, the Na-THF solution was kept at liquid nitrogen temperature until the EPR instrument was set up. The experiments were performed at -20 C, again to retard sample decomposition. The sample temperature was maintained by passing a regulated stream of cold nitrogen around the sample which was in a quartz dewar in the EPR cavity. The temperature was measured using a copper-constantan thermocouple.

Figure 4-1 is a dark spectrum of the Na-THF-C222 solution recorded with the 2 MHz EPR spectrometer. The sweep range is 10 Gauss. The observed singlet which is distorted by the 2 MHz modulation frequency (see Chapter 3), is attributed to the $e^-_{(solv)}$. In an attempt to observe hyperfine splitting due to the sodium monomer, the spectrum of Na-THF was scanned in increments of 10 Gauss, over a 50 Gauss region on either side of the $e^-_{(solv)}$ resonance line. The presence of a monomer escaped detection. Based on the reported coupling constants for K and Rb in THF (25 and 150 G [FR77]), resonance lines for the sodium monomer should fall within the region investigated.

An experiment to determine the kinetics of the photoelectron by monitoring the $e^-_{(solv)}$ resonance line was undertaken using the time-varying data acquisition procedure discussed in Chapter 3. The magnetic field was adjusted to allow observation of the $e^-_{(solv)}$ resonance line near its maximum absorption and then the computer, running program TIMEDA, flashed the lamp and acquired the time-

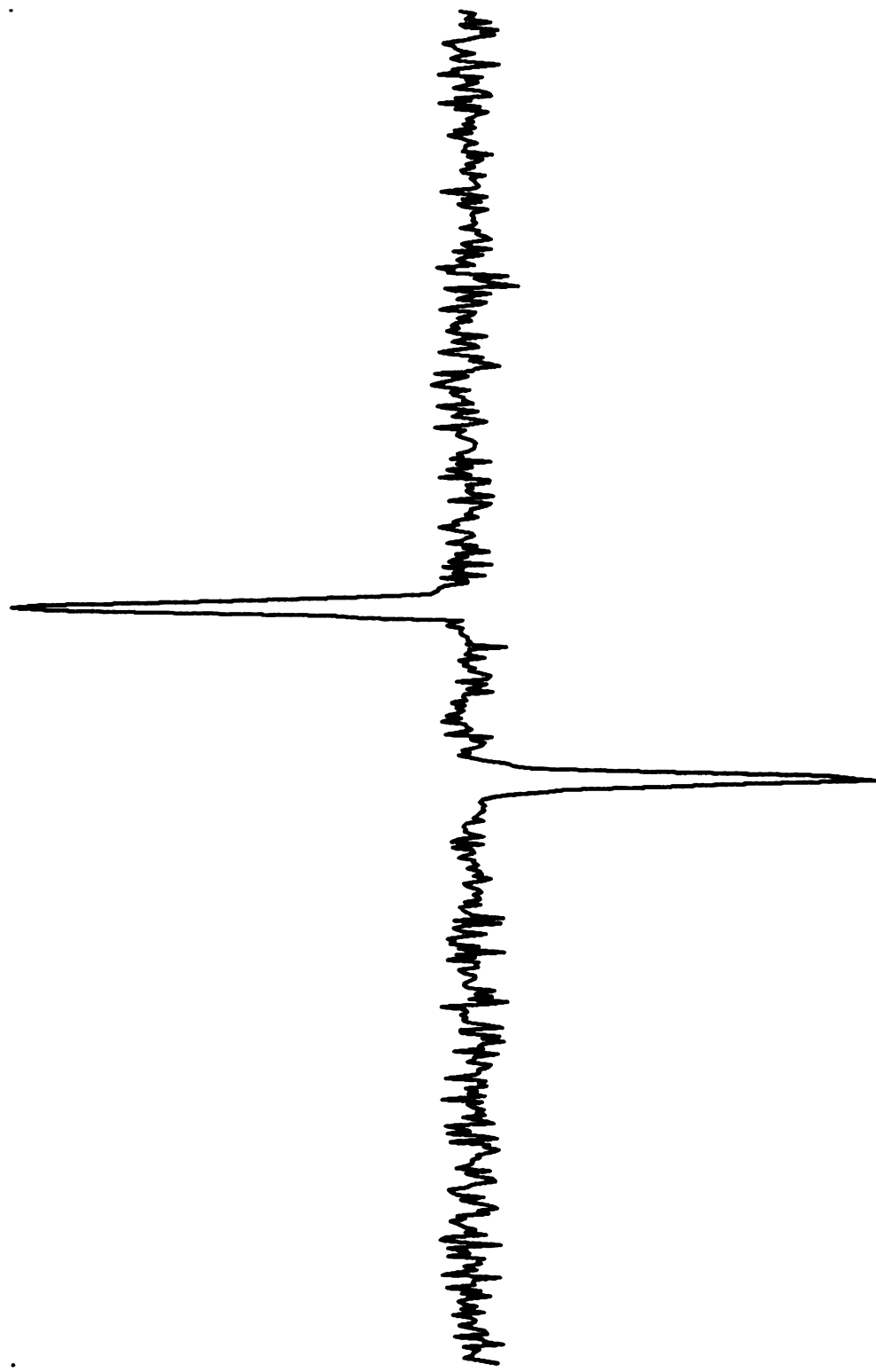


Figure 4-1: A spectrum of Na-THF-Crypt recorded with 2 MHz field modulation.

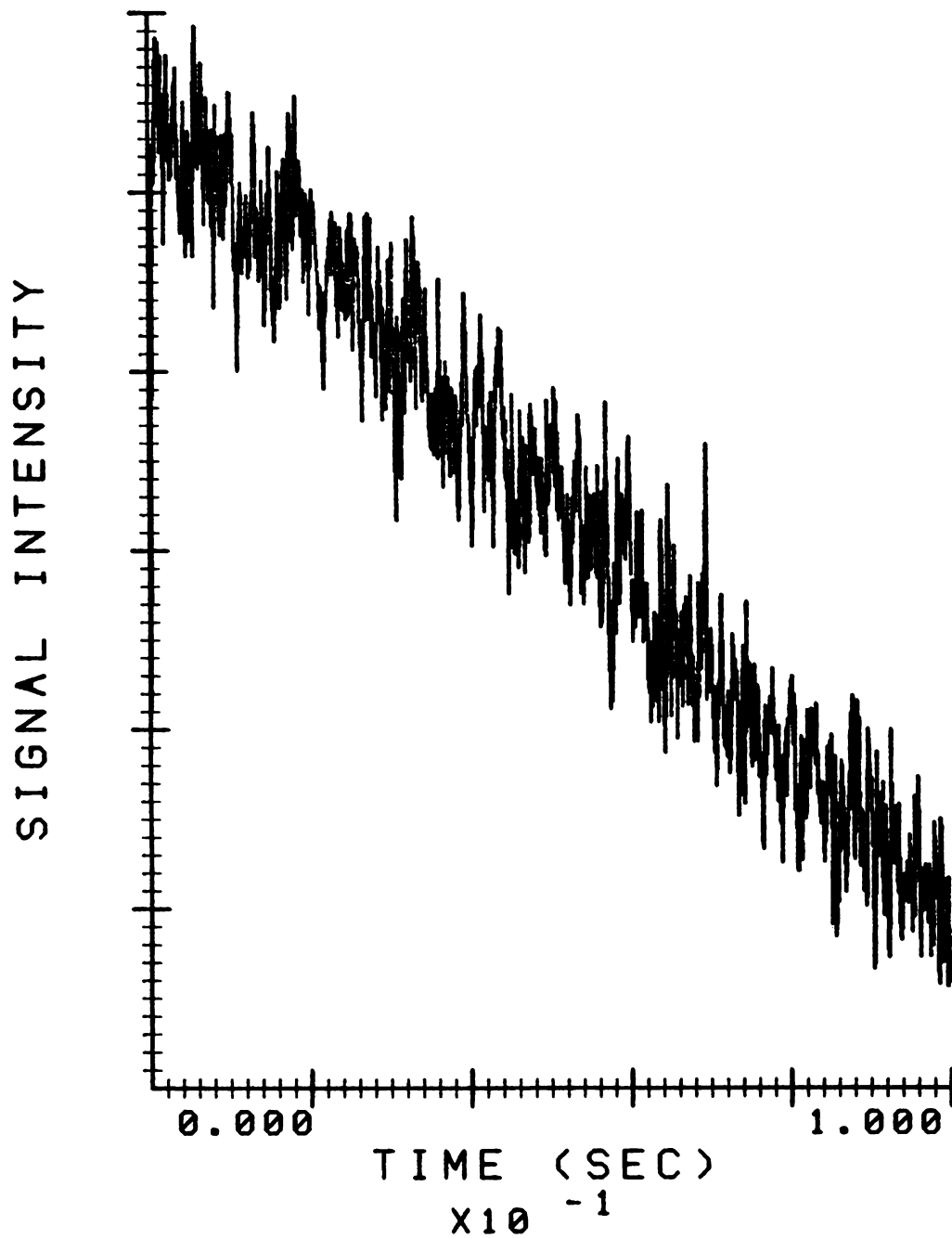


Figure 4-2: The $e^-_{(sol)}$ signal as a function of time after a perturbing illumination pulse recorded with 2 MHz modulation and a 1 ms filter time constant.

varying data. Figure 4-2 shows a decay curve obtained from 16 averages using a response time constant of 1 ms. The disappearance of the photoelectron signal was extremely slow making averaging (the only method available to increase the S/N lost when the response time of the instrument was reduced) a very lengthy process. The lamp-trigger signal was delayed an additional 10 seconds after the data were collected, but this time interval was not nearly long enough to allow the total decay of the $e^-_{(solv)}$ line. The long decay time of this signal is not best suited for study using a 2 MHz instrument because of the need to average to obtain a reasonable S/N (for random noise, S/N improvement is proportional to the square-root of the number of averages). The S/N ratio is needlessly reduced in this kinetic experiment by using the wide bandwidth of the 2 MHz spectrometer. Since the microwave cavity being used was a Varian cavity with 100 KHz modulation coils on the sidewalls and a 2MHz internal modulation loop, the Micro-Now 2 MHz EPR field modulation and phase detection electronics were replaced with the Varian 100 kHz modulator and phase detector and the experiment was repeated using the analog output normally used for the 100 kHz oscilloscope display. The time constant for this signal output is 300 μ s; however, additional RC filtering (20 ms) was used. The 0.3 and 20 ms time constants were experimentally verified.

A dark spectrum of the Na-THF solution at -20 C recorded with 100 kHz modulation is shown in Figure 4-3. Because of the decreased modulation frequency (sidebands at 36 mG intervals instead of 720 mG), the $e^-_{(solv)}$ resonance line appears as a conventional first derivative signal. Again, scanning around the $e^-_{(solv)}$ signal did not reveal the presence of the monomer.

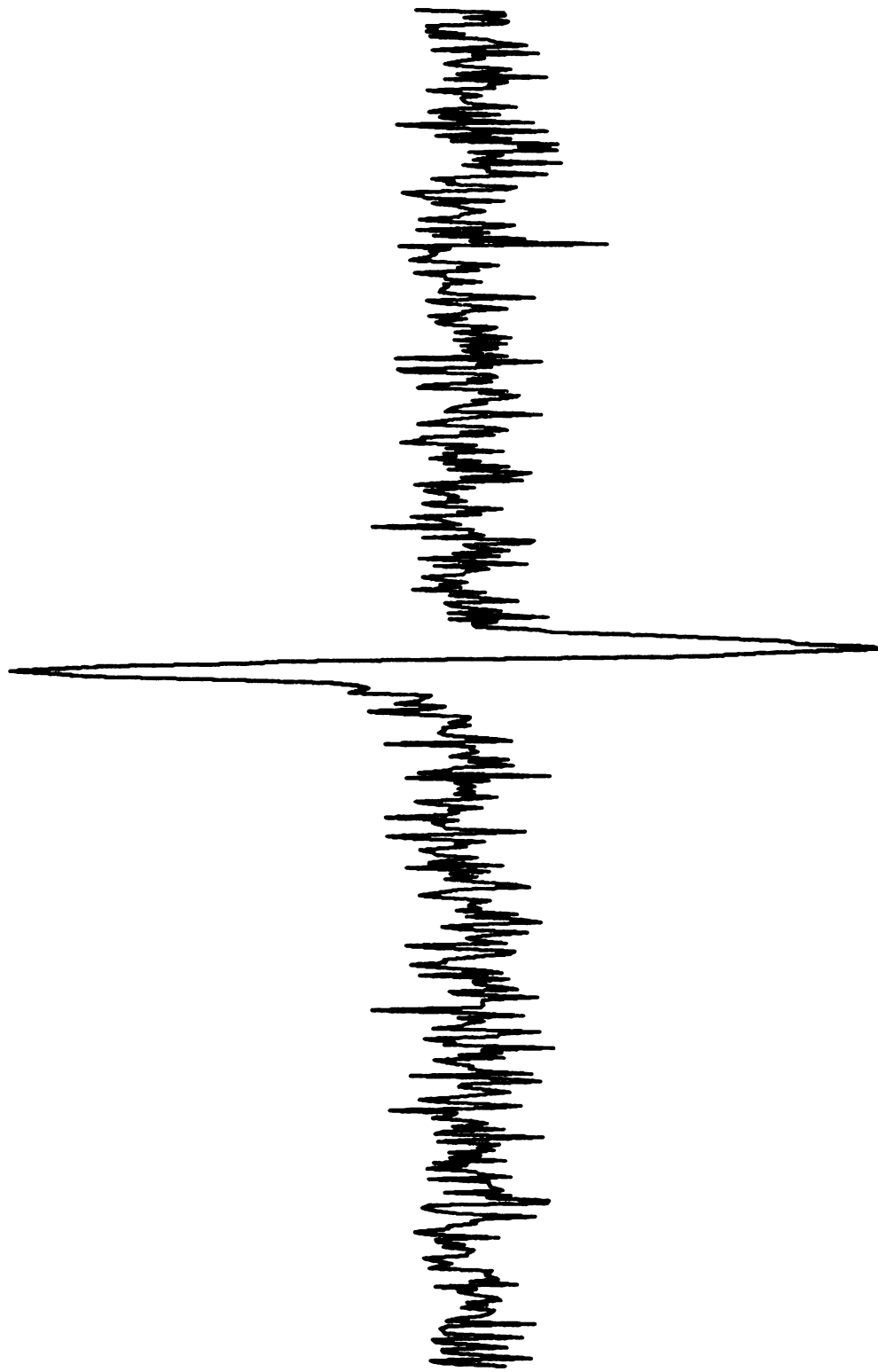


Figure 4-3: A spectrum of Na-THF-Crypt recorded with 100 kHz field modulation.

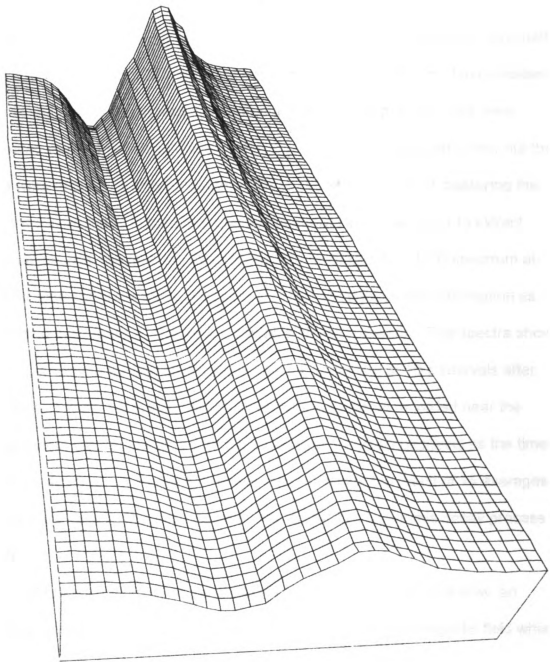


Figure 4-4: A time-resolved spectrum of $e^-_{(solv)}$ employing 100 kHz field modulation.

A time-resolved spectrum of the $e^-_{(solv)}$ resonance was recorded using computer program TIME12 and is shown in Figure 4-4. The data were recorded with a time constant of 20 ms and at intervals of 0.1 s (5 times the time constant). The flashing of the lamp was delayed an additional 20 s after the data were collected to allow for a total decay of the signal. No averaging was done, but the data were digitally smoothed before plotting. Another method of displaying the information encoded in the time-resolved spectrum in Figure 4-4 is to extract information from the time-resolved data set to reconstruct an EPR spectrum at various times after the flash. Program DSTRIP will remove this information as described in Chapter 3. Figure 4-5 contains six such spectra. The spectra show the $e^-_{(solv)}$ resonance line starting at 0.1 s and continuing at 10 s intervals after the flash. Figure 4-6 shows the decay of the $e^-_{(solv)}$ signal recorded near the maximum of the resonance under the same experimental conditions as the time-resolved spectrum in Figure 4-4 except that this plot is the result of 16 averages. These data have not been smoothed. The calculated $t_{1/2}$ for this decay process is 25 s.

Because the decay of the photolytically produced species is slow, an attempt was made to observe the monomer by scanning the magnetic field while manually triggering the flash lamp every few seconds. For a long-lived species, this process should build up an observable population of the radical; however, the experiment produced negative results.

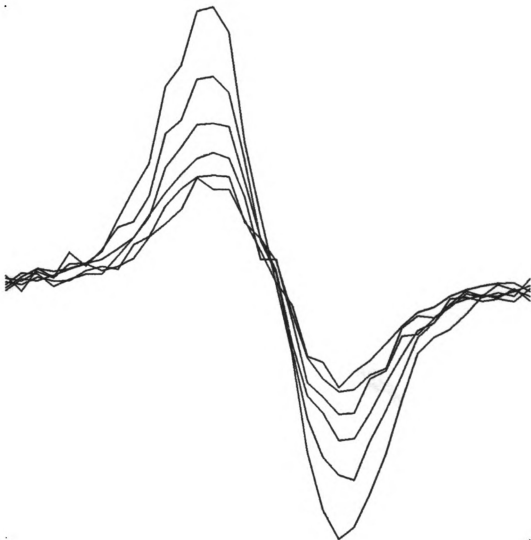


Figure 4-5: Spectra extracted from the time-resolved data set in Figure 4-4 showing the spectrum at 0.1 ms after the flash and continuing at 10 s intervals.

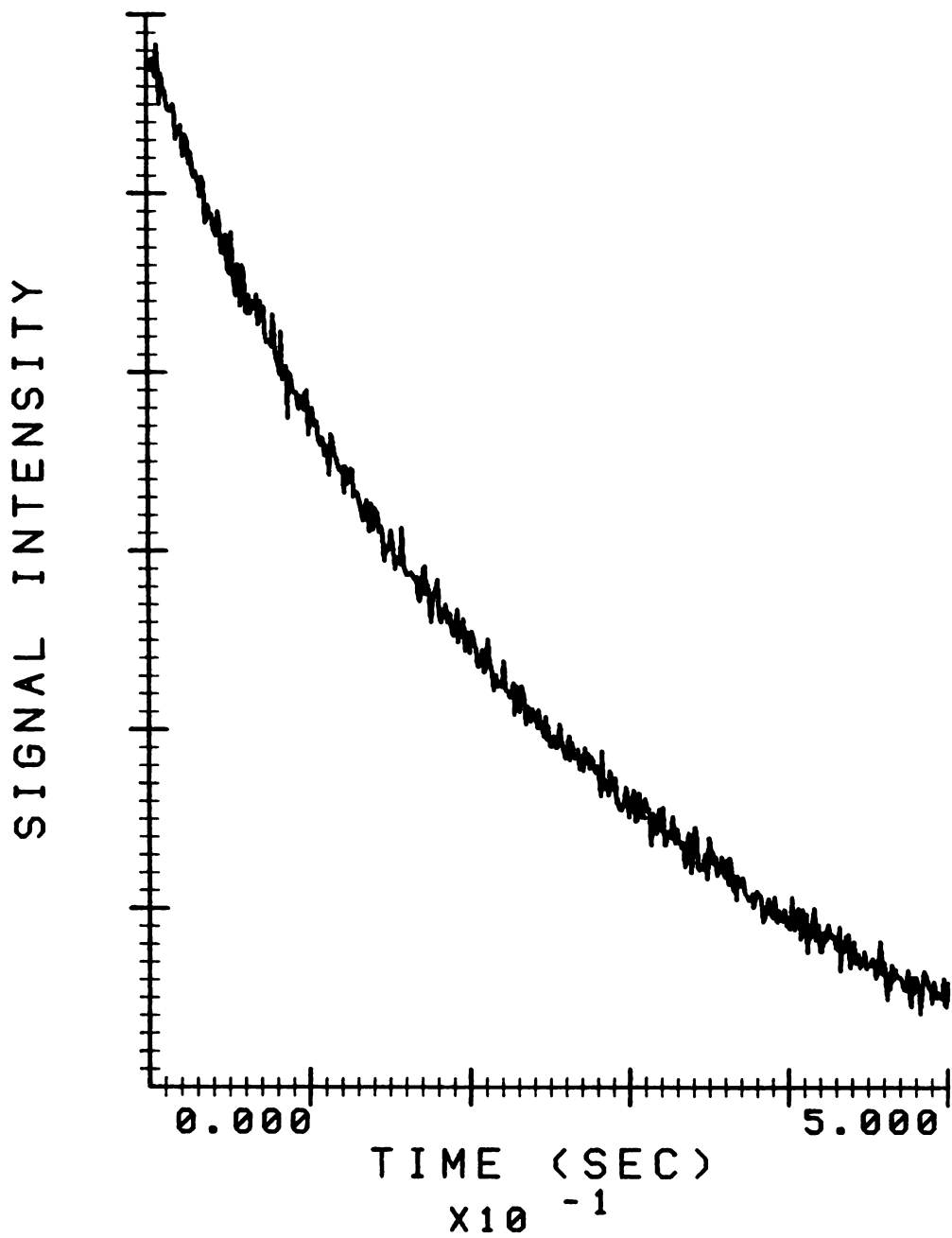


Figure 4-6: The decay of the $e^-_{(soln)}$ signal as a function of time recorded with 100 kHz field modulation and a 20 ms filter time constant.

Discussion

The absence of a hyperfine multiplet for sodium, as well as for some other alkali metals in THF, has been previously observed. Catterall et al. [CA77] stated that EPR spectra indicate the higher alkali metals in THF will yield a singlet from the solvated electron and a hyperfine multiplet from the monomer while spectra of lower alkali metals will be a single resonance line. Catterall described this phenomenon as a time-average of the two possible environments for the unpaired electron. He indicated that even spectra of potassium solutions have been reported as a single line. However, since that article, EPR spectra containing hyperfine splitting attributed to potassium monomer have been reported [FR77]. Hyperfine splitting of K in THF was observed under continuous illumination without the addition of a cation-complexing agent and was also observed in the dark spectrum with the addition of a small amount of crown ether, CR, as a cation-complexing agent. However, at CR concentrations above 10^{-4} M, a monomer spectrum was no longer detected. Friedenber and Levanon [FR77] suggest that the disappearance of the monomer spectrum is due to ion-pair formation, which exchanges with the monomeric species yielding a single average resonance line. When documenting the detection of the potassium monomer, Friedenber and Levanon [FR77] included a spectrum of a K-Na-THF solution, which showed only the same lines as the lines observed in the pure K-THF solutions. Even under conditions that produced a K spectrum, Na was not observed. This does not, however, imply that the same results would be

obtained with the addition of cryptate, a much stronger cation-complexing agent. Under the proper reagent concentrations, the monomer may be observed.

If hyperfine splitting from sodium is to be observed, the chance of detecting it would increase by studying the solution at room temperature or above rather than at -20 C (253 K) which was used during these experiments. Friedenbergs and Levanon did not observe the potassium monomer below 230 K , while at room temperature; they observed hyperfine splitting in a dark spectrum of K-THF with crown ether added.

There is a limited amount of reported research on the kinetics of sodium-ether solutions. Studies have been hampered by the limited solubility of sodium in these solvents. Glarum and Marshall [GL70] reported a kinetic EPR study of potassium, rubidium and cesium; however, they were not able to dissolve sodium in DME. DME left in contact with sodium for several days, was pale green in color and absorbed light at 480 nm instead of the usual 670 nm Na^- band. However, the solvated electron signal was observed and its amplitude increased upon illumination; but they believed that the species in solution were decomposition products rather than the desired Na^- .

To prevent irradiation of the 480 nm absorption band attributed by Glarum and Marshall to decomposition products, a red filter was inserted between the flash lamp and the sample. The addition of the filter had no effect on the observed results. The calculated $t_{1/2}$ for the decay of the $e^-_{(\text{soln})}$ resonance line in the Na-THF solution reported in this study is 25 seconds – much longer than was expected. However, the sodium solutions previously studied did not contain a complexing agent. Friedenbergs and Levanon [FR77] studied potassium,

rubidium and cesium in THF with crown present and reported that the recombination rate constants were dependent on the crown concentration. They proposed the process below to account for the decrease in the rate constant with an increase in the CR concentration:



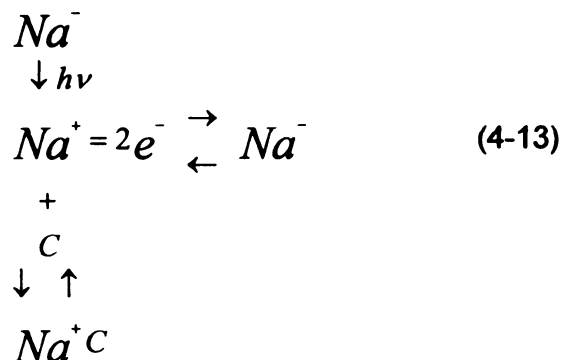
This process competes with the recombination process:



The proposed ion pair (e^{-} , MCR^{+}) would have a broad EPR signal that would be masked by the solvated electron signal.

Friedenberg and Levanon [FR77] reported a factor of 13 decrease in the observed rate constant for potassium in a 2×10^{-4} M CR solution compared to a solution without CR yielding a $t_{1/2}$ of 0.1 s.

Since the reaction rate recorded for Na-THF is still significantly longer than that reported for potassium above, it is possible that we are observing a different phenomenon. The cryptate, C222, is in excess in the Na-THF solutions. Thus, the species in solution are $Na^{+}C$, Na^{-} , C , $e^{-}_{(solV)}$. Irradiation with light containing wavelengths around 670 nm, the region of that Na- absorption band, will remove one electron [HU70, GA70]. The monomer produced is in an excited state and will decay by losing another electron. The newly created cation has two reaction paths to follow as shown below:



The complexation reaction between Na⁺ and C222 is known to be fast. An estimate for the recombination rate for sodium can be obtained from the flash photolysis work of Kloosterboer et al. [KL71]. They optically observed a t_{1/2} approximately equal to 0.15 s for the disappearance of the e⁻_(solv) signal. Even though it is generally accepted that the product being formed was K⁻ due to potassium contamination rather than Na, the observed lifetime can be used as an upper limit for the sodium recombination since K⁻ formed more rapidly than Na⁻. This number is only an estimate because both the solvent (DME) and the temperature (-60 C) in Kloosterboer's study were different that in the current work. The e⁻_(solv) will not displace the Na⁺ from the crypt; therefore, the disappearance of the e⁻_(solv) signal would depend upon the rate of release of the Na⁺ from the crypt. This release rate via the proposed mechanism below has been measured using Na²³ NMR [CE77].



The release rate of Na⁺ from C222 was determined at 298 K for the Na-THF-C222 solution and was reported along with the thermodynamic parameters ΔH₀[‡],

ΔS_0^\ddagger , and ΔG_0^\ddagger . Using these parameters, ΔG_0^\ddagger and the release rate constant (k_{-1}) and $t_{1/2}$ at a different temperature can be calculated by Equations 4-15, 16, 17:

$$\Delta G_0^\ddagger = \Delta H_0^\ddagger - T \Delta S_0^\ddagger \quad (4-15)$$

$$k_{-1} = \frac{K \beta^T}{h} e^{-\Delta G_0^\ddagger / RT} \quad (4-16)$$

$$t_{1/2} = \frac{0.693}{k_{-1}} \quad (4-17)$$

The calculated $T_{1/2}$ at 253 K is 6.5 s. This number is respectably close to the measured 25 s $T_{1/2}$. The reaction rate measured was probably the rate of release of Na^+ from C222, not the recombination rate of Na^+ and $2e^-$.

Recommendations

The complex chemistry of alkali-metal solutions in ethers and amines is not completely understood. There is still much controversy about the nature of the species in solution. Many mechanisms have been proposed to explain the observed and unobserved experimental evidence. A systematic transient EPR investigation of sodium solutions (the alkali metal lease studied) could possibly reveal some very important data on the species in solution. A series of sodium solutions, with varying concentrations of cryptate, could either allow the observation of the monomer under the "proper" reagent concentrations or provide very strong negative evidence that would support ion-pair formation and exchange mechanisms.

The study of alkali-metal solutions could be greatly enhanced by the addition of an optical spectrometer to the EPR system to allow direct comparison of EPR and optical kinetic data. A simultaneous optical and ESR spectrometer (SOESR) [WA76] could yield the correlation between optical and EPR data necessary for understanding the chemistry involved in alkali-metal solutions.

The 2 MHz EPR spectrometer could be enhanced considerably by adding a pulsed laser source for the kinetic studies. The biggest problem with the 2 MHz spectrometer is the signal-to-noise ratio. The current experiments were performed under conditions near the limit of detection for this instrument. The addition of an intense, collimated source might produce a large enough signal to make the 2 MHz instrument a viable kinetic tool.

CHAPTER 5

Characterization of the Flash Lamp

Introduction

Since the mid 60's, EPR has been used to investigate transient radicals generated by photochemical, electrochemical, and electron irradiation processes. More recently, it has become possible to obtain kinetic information on radical reactions, which can be carried out in the EPR sample cavity. Modifications to existing EPR instrumentation have enabled experimenters to follow rapid changes in radical concentrations as a function of time. Free radicals investigated in this way have been produced by flash photolysis [BE67, AT70, FI67], pulsed electrolysis [GO71, GO74], and pulsed radiolysis [FE73, SM71]. The technique involves applying a perturbation pulse to the sample and averaging the transient response obtained from the EPR.

Early flash photolysis experiments were carried out using a continuously operated light source in conjunction with a rotating slotted disk to provide intermittent illumination of the sample [GA70, HAM70]. The main limitation to this approach is the mechanical problem associated with the very high-speed rotating disk, which is necessary for observation of radical lifetimes on the order of ms and below. Since the perturbation pulse must be significantly shorter than the lifetime of the radical under study, the rotating disk method is restricted to studies of long-lived species. Several investigators have overcome this problem by using lasers [AT73, HAL72] to produce intense light pulses of short duration (<1

μs). These short, intense light pulses make a laser an ideal irradiation source, but unfortunately, lasers are only available in a relatively narrow range of wavelengths, which does not include much of the ultraviolet, a region in which a great number of photochemical reactions occur.

This chapter is devoted to the approach taken by this investigator – a fast-extinguishing flash lamp that has a spectral output from the ultraviolet to the infrared. In this chapter, the flash-lamp trigger and flash-detection circuitry are presented and the flash lamp is characterized. Finally, the chemical photon-counting technique called actinometry, used to measure the ultraviolet light intensity available in the EPR cavity, is discussed.

The Flash Lamp

The flash lamp was purchased from Photochemical Research Associates, University of Western Ontario, London, Ontario.

The circuit in Figure 5-1 shows the flash lamp with the associated high voltage supply and trigger circuitry. A thyatron was placed in series with a Xenon Corporation Suntron 6C flash lamp to give control over timing of the flash and to allow the flash lamp to be operated at voltages above the normal hold-off voltage of the lamp. In this circuit, capacitor C3 is charged to 400 Vdc by the voltage doubler made up of diodes D1, D2 and capacitors C1, C2. A 5-volt pulse at the trigger input of the lamp causes the SCR, S1, to turn on, discharging capacitor C3 through the primary of transformer T3. The secondary of T3 is

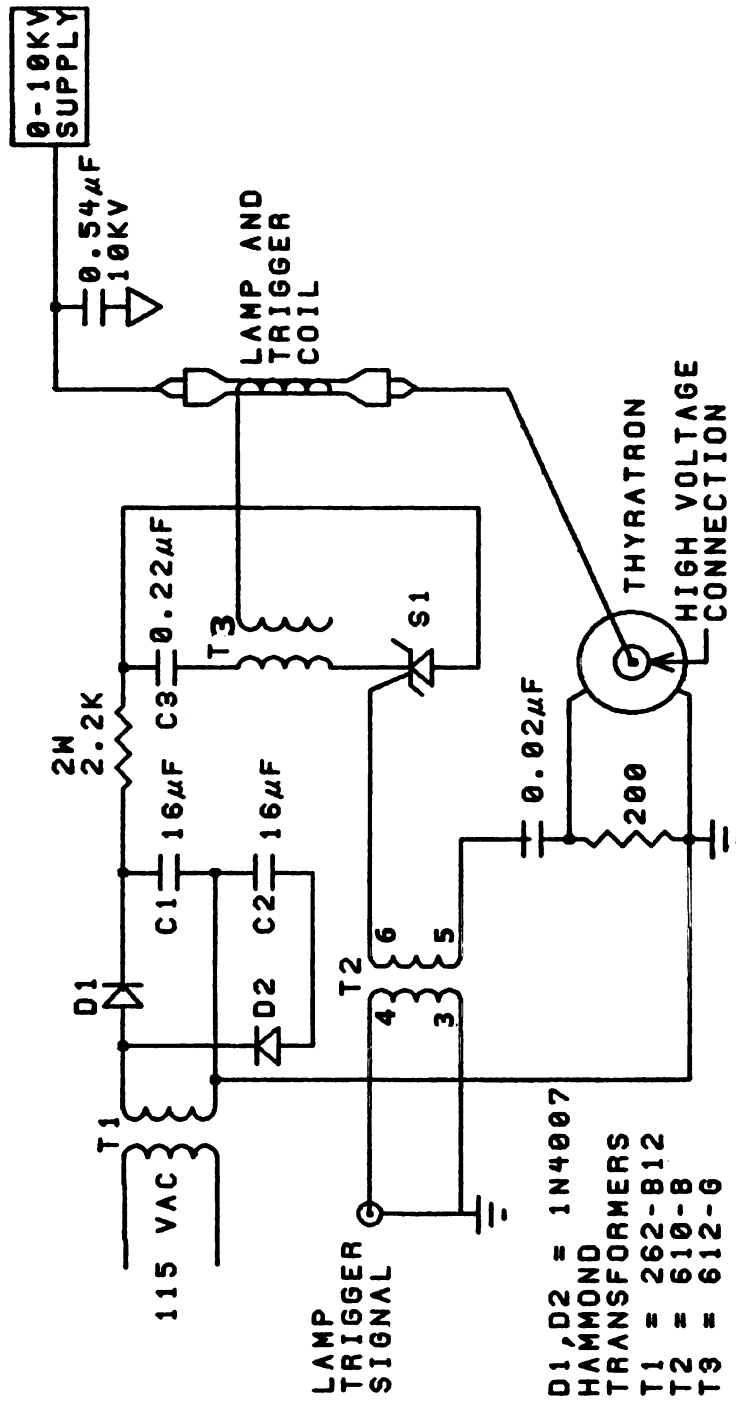


Figure 5-1: Circuit diagram showing the flash lamp and associated trigger circuitry.

connected to a wire wound a couple of times around the body of the flash lamp. This coil starts the ionization of the filler gas in order to insure a reliable trigger of the flash lamp. At the same time, a trigger pulse to the thyatron causes it to turn on and discharge the main storage capacitor, C4, through the flashtube.

The Suntron 6C flashtube is a fast-extinguishing lamp that will produce a spectral output, which is an almost pure continuum above 3000 Angstroms when operated at high current density [XENO]. The recommended operating condition, taken from manufacturer's literature, is 10 kV with a 1 μ F capacitor. The maximum average power that the lamp will dissipate safely in free air is 100 watts. The flash-lamp housing contains a forced-air cooling system to help dissipate heat generated by the lamp.

The computer controls the timing of the flash lamp through the circuit shown in Figure 5-2. A trigger command is issued by the PDP 8/E computer by moving a digital word which contains a 1 in bit 11 to the digital output buffer provided on the laboratory peripherals option of the computer. The rising edge of bit 11 triggers a monostable wired for a 20 μ s pulse. Twenty microseconds is an experimentally determined minimum time, which produces a reliable flash-lamp trigger. The monostable pulse is then driven to the receiver box at the flash lamp by a noninverting buffer. In the receiver box, an optical isolator receives the pulse and causes the final output transistor to conduct the current pulse necessary to the trigger transformer in Figure 5-1. An optical isolator was employed in order to isolate the power and ground in the computer from the electrically noisy ground of the flash lamp.

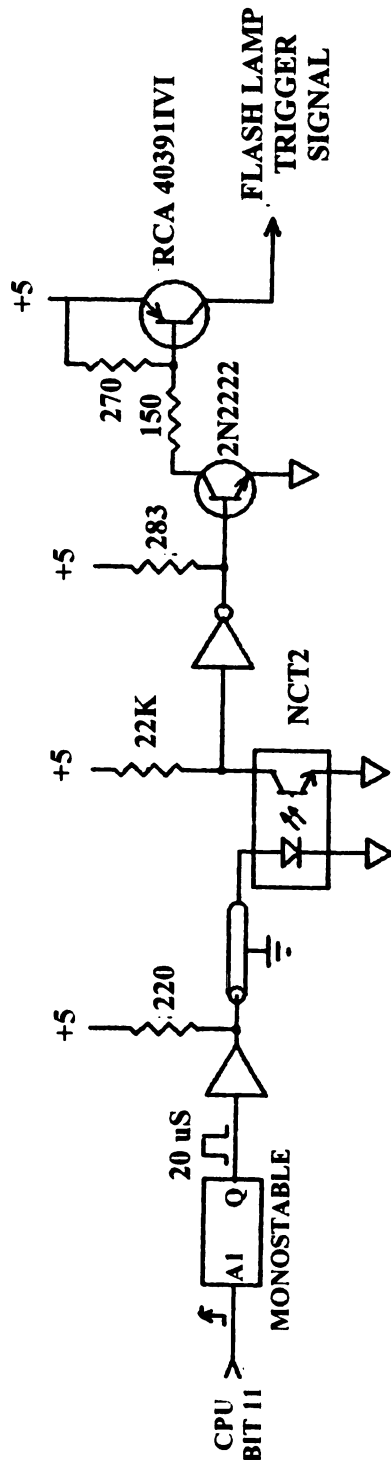


Figure 5-2: The flash-lamp trigger interface to the PDP 8/E computer.

Since the timing of the data acquisition should start when the lamp actually flashes instead of when the computer requests a flash, a "lamp-flashed" signal is generated at the lamp by the circuit in Figure 5-3. An ultra fast response (<1.0 ns) PIN silicon photodiode is mounted on the outside of the flash-lamp housing. A small hole was cut in the lamp housing allowing some of the light from the lamp to strike the photodiode. When the photodiode starts to conduct, a TTL signal is sent to a Schmitt trigger input on the analog peripheral option of the PDP 8/E. The analog control board in the computer was modified so that a Schmitt trigger pulse could be used to start the crystal controlled clock without requiring software intervention. DEC literature indicates that this function is available on the lab peripherals option; however, it was not previously implemented on this particular computer. It now works as stated in DEC's documentation.

A second photodiode is used to obtain the integrated intensity of the light pulse so that the variations in each light pulse can be taken into account in the data manipulation. The circuit is shown in Figure 5-3. The capacitor on the input of the integrator is used to prevent the negative operational amplifier input from saturating and thereby losing the intensity information. A sample-and-hold amplifier samples the integrator output after 70 μ s to allow time for the integrator to drain all the charge from the input capacitor. The sample-and-hold amplifier "holds" the voltage output of the integrator until the computer has time to sample the signal. The integrator is discharged by a resistor across the integrating capacitor of the operational amplifier. The time constant of the discharge, 50 ms, is long enough so that it will not affect the integrated light pulse signal before the

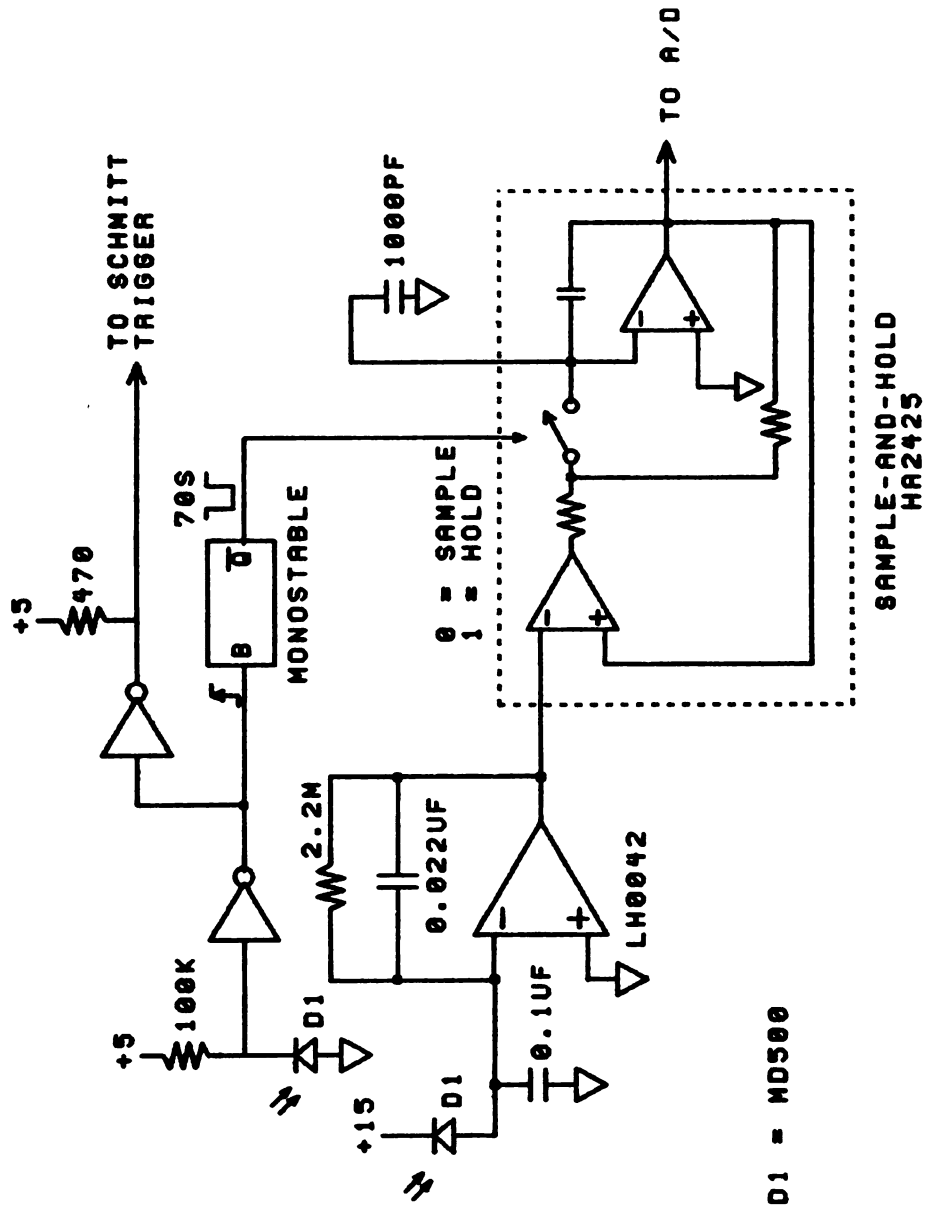


Figure 5-3: The lamp-flashed detector and light integrator.

sample-and-hold amplifier captures the signal (70 μ s). Since the maximum lamp repetition rate is 4 Hz with a 10 kV supply voltage, the discharge resistor has sufficient time to discharge the integrator (5 time constants). The discharge resistor approach was taken to eliminate the need for another control line from the computer to the flash lamp to control a shorting switch across the capacitor. The sample-and-hold amplifier timing is controlled by the flash detection photodiode.

Characterization of the Flash Lamp

The total energy dissipated by the lamp during a flash is determined by the capacitance across the tube and the supply voltage to the capacitor according to Equation 5-1

$$E = 1/2 CV^2 \quad (5-1)$$

where E is the energy in joules, C is the capacitance, and V is the applied voltage. The capacitance of the storage capacitor was determined by using it as the integrating element of an operational amplifier (O.A.) integrator. A Heath [HEAT] voltage reference source (VRS Model EU-80A) with an optional current probe was used as a constant current source to charge the integrator. The test circuit is shown in Figure 5-4. The OFF-ON switch controls the current to the integrator and the start and stop of a Heath Universal Digital Instrument (UDI) in timer A-B mode. The capacitance is calculated using Equation 5-2

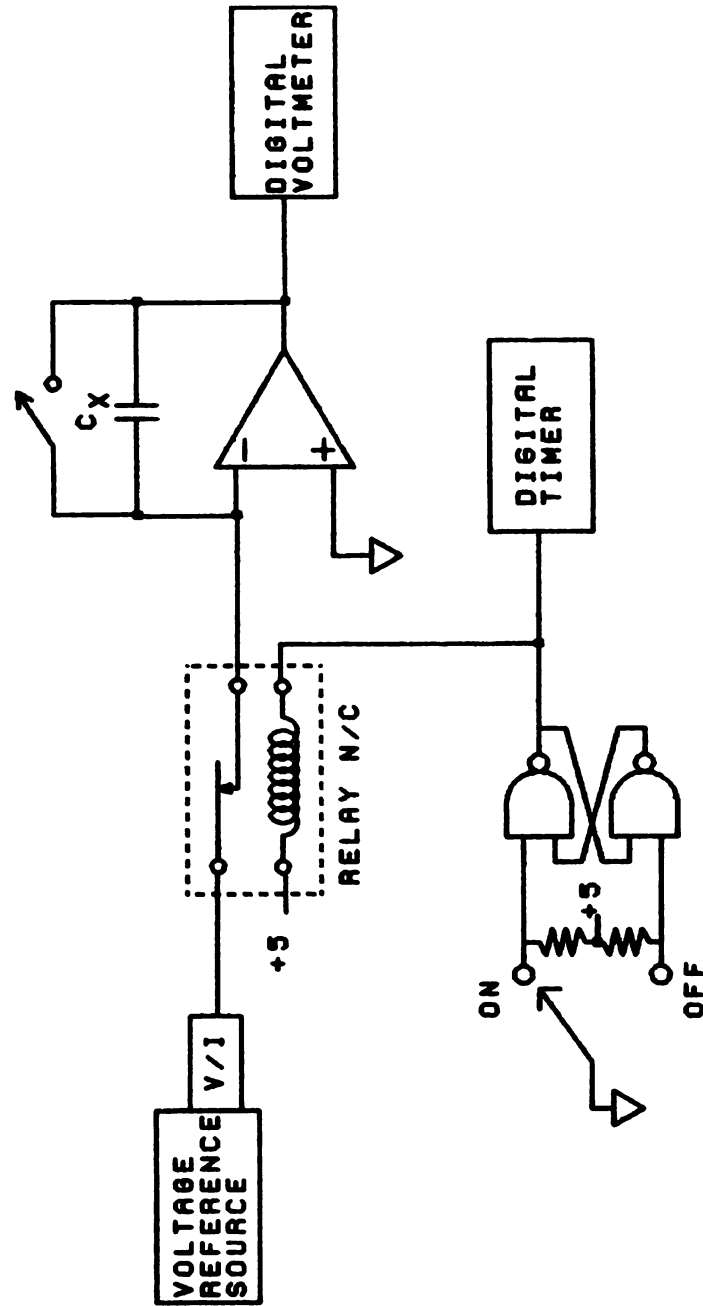


Figure 5-4: A digital capacitance meter.

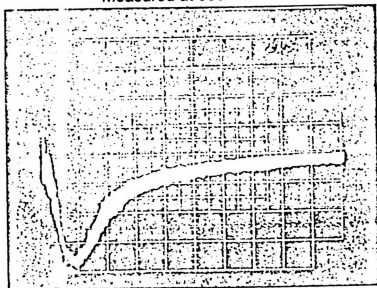
$$C = \frac{Q}{V} = i * \frac{t}{V} \quad (5-2)$$

where I is the current, t is the time and V is the voltage of the integrator measured at the end of the integration time, t . The measured capacitance was $0.540 \mu\text{F}$. The maximum recommended operating voltage of the lamp is 10 kV ; therefore, the maximum energy dissipated in the lamp is 27 joules/pulse . This, unfortunately, is below the $100 \text{ joules per pulse}$ recommended by the manufacturer for optimum spectral output. The small capacitance is a trade-off that had to be made to decrease the flash pulse-width to the desired $<10 \mu\text{s}$ value since the size of the capacitance affects the length of the flash.

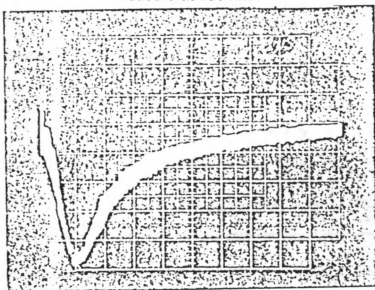
The characteristic of a flash lamp, which limits the observable reaction rate is the pulse width. This was determined by placing the lamp in front of the entrance slit of a Heath (Model EU-700) monochromator and observing the photomultiplier voltage output on a Tektronix 7623A storage oscilloscope. This measurement was made at several wavelengths and supply voltages. The results are shown in Figure 5-5. The full width at half maximum for the pulse is about $2 \mu\text{s}$ with the entire flash over in an absolute maximum of $10 \mu\text{s}$ at all supply voltages used.

The most important characteristic of a flash lamp, optics and sample chamber system is the number of photons of an appropriate energy that arrive at the sample. This number depends on the intensity of the flash lamp, the collection efficiency of the optics, and the size of the opening in the microwave cavity. This number is most easily determined using a photon counting solution in the EPR cavity. The chemical photo-counting technique is called Actinometry.

Measured at 360 nm



Measured at 450 nm



2 μ s/Div.

Figure 5-5: The flash-lamp pulse shape with a 10 kV lamp supply voltage. The abscissa is 2 μ s/div.

A potassium-ferrioxalate actinometer was used as the photon counting solution. The ferrioxalate actinometer, rated as the best solution-phase actinometer available today [CA66], is easy to use and sensitive over a wavelength range of 250–480 nm. A detailed discussion of the actinometer, including its nature, preparation, purification and use, has been published by Hatchard and Parker [HA56, PA53]. However, a brief discussion will be presented here to acquaint the reader with the technique. When sulfuric acid solutions of $K_3[Fe(C_2O_4)_3]$ are exposed to light in the range of 250–480 nm, a simultaneous oxidation of the oxalate and reduction of iron to Fe(II) occurs. The quantity of Fe(II) produced can be determined by first complexing it with 1,10-phenanthroline in an acetic-acid, sodium-acetate buffer of pH 3.5 and then measuring the absorbance of the complex at 510.0 nm. The high molar absorptivity of the Fe(II) complex, $E=1.11 \times 10^4 M^{-1} CM^{-1}$, makes it possible to determine very low photon levels.

Stock solutions were prepared, as recommended [HA56], from solid $K_3[Fe(C_2O_4)_3] \cdot 3H_2O$ which had been recrystallized three times from deionized water. Weighed quantities of the recrystallized solid were dissolved in 0.1 N H_2SO_4 and diluted to volume in volumetric flasks. Since the actinometer is highly sensitive to normal room light, all solutions were prepared in a dark lab and stored in a closed cabinet until use.

Preparation of the Working Curve

A calibration curve for the 1,10-phenanthroline iron(II) complex was prepared using ferrous ammonium sulfate [C162] as an iron standard instead of

using the iron standardization procedure published by Hatchard and Parker [HA56]. The Fe(II) stock solution was prepared by dissolving the ferrous ammonium sulfate in 0.1 N H₂SO₄. A standard 5.0 x 10⁻⁴ M Fe(II) solution was prepared from the stock solution. This procedure requires all of the iron in the standard solution to be in the Fe(II) oxidation state, so hydroxylamine hydrochloride was added to reduce any Fe(III) present. Another departure from the method of Hatchard and Parker was a 20-fold excess of 1, 10-phenanthroline used to ensure total complexation of Fe(II).

The following volumes of the Fe(II) solution were added to eleven 25 ml volumetric flasks: 0 (blank), 0.5, 1.0, ..., 5.0 ml. Added to each flask was 5 ml of buffer, 4 ml of 1, 10-phenanthroline, 1 ml of hydroxylamine hydrochloride and sufficient 0.1 N H₂SO₄ to bring the total number of milliequivalents of acid to 1.25. The solutions in the flasks were diluted to volume, mixed and allowed to stand at least one-half hour. The absorbance was measured using a McPherson Model EU-700 Spectrometer with an oscillating sample cell. Figure 5-6 shows the fitted results of the working-curve data. The least squares fitted slope of the working curve, E, was 1.11x10⁻⁴M⁻¹CM⁻¹, numerically equal to previously reported molar absorptivity values [HA56, HO69].

Photolysis Experimental Setup

The EPR cavity was removed from the microwave bridge of the EPR instrument and clamped to a ring stand on a lab bench for easier access. The task of focusing the lamp on the sample in the Micro-Now EPR cavity was a very

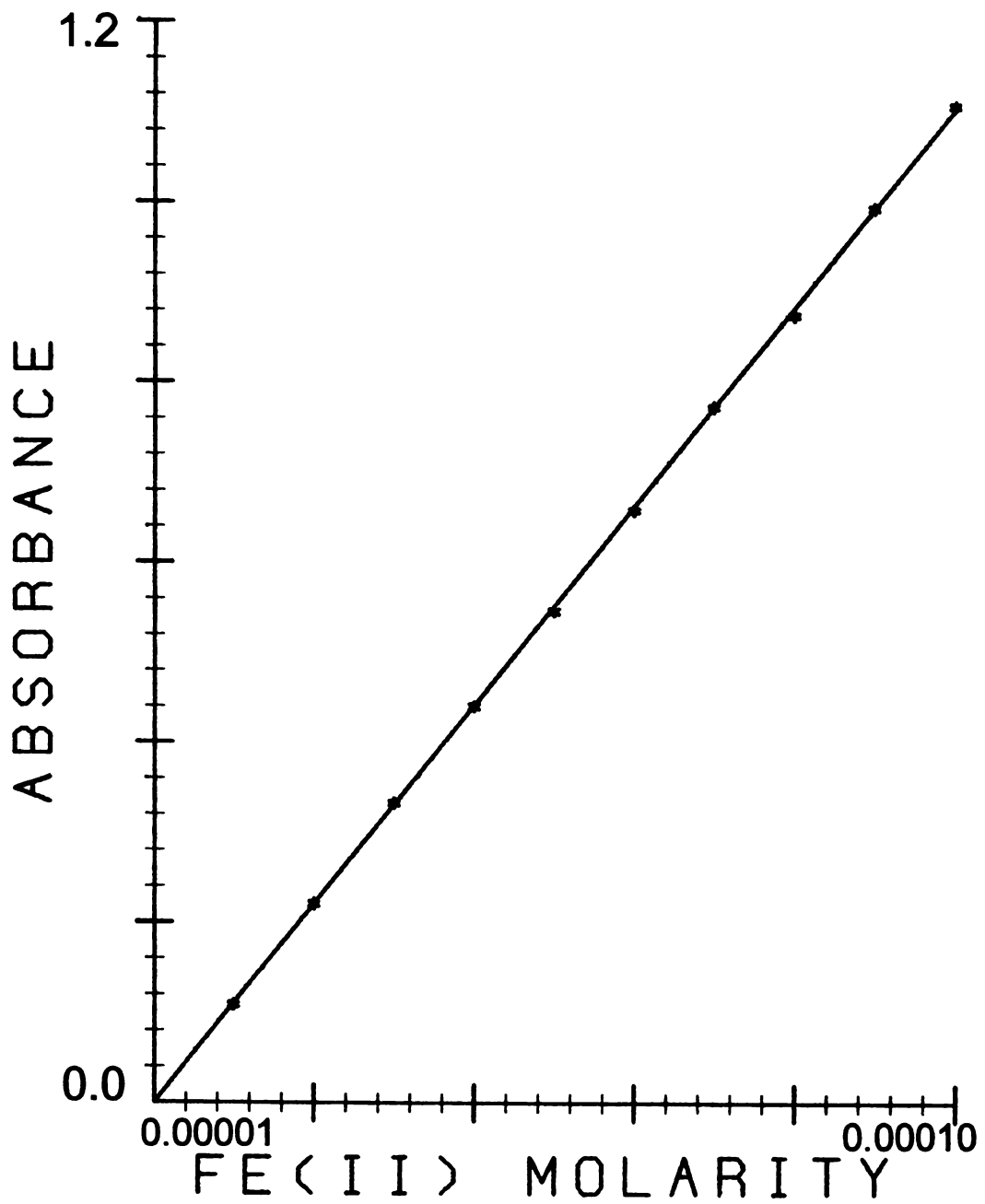


Figure 5-6: A calibration curve of absorbance of 1,10-phenanthroline Fe(II) complex as a function of Fe(II) molar concentration.

difficult one. According to manufacturer's literature, previous Micro-Now cavities were designed for coupling with a linear accelerator beam. Such a well-collimated source does not require a large opening in the sample cavity wall. The actual opening in the cavity wall of this micro-Now cavity is a rectangle 0.6 cm wide by 0.2 cm high. To prevent the microwave in the cavity from leaking out through the hole, a cylindrical waveguide "beyond cutoff" was welded around the rectangular hole in the cavity wall. The cylindrical waveguide is 0.6 cm inside diameter and longer than one half wavelength, 3.0 cm. It is too long and too narrow to support a standing wave at the frequency of cavity resonance and thus no microwave will leak out of the opening.

This small entrance would not present a problem for a collimated source such as an electron or laser beam; however, the flash-lamp source used in these experiments is not collimated. Neither is the lamp a point source, but instead a column and the optics of the lamp focus to give a reduced size image of the column at 3.5 cm from the end of the lamp optics. This would not be a problem in an EPR experiment since the height of the focus image, 1.2 cm, is shorter than the active sample region in the microwave cavity. However, the geometry of the opening in the Micro-Now cavity prevents optimum focusing. The problem is the small area presented by the end of the cylindrical waveguide.

Observation of the shape of the light beam at various distances from the end of the lamp optics revealed that at 1.5 cm, the beam had converged to its smallest diameter before diverging into a focused image. A diagram of the light beam is shown in Figure 5-7. The flash lamp was placed so that the entrance to the waveguide is 1.5 cm from the optics. A considerable amount of light was lost

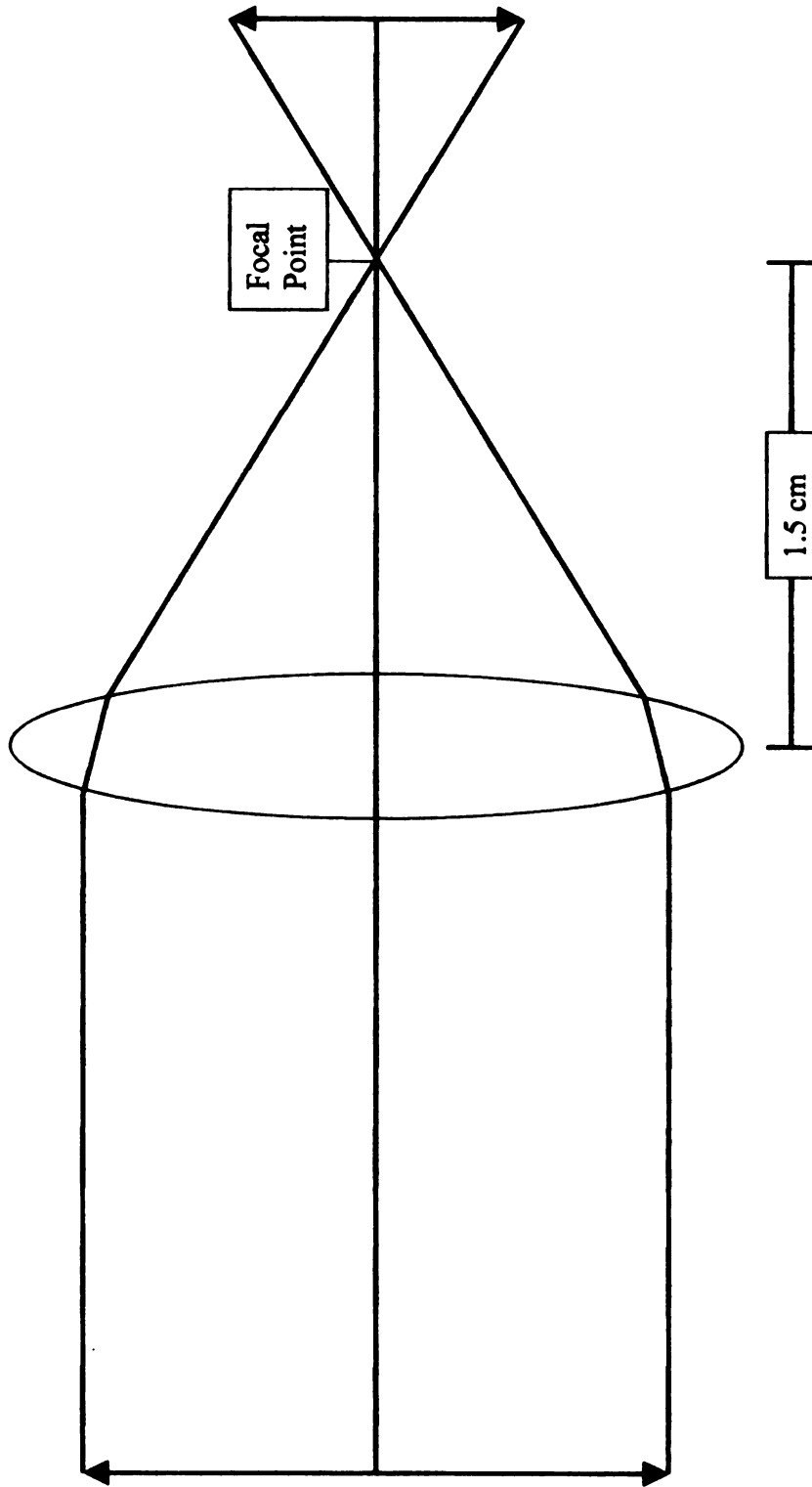


Figure 5-7: Diagram of the focused light beam of the flash lamp.

because the minimum beam spot is still not as small as 0.6 cm. As the light starts to diverge in the cylindrical waveguide, the internal surface of the waveguide should act as a light pipe and reflect the light toward the sample. Once the light is in the waveguide, the limiting parameter is the height of the slit presented by the rectangular opening in the wall of the cavity. The slit width, 0.2 cm, will only allow about 40 percent of the light in the waveguide to enter the cavity (based on areas). The study was also conducted in a second EPR cavity to determine the amount of light lost by using the Micro-Now cavity. This cavity was a Varian transmission cavity, i.e. openings in both front and back walls of the cavity for light to pass. The opening into the waveguide and cavity were rectangles 1.2 cm high by 0.6 cm wide. This made it much easier to focus the lamp and, as it turned out, allowed more light to enter the cavity.

Photolysis of the Actinometer Solution

The wavelength sensitivity of the potassium ferrioxalate actinometer is concentration dependent. Plots of absorbance and quantum yield of Fe(II) versus wavelength for several concentrations are shown in a paper by Hatchard and Parker [HA56]. Selection of the concentration of the actinometer gives a natural cut-off filter. A concentration of 0.15 molar was selected which according to Hatchard and Parker absorbs all light below 450 nm.

The actinometer solution was placed in a quartz NMR tube and inserted in the EPR cavity. Flash-lamp supply voltages of 8, 9, and 10 kV were used. Each

sample was flashed 50 times to build up an Fe(II) concentration large enough to optically measure. The sample was stirred after every ten flashes.

The analytical procedure used for the unknown was identical to that used in preparing the working curve, except the 4 ml of photolyzed solution replaced the standard Fe(II) solution and the hydroxylamine hydrochloride was excluded.

The quanta of light absorbed can be calculated by the following equation [HA56]:

$$Quanta = \frac{A_s V_1 V_3 (6.023 \times 10^{20})}{EL V_2} \quad (5-3)$$

where

V_1 = volume of actinometer solution photolyzed (5 ml)

V_2 = volume of aliquot taken for analysis (4 ml)

V_3 = the final volume to which V_2 was diluted (25 ml)

A_s = the measured absorbance of the solution at 510.0 nm

L = the path length of the cell (0.9 cm)

E = the molar absorptivity of the Fe(II) complex ($1.11 \times 10^4 \text{ M}^{-1} \text{ cm}^{-1}$)

Q = the average quantum yield for Fe(II) formation for light in the range of analysis (1.2)

The results of this study for both the Micro-Now and Varian cavities are shown in Table 5-1.

At the time these experiments were performed, the Varian cavity was not being considered as a possible alternative to the Micro-Now cavity; therefore, a complete set of supply voltages were not used. The only reason for the Varian

Table 5-1: Measured Quanta of Light per Pulse Available in the Micro-Now and Varian Cavities.

Supply Voltage (kV)	Micro-Now Cavity Quanta/pulse) x10⁻¹⁵	Varian Cavity Quanta/pulse) x10⁻¹⁵
8	1.02 +/- 0.29	3.14 +/- 0.37
9	1.46 +/- 0.54	
10	2.05 +/- 0.48	

cavity's inclusion was to determine the effect the small entrance to the Micro-Now cavity had on its total light gathering capability. As expected, the Varian cavity collected more light than the Micro-Now cavity but the difference is more than can be explained by comparing the areas of the entrance waveguides of the two cavities. The rectangular waveguide in the Varian cavity captures a larger fraction of the total light because the shape is similar to the focused image of the lamp.

The number of photons per pulse is a disappointingly small number for both cavities considering the range of wavelength absorbed by the actinometer solution. Fortunately, most molecular absorption bands are very broad and will absorb light in a range of wavelengths.

Even though this actinometer study did not yield any specific data about the quanta of light of wavelengths of interest for the photochemical experiments done in this research, it is important for several reasons. The results indicate that the focusing of the lamp on the sample cavity opening was not as critical as was first thought. The experiments were performed with the lamp at several slightly different positions with very similar results. This is important because

when one tries to focus the lamp on the cavity when the cavity is between the EPR magnet pole tips, it is difficult to see if it is perfectly focused. Secondly, the ultraviolet region is of importance in a great number of photochemical reactions. The results of this experiment suggest that such reactions could be studied with this lamp and cavity system. Also, from the spectral response curve of the flash lamp, an estimate of the quanta of light in other wavelength regions can be made. The comparison between the openings in the Micro-Now and Varian cavities suggest that if a new cavity were to be built, an opening similar to the one in the Varian cavity should be used.

CHAPTER 6

System Modifications

Introduction

The original goal for this research project was the design and fabrication of a computer interface to a fast EPR spectrometer with a pulsed light source, which would allow EPR data to be acquired either as a conventional absorption spectrum or alternately, as a function of time for reaction-rate studies. Computer programs to synchronize events and to record, average and manipulate the data were to be written. The resulting system would be applied to the studies of radical reaction rates in situ in the EPR sample cavity. When it was discovered that the Micro-Now 2 MHz EPR spectrometer was not appropriately designed for the fast reaction-rate studies intended, a major change in emphasis for this research project became necessary. The new goal was to develop a functioning transient EPR system.

In this chapter, modifications made to the EPR system will be discussed in detail. First, the interface design, which was necessary to complete the research project as originally conceived will be presented. Finally, the modifications made to the Micro-Now system in an attempt to create a working spectrometer will be reported.

The Fieldial

To use an EPR spectrometer as a kinetic tool, it is necessary to maintain a constant magnetic field at the point of resonance, apply a perturbation pulse to the sample and record the transient response from the EPR. To obtain an EPR absorption spectrum, the magnetic field is varied and the EPR output signal is recorded as a function of magnetic field strength. The two experimental techniques have been combined to give an EPR spectrum of a transient radical. This has been accomplished by both allowing the magnetic field to scan slowly while the lamp is flashed and the data are acquired [AT68b, FI67, HO72] and also by adding auxiliary field-sweep coils to the magnet pole tips [HI68, HS73]. Data collected using the former technique were acquired without signal averaging on multichannel X-Y or magnetic tape recorders. Using field-sweep coils, data are collected using a signal-averaging device, which is synchronized with both the field sweep and an excitation pulse to produce data collected as a function of time over a narrow magnetic field range. There are several problems with the latter technique [BO39]: 1) the sweep fields are often nonlinear with time, 2) the auxiliary field may disrupt the static magnetic field, 3) I-r heating of the coils limits the sweep field to a range of +/- 25 to +/-100 Gauss from the static field, and 4) field homogeneity decreases as the applied field increases. The technique is also limited in the rates of reactions it can follow.

The system discussed above does not benefit substantially from the use of a computer because there is no provision for allowing interactive control of the

EPR spectrometer. The addition of a computer does not eliminate any of the limitations, but does, of course, simplify data acquisition and reduction.

More recently, Goldberg et al. [GO75] reported an interactive computer controlled system, an O. S. Walker magnet in conjunction with an FCC-4 controller, which has an external analog voltage input that allows remote control of the magnetic field. Varian, in fact, offers an accessory for their Fieldial that allows external control of the magnet field sweep rate; however, it requires that the Fieldial be modified at the factory. S. H. Glarum [GL73] reported a circuit that he installed in a Varian Fieldial Mark I allowing replacement of the original Fieldial potentiometer with a more accurate external potentiometer. This published circuit was modified to enable input from a DAC to replace the potentiometer. Some of the electronics were updated and the circuit was installed in the MSU Fieldial Mark II.

The basic circuit for the externally controlled Fieldial is shown in Figure 6-1. A 1290 Hz oscillator excites a loop, which contains a Hall-effect transducer, the field selector resistors, and a transformer, T1, that drives the modulator circuit. The modulator circuit is basically an analog multiplier with the 1290 Hz sine wave at one input and the DC sweep-input voltage applied to the second input through a DAC. The product of these two signals appears at the output, passes through the sweep-range selector and is combined with the outputs of the Hall-effect transducer and field selector to produce an error voltage that is used to maintain the desired magnetic field.

The modulator was installed in the Fieldial Mark II at the corresponding position chosen by Glarum [GL73] for the Fieldial Mark I circuitry. The modulator

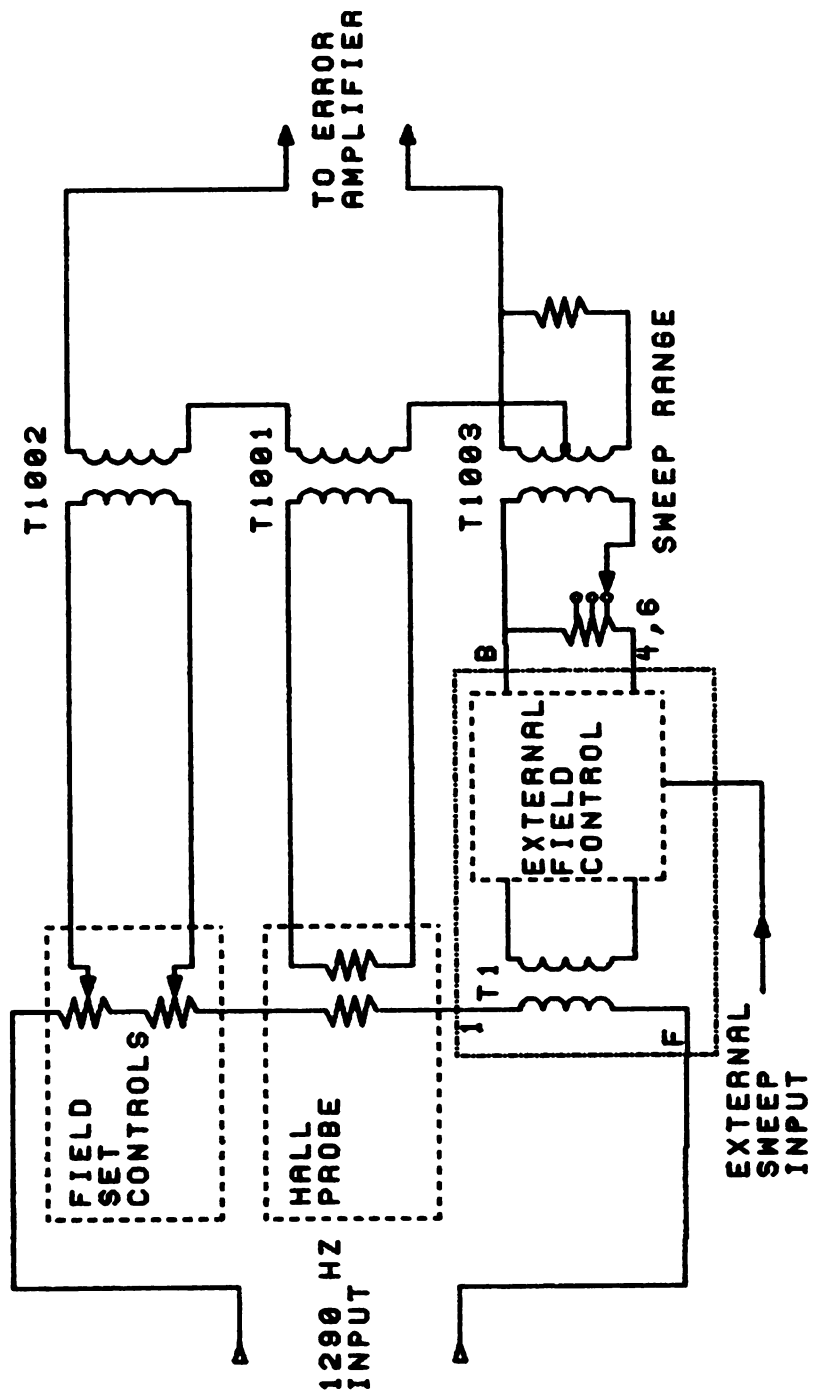


Figure 6-1: The simplified schematic of the externally controlled Fieldial magnetic field regulator.

circuit with transformer T1 is shown in Figure 6-2. The heart of the modulator is a Burr Brown 4204 four-quadrant analog multiplier. The output from the digital-to-analog converter (range = +/-5 volts) is sensed by an Analog Devices AD521J instrumentation amplifier configured with a gain of 2. The resulting output (range = +/-2 volts) makes full-scale use of the X analog-multiplier input. The 1290 Hz reference signal is connected through a double-pole double-throw switch to a step-up transformer and a reference-level potentiometer to adjust the reference signal to 20 volts peak-to-peak. However, because of differences in the circuits of a Mark I and Mark II Fieldial regulator, this signal was a maximum of only about 10 volts peak-to-peak. The output of the analog multiplier ($X*Y/10$) passes through a phase-shifter amplifier to the output amplifier. The output amplifier is connected to the sweep-range selector by a second double-pole double-throw switch. The two switches were inserted in the circuit to allow the selection of the standard Fieldial arrangement. This was necessary because the computer used as the controller in this research is used by many other researchers in the department and could not be dedicated to the EPR spectrometer. Without the switches to return the Fieldial its original condition, the EPR would be inoperable whenever the computer was needed elsewhere. The circuit diagram in Figure 6-2 does not include the trim potentiometers necessary for the analog multiplier or offset and gain-adjust potentiometers for the various amplifiers.

Connections were made to the Mark II Fieldial by inserting the modulator circuit between point 1 of the CB1101 oscillator and phase detector reference assembly and point B of switch S1007 and point F of J1001 and the wire that eventually goes to terminals 6, 6 of transformer T1003. The labels here and in

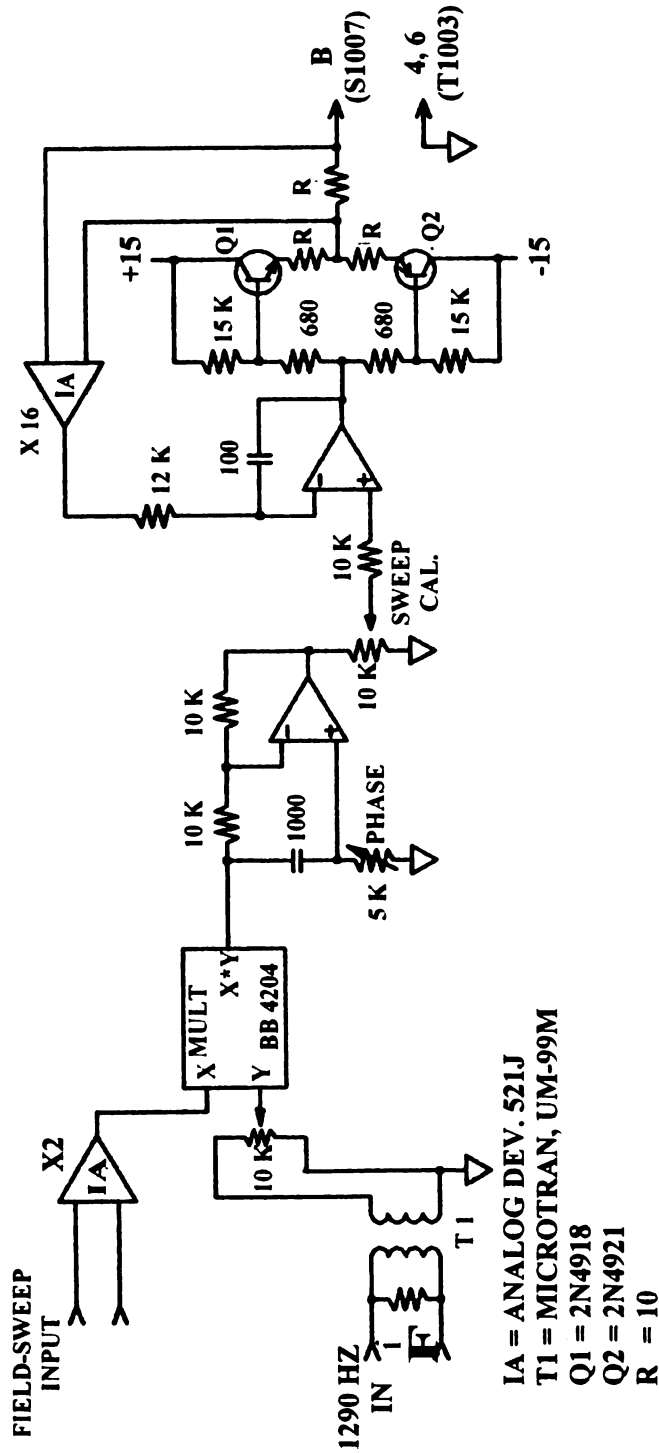


Figure 6-2: Circuit diagram of the modulator enabling external control of the magnetic field.

Figures 6-1 and 6-2 refer to the labels on Varian publication number 87-165-708 for the Mark II Fieldial Regulator. Once inserted in the Fieldial, electrostatic balance, signal phasing and reference tuning were performed according to the procedures outlined in the Varian Fieldial manual. Adjustment of the analog multiplier was performed following the manufacturer's instructions.

The DC analog voltage is derived from a 10-bit DAC within the computer and gives a resolution of slightly better than 0.1% of the field-sweep range selected. This resolution is adequate for the small field-sweep ranges used in this research, but at a sweep range of 1 kG, the resolution is only 1 G, which is wider than many EPR lines. The DAC should be replaced with a 12-bit DAC (resolution of 1 part in 4096) for general use.

The linearity of the field sweep was determined by applying a DC voltage to the field-sweep input of the analog multiplier and measuring the resultant magnetic field with a home-built gaussmeter which utilizes the NMR resonance of the proton. The results are shown in Figure 6-3. The nonlinearity in the center of Figure 6-3 is due to the nonideal behavior of the analog multiplier. When the sweep-input voltage is zero, the analog multiplier output should be zero; however, a small amount of the signal at the second input feeds through to the output (maximum of 10 mV_{p-p} for this multiplier). The nonlinearity could be reduced by replacing the Burr Brown analog multiplier with a unit having a better feed-through specification. A linearity test at sweep-width settings of 10, 100, 500 and 1000 Gauss indicated that the linearity within $\pm 10.25\%$ of the sweep width. This value is better than the linearity specification quoted by Varian in its Fieldial literature (0.5% of sweep width).

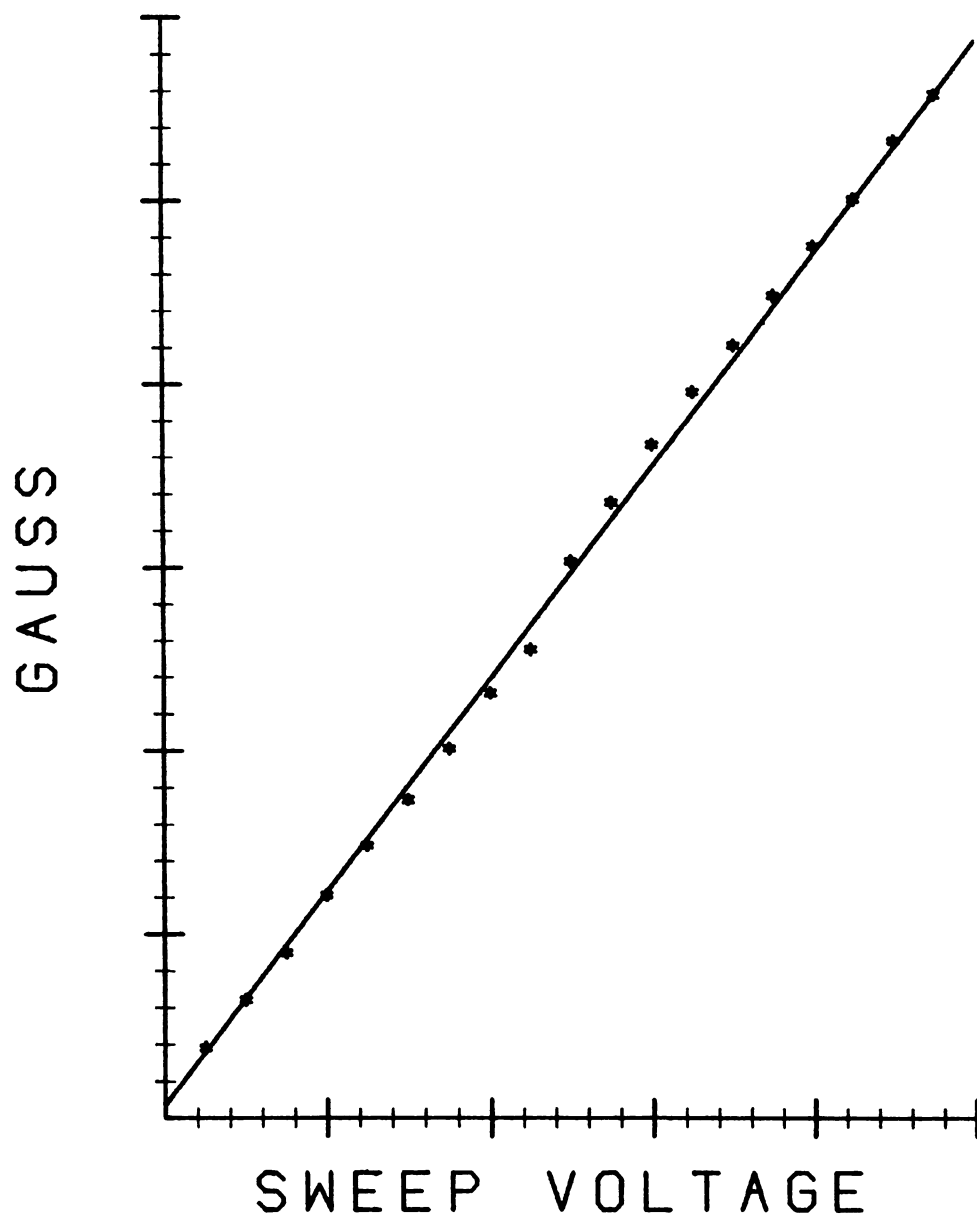


Figure 6-3: The magnetic field as a function of the external sweep voltage at a sweep width of 100 Gauss.

The short-term stability of the field was difficult to measure with the home-built gaussmeter used in this analysis since it was not a tracking gaussmeter and had to be manually adjusted. The frequency to establish proton resonance was selected using a variable capacitor. One's hand had to be kept on the adjustment knob during the entire integration period of the frequency meter to keep the frequency from changing, and this prevented continuous monitoring of the magnetic field. The short-term stability results are based on five readings made over about one minute. At sweep-range settings of 50 and 100 Gauss, with zero volts applied to the sweep input, the maximum field deviation seen was 25 mG. This change corresponds to 7 parts per million in the measured frequency. Considering the manual method of adjusting the frequency of the gaussmeter, this error may not be significant. The error value is about 25 times larger than the value reported by Glarum [GL73]. With a voltage input of +5 volts, the maximum field excursion detected was 35 mG.

Fieldial Error Signal

After a new magnetic field has been selected by the computer, it is necessary to know when the Fieldial has established the correct field. The best approach to this problem is to insert a tracking gaussmeter into the field and monitor the field strength until it stabilizes; however, such a gaussmeter was not available. An indirect approach to determining the field stability is to monitor the Fieldial internal error signal. The error signal was experimentally determined to be an AC signal with an average voltage near zero when the Fieldial is at null.

The small AC signal and its common are superimposed on a constant -58 volt signal. When the field is changed, information appears on both the common and signal lines so it was necessary to compare both signals with a differential amplifier to obtain a valid result. The circuit built to process the error signal to produce a signal useable by the computer is show in Figure 6-4.

The differential amplifier is an Analog Devices AD521J instrumentation amplifier. The error signal and common are capacitively coupled to the inputs of the amplifier to remove the -58 volt offset that is only present when the Fieldial power is switched ON. Diodes to the power supply of the instrumentation amplifier protect its inputs when the Fieldial is being used without the computer for control. The output is connected both to a comparator and to a half-wave rectifier circuit. The output of the half-wave rectifier is divided to ensure that the voltage does not exceed the maximum limit of the ADC input (± 5 volts). The $1\text{ M}\Omega$ resistor shown connected to the output terminal is the terminating input resistance of the ADC in the computer. The analog output is not filtered enough to be a smooth DC signal but contains a component of the 1290 Hz excitation signal that is used to generate the error signal. Therefore, random sampling of the signal with the analog-to-digital converter might never yield several points in a row with the same value. It was necessary to add a comparator with a variable trigger threshold to the amplifier output to generate a clock pulse to control data acquisition. The period of the clock signal is approximately 0.38 ms. To keep the comparator from ringing as it changes states, it was necessary to add hysteresis to the comparator. The comparator output is connected to a Schmitt trigger input on the laboratory peripherals panel of the computer and used as a

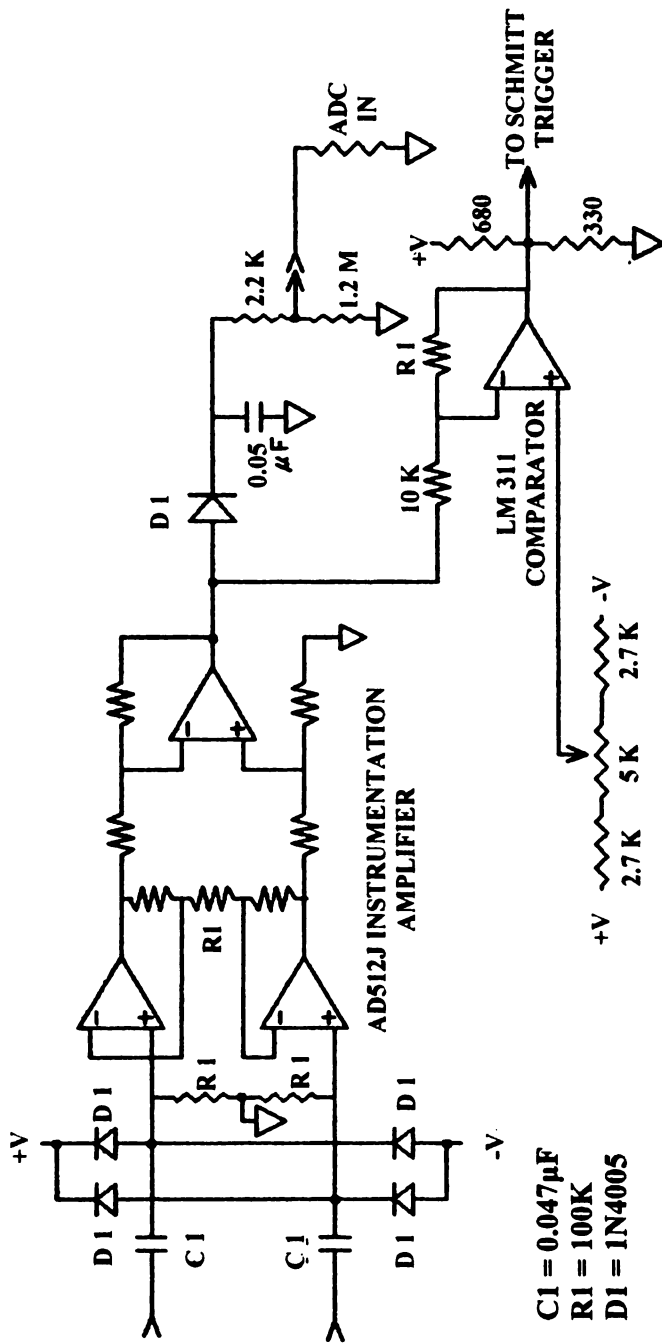


Figure 6-4: The computer interface to the Fieldial internal error signal.

hardware start for the ADC. To display the error signal when the magnetic field is suddenly changed, a minor variation of the program TIMDA (TIMed Data Acquisition) changes the DAC output, which causes the magnetic field to change and immediately starts to acquire data from the error signal output. Three examples of the error signal resulting from an instantaneous change in the selected field are shown in Figure 6-5. Figure 6-5a was recorded after a 500 G increment while a scan-width range of 1 kG was selected. The noise level at the 1 kG scan width is considerably higher than the noise at the 500 G scan width selected for the other two plots. This is probably due to noise on the DAC sweep signal and modulator electronics since at the 1 kG setting, the Fieldial is more sensitive to small changes in the reference signal than it is at smaller scan widths. Figure 6-5b is the result of a 250 G increment at a 500 G sweep-range setting. The final plot (6-5c), is a 5 G change at the 500 G sweep-range setting. A 5 G increment is larger than a normal change of field when recording a spectrum. The large change in the first two plots could be the result of jumping from one end of the sweep range to the other to repeat a scan or to initialize the field before starting a scan. A subroutine called ERRSUB (ERRor SUBroutine) is called by the main program before EPR data are taken to ensure that the field has settled. When called, subroutine ERRSUB acquires groups of 100 points, divides by 100 and compares the result to previously acquired results until three consecutive results agree to ± 1 . When null has been determined, ERRSUB returns to the calling program. The minimum time for null to be declared is 0.11 seconds. The ERRSUB approach may fail if the magnetic field change is large. In Figure 6-5a, sections of the curve are flat because the electronics in the error

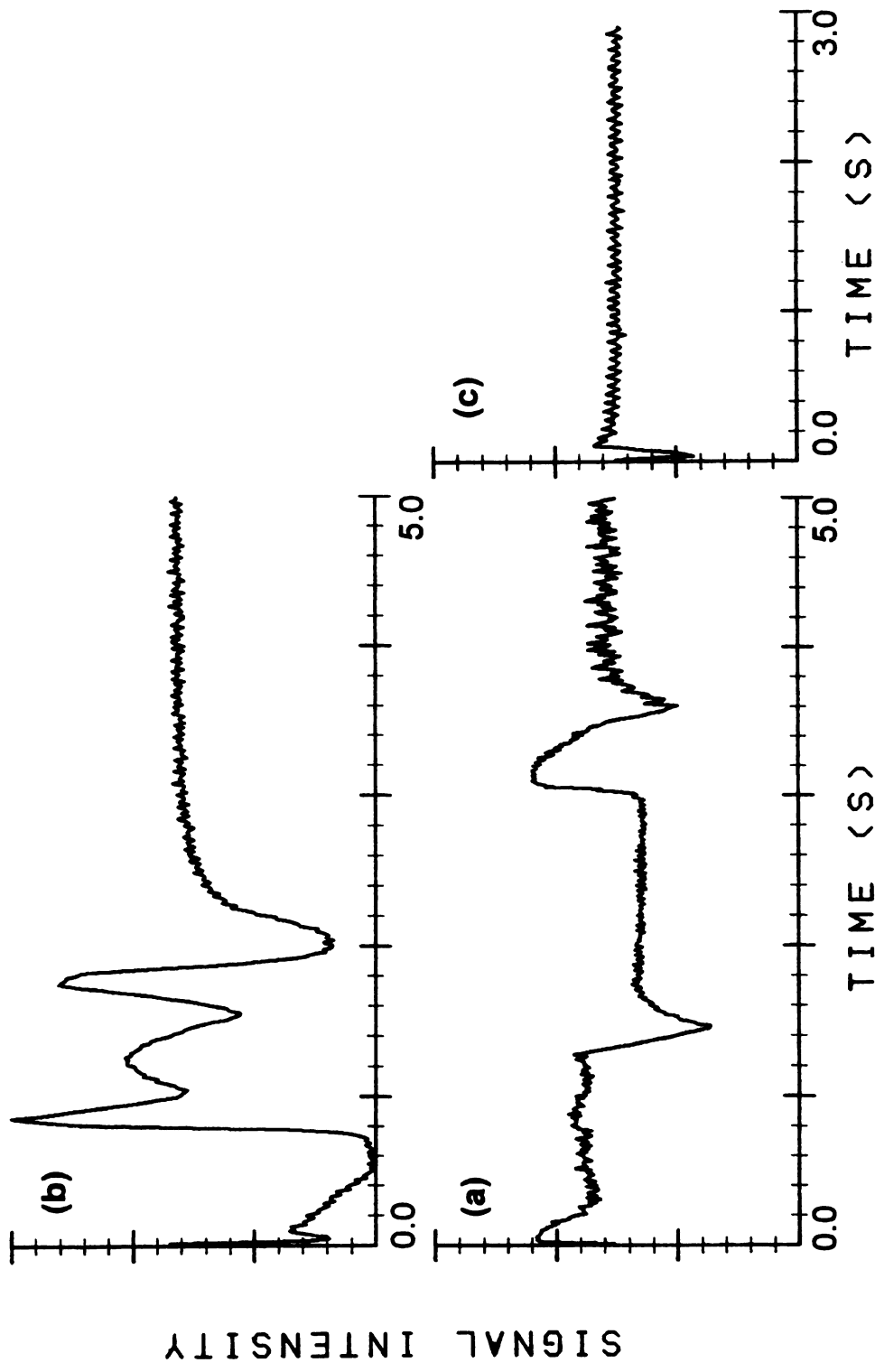


Figure 6-5: Computer-recorded error-signal data as a function of time after a magnetic field increment. (a) A 500 G increment at a 1 kG sweep range. (b) A 250 G increment at a 500 G sweep range. (c) A 5 G increment at a 500 G sweep range.

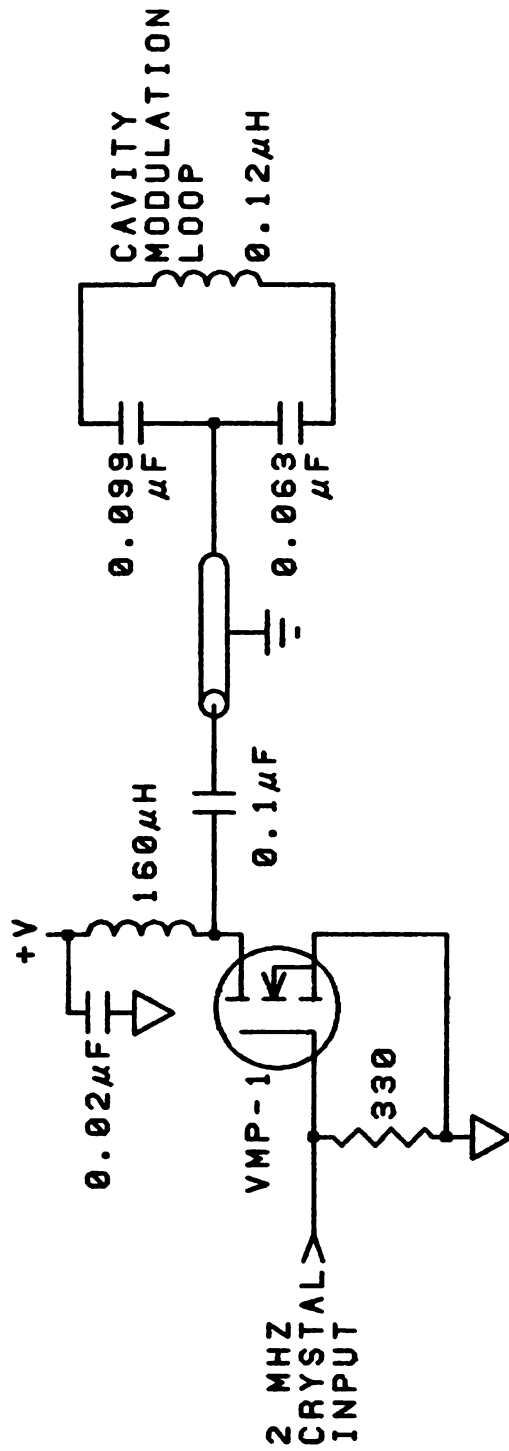


Figure 6-6: The 2 MHz power amplifier and cavity modulation loop with its associated impedance matching capacitors.

detector circuit have saturated due to the large error. These flat sections may be incorrectly interpreted by ERRSUB as null. To prevent this from happening, the starting field-strength value is always determined first through the introductory dialogue and updated immediately to allow time for the field to stabilize while the remaining parameters are specified by the operator.

The Flash Lamp

The details of the interface to the flash lamp and the tests performed on the flash lamp are discussed in detail in Chapter 5 and will not be reiterated in this chapter.

The 2 MHz Modulator

The modulation system consists of a 2 MHz crystal oscillator/preamp, a power amplifier and the modulation coil inside the microwave cavity. In Chapter 2 it was mentioned that problems developed with this system. After the Micro-Now EPR had been taken apart a few times to allow the Q-band EPR to be set up (the 2 MHz spectrometer shares the magnet, AFC, and power supplies with the Q-band instrument), it would not produce a spectrum of strong pitch. The problem was diagnosed as a lack of 2 MHz modulation in the cavity. The 2 MHz power amplifier, including the fusible output transistor, was operating; however, no measurable modulation was detected in the EPR cavity. The problem was blamed on improper termination of the coaxial cable carrying the 2 MHz

modulation to the cavity. The modulation loop in the cavity was approximately zero ohms and the coaxial cable carrying the modulation was 50 ohms. This impedance mismatch could cause a total reflection of the modulation at the junction of the cable and the modulation loop. Micro-Now dealt with this problem by supplying a specific cable to use between the power amplifier and the modulation loop that worked with the system. While it was believed that the cable being used was the original cable, something in the system had changed. Rather than experiment with Micro-Now's power amplifier and cable, the modulation system was redesigned.

The power amplifier was redesigned as show in Figure 6-6 and will no longer fuse if the output cable is accidentally disconnected while the power is ON.

To terminate the cable properly, the cavity modulation loop was used as the inductor in the tuned LC circuit shown in Figure 6-6. The capacitors establish the resonant frequency of the tuned circuit and also the input impedance of this terminator. High-Q capacitors were selected to present approximately 50-ohm impedance at the input thus terminating the coaxial cable at its characteristic impedance. The resonance frequency of the LC circuit was established by using a Texscan Model VS-40 RD sweep generator as the frequency source to drive the LC circuit. The output of the modulation coil was picked up by an antenna connected through the sweep generator to the vertical input of a scope. The sweep generator allows a marker frequency to be combined with the antenna signal to establish an absolute frequency index on the scope display. The 2 MHz crystal output from the Micro-Now EPR was chosen as the marker. The

horizontal scope input was a voltage proportional to the frequency being put out by the sweep generator. The resulting scope display looks like a bell-shaped curve with the amplitude of the antenna-coupled signal increasing to a maximum at the resonant frequency of the LC circuit. The capacitors were had selected to center the maximum of the response curve on the 2 MHz marker. The Q of the LC circuit was measured using a variable frequency marker connected to a frequency meter and measuring the width, in Hertz, of the response peak at the half-power pint ($0.707 V_p$) and dividing the central frequency by the width of the resonance peak. The measured Q was 20. Since Q is the energy stored divided by the energy dissipated per cycle, the circulating current in the tuned LC circuit will be 20 times the current arriving at the input of the circuit.

Based on the current circulating in the LC circuit, a theoretical modulation amplitude can be calculated. The modulation loop, which acts as the inductor in the LC circuit, is shown in Figure 6-7. To calculate the magnetic field intensity at the sample in the center of the modulation loop, each side of the loop can be treated as a long straight wire. The magnetic field at a distance, r , from the wire is given by [HA62]

$$\beta = \frac{\mu_0 i}{2\pi r} \quad (6-1)$$

where $\mu_0 = 4\pi \times 10^{-7}$ webers/amp-meter

r = distance in meters (6.4×10^{-3} M)

I = current in amps

Because the current is flowing in a different direction in both wires, the magnetic field at the sample is the sum of the magnet fields from both wires. This is show

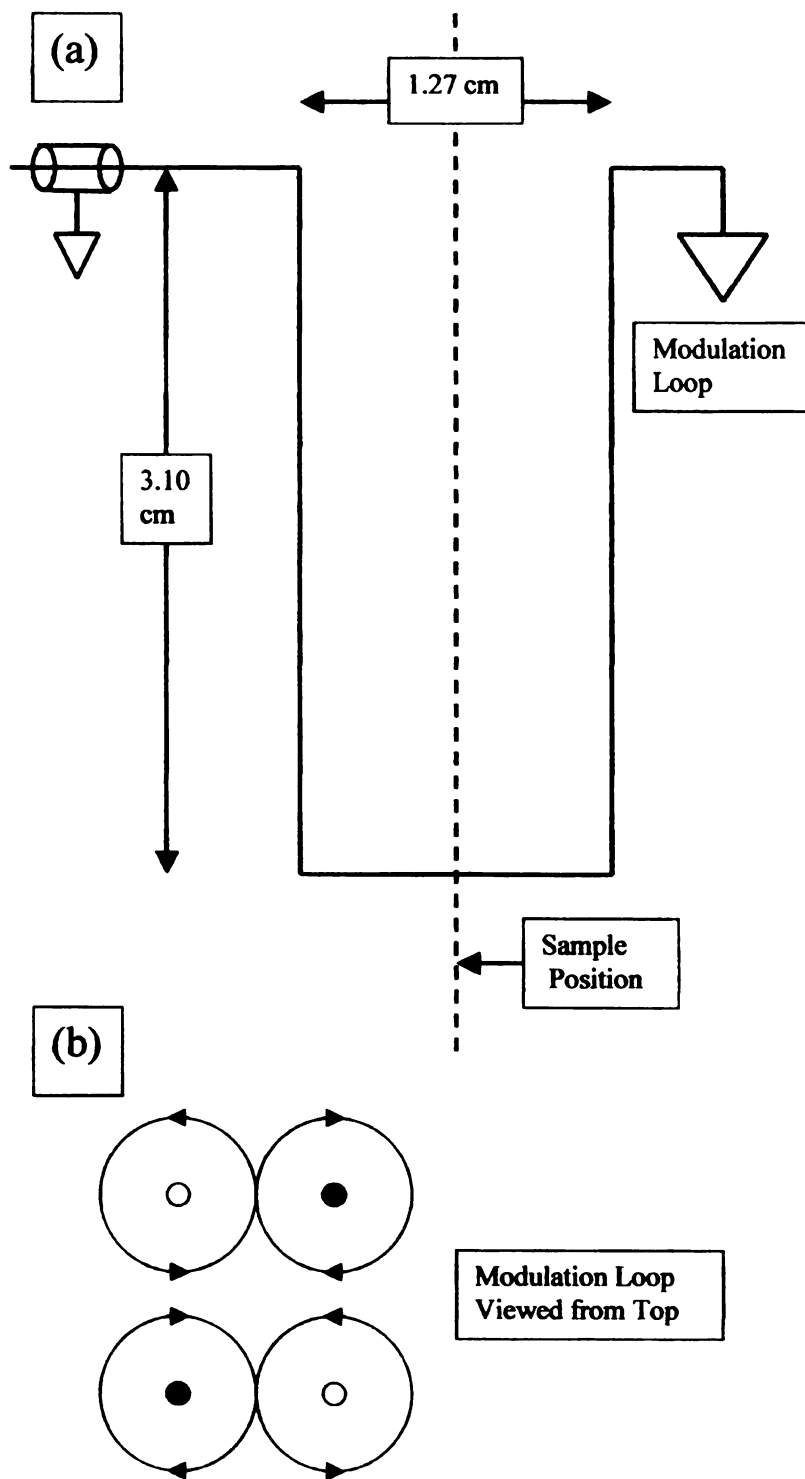


Figure 6-7: The Micro-Now internal 2 MHz modulation loop. (a) A side view showing the dimensions of the loop. (b) A top view showing the addition of the magnetic field from the individual wires.

in Figure 6-7 where a black dot represents current flowing into the page.

The current flowing through the wire was determined by measuring the voltage across capacitor C1, in Figure 6-6, with a high impedance (10 M Ω) oscilloscope and dividing by the input impedance of the circuit (50 ohms). Since the Q of the circuit is 20, the true circulating current is 20 times the current calculated on the basis of the 50 ohm input impedance.

An ammeter was placed between the power supply for the modulation power amplifier and the output stage of the amplifier. The theoretical peak-to-peak modulation amplitude, $H_{m(p-p)}$, in the cavity was calculated by the above method for many ammeter readings and a plot of calculated modulation as a function of power-supply current was made. The plot, shown in Figure 6-8, can be used to estimate the modulation amplitude in the Micro-Now cavity.

The actual modulation amplitude in the cavity can be determined by observing the effect of the modulation on the shape of a resonance line. A detailed analysis of line shapes for Lorentzian [WA61] and for Gaussian lines [SM64] revealed that a line will be broadened by modulation amplitudes greater than 0.2 times the true peak width of the resonance line. As the modulation amplitude is increased, two phenomena occur: the signal amplitude passes through a maximum when $H_{m(p-p)}$ is approximately 3.5 times the peak width for Lorentzian lines (1.8 times for Gaussian lines) and the peak width broadening increases. When the modulation amplitude is much larger than the true peak width, the measured peak width is equal to the modulation amplitude. Since the maximum calculated modulation amplitude for the Micro-Now cavity is approximately 2 Gauss, the condition requiring H_m to be much larger than the

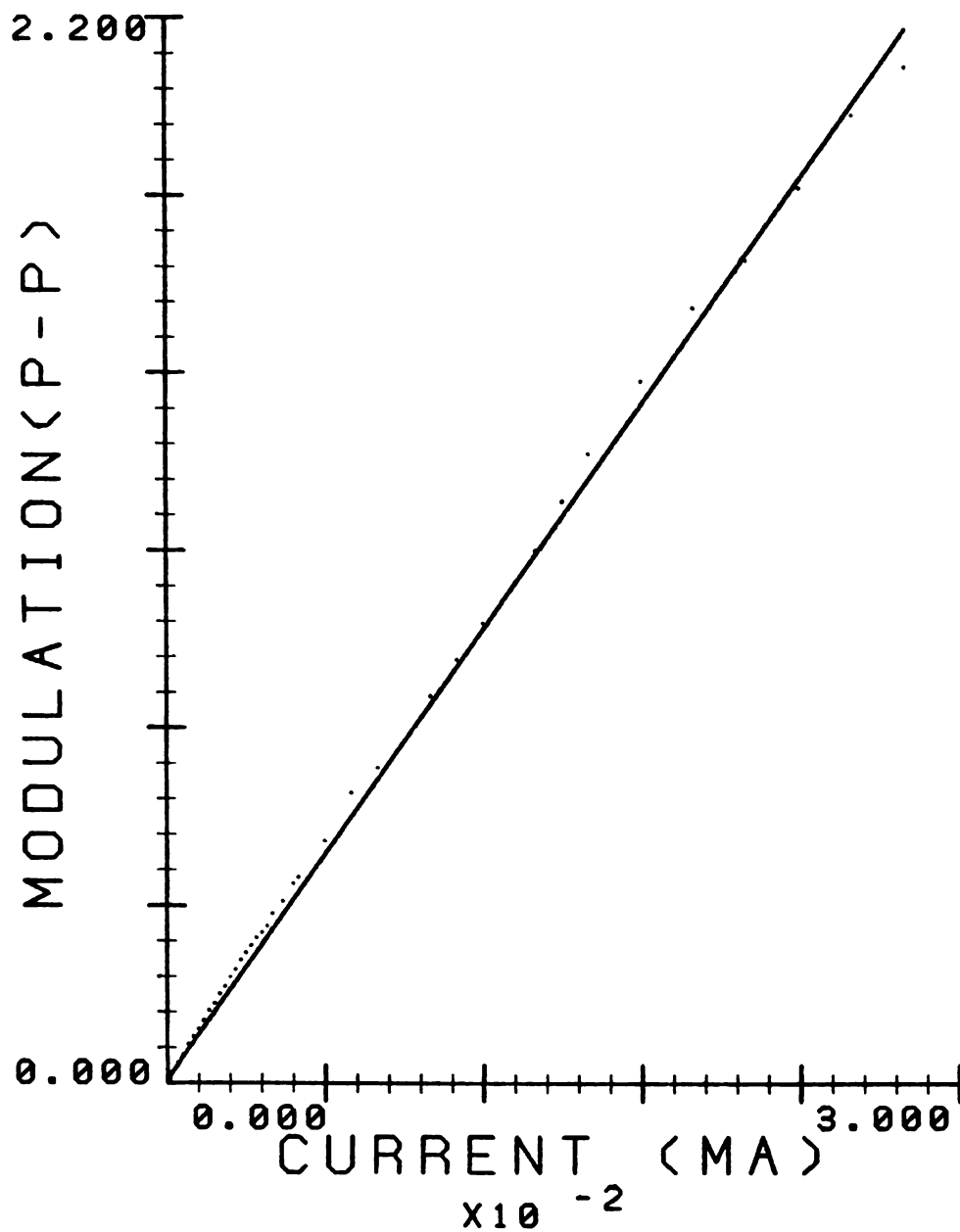


Figure 6-8: A plot of calculated $H_{m(p-p)}$ as a function of the power amplifier supply current.

peak width is difficult to fulfill. Narrow line spectra are distorted by the presence of prominent sidebands at intervals of the modulation frequency, 720mG, as discussed in Chapter 3. Lines that are broad enough not to show the effects of modulation sidebands are too broad to fulfill the condition stated above. However, attempts to over modulate diphenylpicrylhyrazyl (DPPH) with an experimentally determined line width of 1.5 G, produced peak broadening that can be used to estimate the modulation amplitude from the equations developed by Wahlquist [SW61] which evaluated the dependence of line broadening on modulation amplitude for Lorentzian line shapes. The estimated $H_{m(p-p)}$ is 3.0 G, slightly more than the 2.1 G modulation amplitude calculated with Equation 6-1.

The Modulator/Demodulator

The problems associated with the Micro-Now modulator/demodulator are discussed in Chapter 2. This section of Chapter 6 will discuss modifications made to the system with only brief descriptions of these problems.

Originally, the Micro-Now EPR output was connected to about 20 feet of 50-ohm coaxial cable and was terminated at the end by the input impedance of the PDP 8/E's ADC, which is 1 M Ω . This is not a problem with slowly varying signals observed when recording a standard EPR spectrum; however, when trying to observe a transient signal, it is important to match all impedances to prevent reflections at the interfaces which could result in erroneous results. A feed-through 50 ohm terminator was inserted at the connection between the coaxial cable and the ADC input to properly terminate the signal at the computer.

The result was that the signal acquired by the computer was reduced to practically nothing. A quick look at the circuit diagram of the source revealed a source impedance of 10 k Ω in the EPR output amplifier. The amplifier circuit show in Figure 6-9 was inserted at the EPR output to correct this problem.

The FET input operational amplifier, (National Semiconductor LH0032C) which functions as the input and amplification stage, is an ultra-fast operational amplifier configured for a gain of 23, the largest gain possible while still maintaining the required bandwidth. The National Semiconductor LH0063C is a high speed FET input voltage follower capable of continuously driving a 50-ohm load with excellent phase linearity up to 20 MHz. The 3 dB roll-off point of the combined amplifiers was 3.5 MHz. Decreasing the gain of the amplifier stage could increase the bandwidth; however, this response is sufficient for this system.

The transient response of the EPR spectrometer was suspect because the results of an experimentally determined reaction rate could not be explained by the chemistry involved. The response of the EPR was determined using the experimental setup in Figure 6-10. The ERP spectrometer was tuned and the magnetic field adjusted to the maximum of the resonance line of a standard pitch sample. The output of the 2 MHz power amplifier was connected to the local oscillator (LO) input of a Mini-Circuits Laboratory, ZAD-1 double-balanced mixer. A debounced switch applied a high or zero level signal at the IF port of the mixer. The switch also generated a time signal that could be connected to the Schmitt trigger of the computer or the trigger of a storage oscilloscope. The signal appearing at the RF port is a mixture of the LO and IF ports. When the IF signal

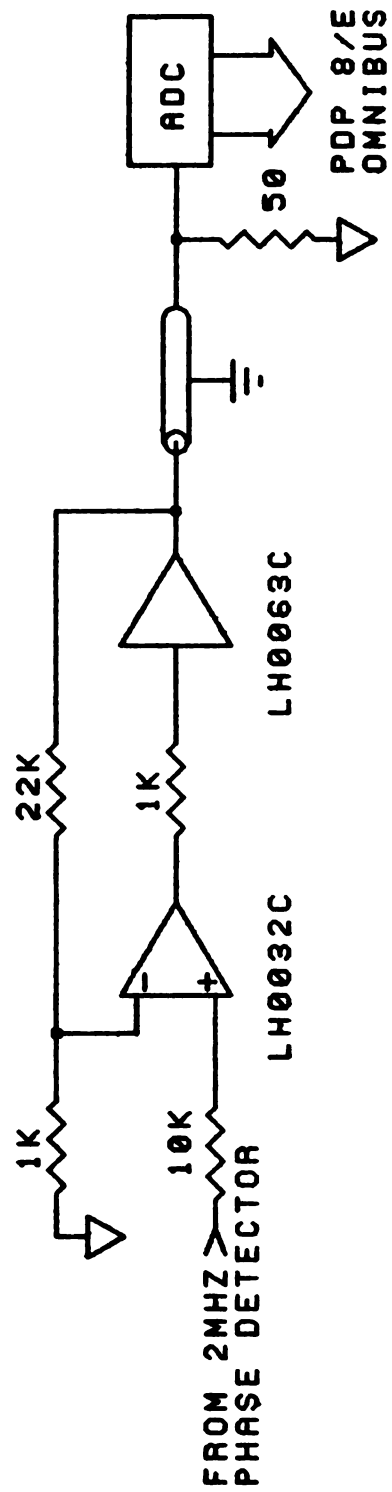


Figure 6-9: The circuit diagram of the EPR output amplifier capable of driving a 50-ohm load.

is zero, a zero signal appears at the RF output. The 2 MHz local oscillator signal is zero, a zero signal appears at the RF output. The 2 MHz local oscillator signal had to be kept below 1 volt (p-p) for the double-balanced mixer to work properly. The fall time of the signal at the RF port of the mixer after the 2 MHz modulation was switched off was 0.1 μ s. The measured time constants were greater than 10000 times longer than indicated on the front panel of the instrument (0.12 s for the 10 μ s filter position). When the capacitors in the EPR output filter were changed to select the time constants labeled on the front panel, the noise level totally swamped the demodulator electronics.

The manufacturer provided a copy of the test data from the MSU EPR take before delivery. The test data reported noise levels and signal gain at two filter values: NONE and 0.01 ms. No time response data were provided. Included with the data was a list of the eight customers who purchased the Micro-Now 2 MHz EPR. Inquiries were made to see what other customers were doing with their spectrometers. The spectrometer sold to Argonne National Laboratory eight months after the MSU model was not being used [ARGO]. F. P. Sargent [SA77] changed the cavity, extensively modified the electronics, used a higher gain preamp, changed the modulation amplifier, and has given up using it because he could not get funding for more modifications. J. K. SA. Wan [WA77] modified the system extensively but is now able to use it only for very large amplitude signals.

The circuits in the Micro-Now demodulation electronics were created on Vector board with wires soldered to the components. The wires were two and three deep in some sections of the circuit boards which is poor construction

practice for electronics operating in high frequency regions because of cross talk between wires. Decoupling capacitors, 0.1 μ F, were inserted in the power-supply lines in an attempt to remove the 2MHz signal picked up by the power supplies. This failed because the power-supply common already had 2 MHz on it. Attempts to clean up the common signal by connecting it directly to the chassis of the instrument were only partially successful.

Rather than attempt to rectify problems in the existing electronics, the decision was made to replace the Micro-Now modules with commercial and home-built equipment and compare S/N ratios to those obtained with the system configured using Micro-Now components. The noise level was determined by connecting a 50-ohm terminator to the input in place of the crystal current and measuring the noise at the output with an oscilloscope. The 2 MHz modulation output from the oscillator circuit was connected through a 0-81 dB attenuator to the crystal current input of the electronics for gain and S/N measurements.

First, a Low Noise Amplifier, LNA [A109], was compared to the Micro-Now preamplifier with the result that the signal-to-noise increased using the LNA. This was expected because the Micro-Now preamp has a frequency range of DC to greater than 7 MHz while the LNA range is limited at the low end to 70 kHz. A look at a typical noise power spectrum shows that major components of noise are $1/f$ and discrete noise and they are largest at low frequencies. The LNA is a high-pass filter and removes much of the low frequency noise. This however, did create a problem with the 10kHz AFC signal and made it necessary to parallel the two preamplifiers at the crystal current input. The Micro-Now preamp was used for the AFC signal while the LNA was used for the EPR signal. The gain of

the LNAS is 37 dB, slightly greater than the Micro-Now preamp. The next module inline was a video amp. A video amp was originally used in the circuit to allow external blanking of the EPR signal via a PIN diode switch. The video amp was not really needed because the blanking option was not included in the purchase; therefore, it was replaced with a 2 MHz narrow band filter and a 55 dB gain tuned amp, both designed locally [A105]. Placing tuned filters and amplifiers in the circuit limits the rise time of the electronics (rise time equals $0.35/\text{bandwidth}$) but in this case, the imposed limit is a worthwhile sacrifice.

The integrated circuit demodulator, Motorola MC1596L, and associated electronics were replaced by a Mini-Circuits Laboratory, ZAD-1 double-balanced mixer. This phase detector requires the input signal amplitude to be less than $1 V_{(p-p)}$ to prevent clipping, which imposes a definite limit on the amount of amplification that can be achieved while the signal is encoded in the 2 MHz carrier. Amplification at the carrier frequency allows discrimination of noise at other frequencies at the time it is phase detected since only signals near and in phase with the reference signal will pass the phase detector. To obtain the same size signal with the new demodulation as compared to the integrated circuit demodulator, DC amplification had to be added to the final output stage (see Figure 6-9). The local oscillator input to the double-balanced mixer is supplied by the Micro-Now 2 MHz reference and phase shifter circuits with minor modifications to improve the rise-and-fall times of the integrated circuit phase-lock loop in the output of phase-shifter circuit.

The results of final tests of the electronics revealed that an input signal level of $3.4 \mu V_{(p-p)}$ produced a 1 V output with a S/N of 1 using a true 10 μs filter.

The S/N of the 3 and 100 μ s filters are 0.8 and 2.5 respectively at the same input signal level. The final time constant test revealed a minimum time constant of 3 μ s. This severely limits the usefulness of the EPR for transient radical studies. These results are based only on electronic noise and do not take into account any noise generated in the klystron, diode detector, or microwave cavity.

The Microwave Cavity

The Micro-Now cavity has several drawbacks that were discussed in Chapter 2. The most serious problem is that the magnetic resonance peak drifts slowly during low temperature experiments using a quartz dewar. The problem is believed to be caused by the cavity's internal modulation loop. If an internal modulation loop is used in a microwave cavity, extreme care must be taken to avoid interactions between the metal wire and the electric field component of the microwave. Such interactions would cause serious loss of microwave energy and according to Equation 2-1, a drop in the cavity Q. A decrease in cavity Q not only causes a decrease in signal power (Equation 2-3), but also decreases the effectiveness of the AFC circuitry.

To minimize the effects on cavity Q, internal wires must be oriented perpendicular to the E field or must pass through a region where the E field is zero [AL68g]. A diagram of Micro-Now's modulation coil is shown in Figure 6-7. The coil is a single piece of wire passing perpendicularly through the E field to the bottom of the cavity where it is bent out into the E field to go around the sample and a quartz dewar and then passes back up through the E field. The

position of this wire does not have a detrimental effect on cavity Q, which was measured by Professor J. Cowen [COWN] as approximately 4000. However, when a quart dewar is placed in the Micro-Now cavity, the bottom of the modulation coil is pushed into the cavity because the bend at the bottom of the coil is not large enough to go around the dewar. The modulation loop not only is not longer perpendicular to the E field, but it is also no longer perpendicular to the sample.

When working with resonance lines that are 200 to 300 mG wide, such as the solvated electron peak, it is important that the resonance peak does not drift during the entire period of the experiment. To determine if the Micro-Now cavity was the cause of the signal drifting, another 2 MHz cavity was constructed. Rather than start from scratch, permission was obtained to modify a Varian Model E-236 Bimodal cavity (Q of 7000) as long as nothing irreversible was done to it.

Smith et al. [SM77] had success reconnecting the modulation coils of a Varian E-4531 cavity in parallel from the original serial configuration and series resonating the coils at 1 MHz. This approach was not taken because of the need to cut and solder wires connecting the modulation coils. The Varian coils could not be resonated at 2 MHz in the standard configuration. The inductance of the Varian modulation coils, measured with an inductance bridge (Boonton Radio Corp. Model 260-A), is 3.7 mH. It would require a series capacitance of 1.7 pF to resonate such a coil at 2 MHz. Stray capacitance in the cables is much greater than this value.

Since the modulation coils could not be used at 2 MHz and the side walls of the Varian cavity were too thick to allow 2 MHz electromagnetic radiation to pass through, they were removed. The side walls were replaced with pieces of G-10 circuit board with a 0.2 mil copper foil epoxied to the inside surface. The skin depth of 2 MHz in copper is 1.8 mils; therefore, 0.2 mil copper foil should not attenuate the 2 MHz modulation to a great extent. The copper foil is, however, greater than the required 5 times the skin depth of the microwave frequency and thus prevents the loss of the microwave through the walls. Copper is an excellent conductor; therefore, the resistive losses in the cavity walls will not increase and the cavity Q should not be affected by changing the walls. To verify this, spectra of a standard sample were obtained with the Varian cavity and 100 kHz modulation before and after the cavity walls were changed. No noticeable degradation of the signal amplitude occurred. Helmholtz coils were wrapped in Plexiglas supports and tuned to 2 MHz. The magnetic field, B, in the center of a set of Helmholtz coils is given by [WI55]

$$\beta = \frac{\mu_0 N I r^2}{(r^2 + \chi^2)^{3/2}} \quad (6-2)$$

where μ_0 is the permeability of free space (1.26×10^{-6} Weber/amp-m), I is the current in amps, r is the radius of the coil, N is the number of turns, and χ is the distance to the center of the Helmholtz coil pair. Unfortunately, this coil arrangement did not produce a spectrum of a standard sample, pitch.

Professor K. M. Chen [CHEN], a microwave specialist in the MSU Electrical Engineering department, suggested that the skin depth of the cavity walls is not the only consideration when you have a finite wall size. The flux lines

passing through the coil must return outside of the cavity and since the cavity is heavy metal everywhere else, the metal outside of the cavity probably attenuated the modulation. Even though Helmholtz coils provide the most homogeneous magnetic field of any coil arrangement, they appear to be of little use at 2 MHz when a metal cavity is used. Possibly constructing a non-metallic cavity for use with Helmholtz coils would solve this problem. Although there was interest in building a non-metallic cavity from a machinable ceramic [PO67d, LA59, CO64], time did not permit such a task. The only remaining coil configuration was an internal modulation loop. The best approach to implementing internal modulation coils is to drill a couple of holes in the top and bottom of the cavity and pass a heavy-gauge wire straight through the cavity without bends. The loop would be continued by connecting the two wires outside of the cavity, avoiding interactions with the microwave field. The wires are supported at both ends of the cavity, which helps to eliminate microphonics that would be present with a coil supported only at one end, such as the loop in the Micro-Now cavity. Because EPR cavities are extremely expensive, drilling holes in an excellent Varian cavity was forbidden. The only opening already in the cavity that could be used to ring wires into this cavity is the cylindrical opening at the top of the cavity provided for the introduction of a sample and dewar. Since a dewar was required for most of the experiments that were planned, a quartz dewar was used as the support for the coil. Since there is not much room between the dewar and the cavity, a small gauge magnet wire had to be used for the modulation loop. The wire was glued down the front and back of the dewar, and the entire assembly was inserted into the Varian cavity. There are, unfortunately, two problems with

this arrangement. A large modulation amplitude requires a lot of current in the wire, but 28-gauge wire has a significant amount of resistance. Also, the wire is in physical contact with the metal cavity for the entire length of the neck of the cavity (1.25 inches), which results in capacitive coupling of the 2 MHz signal to the cavity and attenuation of the modulation signal. Because of these two problems, the Q of the tuned LC circuit containing the modulation loop was measured as 2. The maximum calculated modulation at the sample was 0.5 G(p-p). Even though the modulation amplitude in the modified Varian cavity is significantly less than the modulation in the Micro-Now cavity, the problem of the drifting resonance peak was removed. The modified Varian cavity was used for all of the low temperature experiments.

APPENDIX

APPENDIX A

Program Listings

The computer programs for instrument control and data acquisition are just as important as the hardware that the computer controls. Thus Appendix A contains commented listings of the main programs that were used to control the instrument and acquire and display the data.

The programs are written in FORTRAN II with in-line inclusion of machine assembly language (SABR) statements. The program statements with an "S" in column one are SABR instructions and are ignored by the FORTRAN compiler.

FILE NAME: EPRMON.FT

```
C      FILE NAME: EPRMON.FT
C
C      ESR DATA ACQUISITION MONITOR
C
C      ALL PROGRAMS ARE WRITTEN AS SUBROUTINES CORESIDENT IN CORE
C      AND CALLED BY MONITOR AFTER SELECTING THE OPTION YOU WISH
C      TO USE.  IF THE PROGRAM IS TOO LARGE TO BE CORESIDENT I.E.
C      DATMON.FT, IT IS LOADED BY A FORTRAN CALL TO CHAIN.  THE
C      PROGRAM MUST BE IN A SAVED FILE ON THE SYSTEM DISK (*.SV).
C      THE VARIABLES IN COMMON IS NOT DISTURBED IN THE CHAIN OPERATION
C      SINCE ALL PROGRAMS HAVE THE SAME COMMON STATEMENT.
C
C      PROGRAMMER: TIMOTHY G. KELLY   OCT. 16, 1975
C      MODIFIED JUNE 13, 1976
C
C      COMMON IADRES, NUMINC, IDATPT, NSCAN, IDELAY, NPTS, ITIME, NAVE, BASE,
C      ISIGMA, IKINSP, YDATA, TIMPPT, NBASE, ISTART, INCREM
C      DIMENSION YDATA(1024)
C
C      100  FORMAT(1X, '1 = EXIT, 2 = ACQUIRE, 3 = DISPLAY, 4 = STORE,
C          15 = FETCH'/' 6 = SETUP, 7 = DATMON')
C      101  FORMAT(' : ', 15)
C      102  FORMAT(1X, '1=ESR SCAN, 2=TIMED DATA ACQUISITION')
C      103  FORMAT('PROMPT? ', A1)
C
C      ENTRY POINT
C
C      1      READ(1, 103) IY
C      S      TAD \IY
C      S      TAD CIAI
C      S      SZA CLA
C      S      JMP \2
C          WRITE(1, 100)
C      2      READ(1, 101) IA
C      3      GO TO (10, 20, 30, 40, 50, 60, 90) IA
C
C      EXIT TO OS/8 MONITOR
C
C      10     CALL EXIT
C
C      CALL DATA ACQUISITION PROGRAM
C
C      20     WRITE(1, 102)
C          READ(1, 101) IKINSP
C          GO TO (70, 80) IKINSP
C
C      DISPLAY DATA ON STORAGE SCOPE
C
C      30     CALL SCPLLOT
C          GO TO 1
C
C      OUTPUT DATA
C
C      40     CALL STORE(2)
C          GO TO 1
C
C      READ DATA FILE INTO CORE
C
C      50     CALL FETCH(1)
C          GO TO 1
C
C      SETUP.FT IS A RAPID SCANNING, FAST DISPLAYING PROGRAM TO
C      HELP OPTIMIZE INSTRUMENTAL PARAMETERS
C
```

EPRMON.FT, CONT'D.

```
60      CALL CHAIN('SETUP')
        GO TO 1
C
C      EPRSCN.FT IS USED TO OBTAIN EPR SPECTRA
C
70      CALL CHAIN('EPRSCN')
C
C      TIMEDA.FT IS A TIMED DATA ACQUISITION PROGRAM
C
80      CALL CHAIN('TIMEDA')
        GO TO 1
C
C      DATMON.FT IS ANOTHER MONITOR LIKE EPRMON.FT USED FOR DATA
C      MANIPULATION
C
90      CALL CHAIN('DATMON')
SCIAY, 4640      /ASCII CODE FOR Y IN A1 FORMAT + CIA
        END
```


EPRSCN.FT, CONT'D

```

GO TO 10
SNOREM, MQA CLA /LOAD MQ INTO AC
S DCA INCR
READ(1,300)NAVE
300 FORMAT('NUMBER OF AVERAGES/POINT ',15)
S TAD \NPTS /SET UP POINTS COUNTER
S CIA
S DCA \IDATPT /IDATPT IS -NPTS
S TAD \NAVE /SET UP AVERAGE COUNTER
S CIA
S DCA IAVE /IAVE IS -NAVE
S TAD (2216 /ADDRESS OF LAST 2/3 OF YDAT(1)
S DCA \IADRES
S TAD \IADRES /GET ADDRESS POINTER FROM COMMON
S DCA STORE
S TAD \IDATPT /GET -NPTS FROM COMMON
S DCA NUMPTS
S TAD XCOUNT
S JMP FIELD
SINGFLD, TAD MAGFLD
S TAD INCR
SFIELD, DILX /LOAD X CHANNEL DAC TO CONTROL
S /MAGNETIC FIELD
S DCA MAGFLD
S DCA HIGH /INITIALIZE LOCATIONS HIGH AND LOW
C DCA LOW
C CALL ERRSUB - MAGNET NULL DETECTION PROGRAM
C
S CALL ERRSUB
S CLA CLL /BE SURE AC IS ZERO
S ADCL /CLEAR ADC FLAGS AND REGISTERS
S TAD (3
S ADLM /LOAD MULTIPLEXER 3, CLEAR AC
S TAD IAVE /GET -NAVE FROM COMMON
S DCA NUMAVE
SCETMOR, ADST
SABC, ADSK /SKIP ON A/D DONE
S JMP ABC
S ADRB /READ A/D BUFFER ,CLEAR DONE FLAG
S ADSE /SKP ON ADC TIMING ERROR
S SKP
S JMS ERR
S SMA /CHECK FOR NEGITIVE NUMBER
S JMP NOTNEG /NO
S TAD LOW
S DCA LOW
S SZL /CHECK FOR OVERFLOW
S JMP TCOMP
S CLA CMA /SIGN EXTEND THROUGH UPPER WORD
S TAD HIGH
S DCA HIGH
S JMP TCOMP
SNOTNEG, TAD LOW /NUMBER IS POSITIVE
S DCA LOW
S SZL /CHECK FOR OVERFLOW
S ISZ HIGH /PLACED HERE TO NULLIFY ISZ
STCOMP, 7000
S CLL
S ISZ NUMAVE
S JMP GETMOR
S 6211 /CHANGE TO DATA FIELD 1
S TAD LOW
S IDCA STORE /AUTO INDEX REGISTER
S TAD HIGH
S IDCA STORE
SDATFLD, 6201 /CHANGE TO DATA FIELD 0
S ISZ NUMPTS /INCREMENT THE MAG FIELD?

```

EPRSCN.FT, CONT'D

```
S      JMP INCFLD          /YES
      CALL FLOTDB
      TIMPPT=0.
      CALL CHAIN('EPRMON')
SCONVRT,1000
SNUMAVE,0
SNUMPTS,0
SIAVE, 0
SXCOUNT,7000          /-5 VOLTS FOR 10 BIT DAC
S INCR, 0
SMACFLD,0              /INCREMENTED NUMBER FOR MAG FIELD
SADCEN, 0000
S HIGH, 0
S LOW, 0
S ERR, 0
      WRITE(1,500)
500    FORMAT(1X,'A/D TIMING ERROR')
      CALL EXIT
S ERR2, 0
      WRITE(1,600)
600    FORMAT('DIVIDE ERROR')
      CALL EXIT
      END
```

FILE NAME: DATA.FT

SUBROUTINE DATA

FILE NAME: DATA.FT

ESR ACQUISITION PROGRAM-KINETIC DATA

THIS SUBROUTINE WAS WRITTEN TO PERFORM DATA ACQUISITION UNDER THE CONTROL OF THE DKB-EP PROGRAMMABLE REAL-TIME CLOCK. WHEN THIS ROUTINE IS CALLED, IT TAKES NUMPTS (VARIABLE NAME) NUMBER OF POINTS AT A TIME INTERVAL SET BY THE CLOCK. THE MINIMUM TIME BETWEEN POINTS IS 25 USEC USING THE ADG-EA A/D CONVERTER.C THE DATA POINTS ARE DEPOSITED IN THE ARRAY YDATA(1024) IN COMMON. ALL INDEXES AND PARAMETERS MUST BE SETUP BY THE CALLING PROGRAM.

ALL ARGUMENTS ARE PASSED THROUGH COMMON

SPECIAL LOADING INSTRUCTIONS!

THIS SUBROUTINE MUST BE LOADED INTO FIELD ZERO. THIS IS REQUIRED BECAUSE THERE MAY NOT BE TIME TO READ THE DATA FIELD AND SETUP A RETURN TO THAT DATA FIELD BEFORE THE A/D CONVERTER HAS THE FIRST DATA POINT; THEREFORE, THE ROUTINE ASSUMES THAT IT IS IN FIELD 0.

PROGRAMMER: TIMOTHY G. KELLY AUG. 8, 1976

COMMON IADRES, NUMINC, IDATPT, NSCAN, IDELAY, NPTS, ITIME, NAVE, BASE, ISIGMA, IKINSP, YDATA, TIMPPT, NBASE, ISTART, INCREM DIMENSION YDATA(1024)

ABSOLUTE SYMBOL DEFINITION

ABSYM	NUMPTS	174	/PAGE 0 ADDRESS
ABSYM	MCOUNT	175	/PAGE 0 ADDRESS
ABSYM	XPONTR	130	/PAGE 0 ADDRESS
ABSYM	POINTR	17	/AUTO INDEX REGISTER
ABSYM	YPOINT	16	/AUTO INDEX REGISTER

ENTRY POINT

6211	/CHANGE TO DATA FIELD 1
CLA CLL	
SGETHOR, ADSK	/SKIP ON A/D DONE
S JMP GETHOR	
S ADRB	/READ A/D BUFFER, CLEAR DONE FLAG
S ADSE	/SKIP ON A/D ERROR FLAG
S SKP	
S JMS ERR	
S IDCA POINTR	/DEPOSIT DATA IN FIELD 1
S ISZ NUMPTS	/HAVE I TAKEN ALL THE DATA POINTS?
S JMP GETHOR	/NO, GETHOR!
S 6201	/RETURN TO DATA FIELD 0
S RETURN	
SERR,	0
500	WRITE(1,500)
	FORMAT(1X, 'A/D TIMING ERROR')
	CALL EXIT
	END

ERRSUB.FT, CONT'D.

S	TAD CLKENB	/LOAD CLOCK ENABLE WORD INTO AC
S	CLOE	/SET AC INTO CLOCK ENABLE REGISTER
S	CLA CLL	
S	SOVER2, CLSK	
S	JMP OVER2	
S	TAD (8777)	/STOP CLOCK AND CLEAR CLK
S		/EXT. START ENABLE
S	CLZE	
S	CLA CLL	
S	SADC, ISZ CHKFLG	/THIS SELF RESTARTING OPTION IS NEEDED
S	SKP	/TO OVERCOME INADQUICIES IN DEC
S	JMP CONTIN	/HARDWARE
S	ADSK	/SKIP ON A/D DONE
S	JMP ADC	
S	ADRB	/READ A/D BUFFER ,CLEAR DONE FLAG
S	ADSE	/SKIP ON A/D ERROR FLAG
S	SKP	
S	JMS ERR	
S	TAD CONVRT	/CONVERT 10 BIT 2'S COMPLIMENT TO BINARY
S	CLL	
S	TAD LOW	/DOUBLE PRECISSION ADD
S	SZL	
S	ISZ HIGH	/INCREMENT HIGH ORDER BITS
S	ISZ NUMAVE	/HAVE I AVERAGED ENOUGH POINTS?
S	JMP GETHOR	/NO
S	CLL	/CLEAR LINK-MUST BE CLEAR BEFORE DIVISION
S	SDIVIDE,MQL	/AC TO MQ
S	TAD HIGH	/MOST SIGNIFICANT BITS
S	DVI	/DIVIDE
S	SDIVSOR,144	/DIVISOR=100
S	SZL	/TEST FOR DIVIDE ERROR
S	JMS ERR2	
S	SWP	/AC TO MQ, MQ TO AC
S	DCA \NUMBER	
S	NUM(I)=NUMBER	
S	CMA	/SET AC=-1
S	TAD \I	
S	SZA	/I-1=0?
S	JMP POS	/NO
S	TAD (5	
S	SPOS, DCA \J	
S	ITEST=NUM(J)	
S	TAD \NUMBER	
S	CIA	
S	TAD \ITEST	/AVERAGE MUST BE WITHIN +/-1
S	SFA	
S	JMP NEG	
S	TAD (7777	/-1
S	SMA SZA	/AC WAS=1 OR 0, MEETS REQUIREMENTS
S	JMP INCI	/OUTSIDE OF LIMITS
S	JMP OK	
S	SNEG, TAD (1	
S	SMA CLA	
S	JMP OK	
S	JMP INCI	
S	SOK, CLA CLL CMA	/SET AC=1
S	TAD \J	/DECREMENT J
S	SZA	
S	JMP NO	
S	TAD (4	
S	SNO, ISZ XPONTR	/MUST HAVE 3 AVERAGES EQUAL
S	JMP POS	
S	RETURN	
S	SHIGH, ●	
S	SLOW, ●	
S	SNUMAVE,●	
S	SCONVRT,1000	/CONVERT 10 BIT 2'S COMPLIMENT TO BINARY
S	SCLKENB,4661	/OVERFLOW+MODE 00+1 MEZ+EXT. START
S		/AND CLOCK INHIBIT+EVENT1

ERRSUB.FT, CONT'D.

```
SADCENB,0200          /ADC ENABLE EXTERNAL START
S ERR,                0
                    WRITE(1,500)
500  FORMAT(1X,'A/D TIMING ERROR')
    CALL EXIT
SERR2,                0
600  WRITE(1,600)
    FORMAT(1X,'DIVIDE ERROR')
    CALL EXIT
    END
```

FILE NAME: FLOTDB.FT

SUBROUTINE FLOTDB

SUBROUTINE FLOTDB.FT

THIS PROGRAM WAS WRITTEN TO FLOAT DOUBLE PRECISION INTEGERS,
 USING THE EXTENDED ARITHMETIC ELEMENT (EAE). THE DOUBLE
 PRECISION INTEGERS ARE STORED IN THE LAST 2/3 OF THE
 ARRAY YDATA(1024). THIS ROUTINE REMOVES THE DOUBLE
 PRECISION INTEGER, FLOATS IT, AND STORES IT AS 3 WORDS
 STARTING AT THE FRONT OF THE ARRAY.
 REAL DATA ON THE B/E IS STORED IN 3 WORDS (36 BITS).
 BIT 0 = SIGN BIT (0 IS POSITIVE, 1 IS NEGATIVE)
 BITS 1-8 = EXPONENT + 200 OCTAL
 BITS 9-35 = MANTISSA

COMMON IADRES, NUMINC, IDATPT, NSCAN, IDELAY, NPTS, ITIME, NAVE, BASE,
 ISICHA, IKINSP, YDATA, TIMPPT, NBASEISTART, INCREM
 DIMENSION YDATA(1024)

ABSOLUTE SYMBOL DEFINITIONS

ABSYM	NUMPTS	132	/PAGE 0 ADDRESS
ABSYM	XCOUNT	17	/AUTOINDEX REGISTER
ABSYM	XPONTR	16	/AUTOINDEX REGISTER
ABSYM	POINTR	131	/PAGE 0 ADDRESS

ENTRY POINT

TAD	\NPTS	
CIA		/SET UP LOOP
DCA	NUMPTS	
TAD	(216	/ADDRESS OF YDATA IN COMMON-1
DCA	XCOUNT	
TAD	(2216	/ADDRESS OF INTEGERS IN COMMON-1
DCA	XPONTR	
TAD	DATFLD	
RDF		/OR DATA FIELD INTO AC
DCA	DATFLD	/SETUP DATA FIELD FOR RETURN
SCETMOR,	6211	/CHANGE TO DATA FIELD 1
ITAD	XPONTR	
NQL		/AC TO MQ, 0 TO AC
ITAD	XPONTR	
NMI		/NORMALIZE-EAE INSTRUCTION
DCA	TEMP1	
TAD	TEMP1	
AND	(4000	/GET SIGN OF NUMBER
DCA	WORD1	
TAD	WORD1	
SNA	CLA	/CHECK FOR NEGATIVE NUMBER
JMP	POS1	
TAD	TEMP1	/YES, IT IS NEGATIVE
SWP		
CLL		
CIA		/CREATE 2'S COMPIMENT OF THE DOUBLE
SWP		/PRECISION INTEGER
CMA		
SZL		/CHECK FOR A CARRY FROM CIA OF LOW WORD
IAC		/INCREMENT HIGH WORD
DCA	TEMP1	
SPOS1,	SCA CLA	/STEP COUNTER CONTAINS NUMBER OF SHIFTS
CIA		
TAD	(27	/EXPONENT IS 27(OCTAL) - NUMBER OF SHIFTS
TAD	(200	

FLOTDB.FT, CONT'D.

```

S      AND (377           /EXPONENT IS STORED AS EXPONENT+200(8)
S      CLL               /MAKE SURE LINK = 0
S      RTL;RAL
S      TAD WORD1
S      DCA WORD1         /WORD1 NOW HAS SIGN AND EXPONENT
S      TAD TEMP1
S      AND (3400         /GET FIRST 3 BITS OF MANTISSA
S      BSW
S      CLL               /MAKE SURE LINK=0
S      RTR
S      TAD WORD1
CS     6211
S      IDCA XCOUNT     /AUTOINDEX REG.
CS     6201
S      TAD TEMP1
S      AND (377         /GET REMAINING 8 BITS FROM WORD1
S      RTL;RTL         /LEFT JUSTIFY BITS
S      DCA WORD1
S      SWP
S      DCA TEMP1
S      CLL
SPOS2, TAD TEMP1
S      AND (7400         /GET 4 BITS TO COMPLETE WORD 2
S      BSW               /MOVE BITS 0-3 INTO POSITIONS 8-11
S      RTR
S      TAD WORD1
CS     6211
S      IDCA XCOUNT
CS     6201
S      TAD TEMP1
S      AND (0377        /GET REMAINING 8 BITS
S      RTL;RTL         /LEFT JUSTIFY
CS     6211
S      IDCA XCOUNT
SDATFLD,6201
S      ISZ NUMPTS
S      JMP GETMOR
      RETURN
STEMP1, 0
SWORD1, 0
      END

```

FILE NAME: STORE.FT

SUBROUTINE STORE(MODE)

FILE NAME: STORE.FT

SUBROUTINE TO OUTPUT A DATA FILE TO STORAGE DEVICE IN
C.G.E.CO. STANDARD FILE FORMAT. FIRST TWO CHARACTERS
ARE CONTROL CHARACTERS.

; = COMMENT
HD = HEADER (FILE NAME, DATE, YOUR NAME)
IN = INTEGER DATA (I5 FORMAT)
RD = READ DATA (E15.8 FORMAT)
AS = ASCII DATA (A6 FORMAT)
ED = END DATA FILE

DATA ARE WRITTEN WITHOUT THE X DATA POINTS IN ALL THREE FORMATS
IN ORDER TO SAVE SPACE ON THE OUTPUT DEVICE. THE X DATA POINTS
WILL BE ADDED TO THE DATA FILE ON THE PDP 11/40 WHEN IT IS READ
IN USING DATMON.LDA UNDER DOS/BATCH.

AN 'AS' DATA FILE REQUIRES THE LEAST SPACE ON THE STORAGE DEVICE
AND IS BY FAR THE FASTEST FORM OF OUTPUT. HOWEVER, THIS FILE
FORMAT HAS THE DISADVANTAGE OF HAVING TO BE TRANSLATED BEFORE
YOU CAN READ THE VALUES OF THE POINTS.

THIS PROGRAM IS USED IN TWO MODES.

MODE:

=1 OPEN DATA FILE AND RETURN TO CALLING PROGRAM
=2 OPEN DATA FILE AND OUTPUT DATA

PROGRAMMER: TIMOTHY G. KELLY JAN. 9, 1976

MODIFIED JULY 29, 1976

DEFINITIONS:

OPDEF	RDF	6214	/READ DATA FIELD INTO AC BITS 6-8
OPDEF	ITAD	1400	/INDIRECT TAD TO FOOL SABB
OPDEF	BSW	7002	/BYTE SWAP IN AC
ABSYH	DMONYR	0135	/PAGE 0 ADDRESS
ABSYH	POINTR	10	/AUTO INDEXING REGISTER

COMMON IADRES, NUMINC, IDATPT, NSCAN, IDELAY, NPTS, ITIME, NAVE, BASE,
ISICMA, IKINSP, YDATA, TIMPPT, NBASE, ISTART, INCREM
DIMENSION YDATA(1024), IYNAME(8)

C

100 FORMAT('ENTER COMMENT TEXT'/'CONTROL C TO END'/)

101 FORMAT('WRITE ENABLE 'A4'/)

140 FORMAT(A1)

150 FORMAT('HD', A6, 2I2, 1I, 8A2, 7I5, F15.6, 2I5)

160 FORMAT(A2)

201 FORMAT('ENTER FILE NAME ', A6)

300 FORMAT('ENTER YOUR NAME: ', 8A2)

400 FORMAT('OUTPUT DEVICE: 'A4)

500 FORMAT('IN' I5)

600 FORMAT('ED')

700 FORMAT('RD' E15.8)

800 FORMAT('AS' A6)

900 FORMAT('1 = IN, 2 = RD, 3 = AS: ' I1)

1000 FORMAT('; FIELDIAL SET (KG): ' F10.3)

1100 FORMAT('; RANGE (KG): ' F10.3)

C

C

C

C

ENTRY POINT

READ(1, 400) DEVICE

STORE.FT, CONT'D.

```

          WRITE(1,101)DEVICE
9         READ(1,201)FNAME
          CALL OOPEN(DEVICE,FNAME)
          READ(1,300)IYNAME
C
C         WRITE HEADER ON OUTPUT DEVICE
C
          IMO =0
          IDAY=0
          IYR=0
S         TAD (7666
S         DCA DMONYR
S         RDF                               /READ DATA FIELD TO SETUP RETURN
S         TAD DATFLD
S         DCA DATFLD
S         6211                               /CHANGE TO DATA FIELD 1
S         ITAD DMONYR                       /DATE IS IN LOCATION 17666
SDATFLD,6201                               /RETURN TO DATA FIELD N
S         DCA AC
S         TAD AC
S         AND (0007                           /LAST DIGIT OF YEAR IS IN BITS 9-11
S         DCA \IYR
S         TAD AC
S         RTR;RAR
S         AND (37                             /DAY IS IN BITS 4-8
S         DCA \IDAY
S         TAD AC
S         RTL;RTL;RAL
S         AND (17                             /MONTH IS IN BITS 0-4
S         DCA \IMO
          WRITE(4,150)FNAME,IMO,IDAY,IYR,IYNAME,IDATPT,RSCAN,IDELAY,NPTS,
          11TIME,NAVE,IKINSP,TIMPPT,NUMINC,NBASE
C
C         WRITE COMMENT ON OUTPUT DEVICE IN C.G.E.CO. STANDARD FILE
C         FORM-CONTROL CHARACTERS ARE : .
C
          READ(1,1000)SET
          READ(1,1100)RANGE
          WRITE(4,1000)SET
          WRITE(4,1100)RANGE
          WRITE(1,100)
S         TAD CR215
S         DCA AC
SNWLINE,TAD (7340                          /; =COMMENT (IN A2 FORMAT)
S         DCA \ICHR
          WRITE(4,160)ICHR,
S         TAD (7671
S         DCA LINE                          /LINE LENGTH OF 72 CHARACTERS
S                                         /SET UP A LINE COUNT
S                                         /CORRESPONDING TO WIDTH OF TTY
SGETMOR,JMS GETCHR                          /GET CHARACTER FROM TTY
S         TAD \ICHR                          /CHARACTER MUST BE SIX BIT ASCII
S                                         /FOR FORTRN FORMAT
S
S         BSW
S         AND (7700
S         TAD (40
S         DCA \ICHR
          WRITE(4,140)ICHR,
S         ISZ LINE
S         JMP GETMOR
S CRLF, TAD CR4040                          /CR IS WRITTEN AS A SPACE
S         DCA \ICHR
          WRITE(4,140)ICHR
S         TAD CR215
S         JMS PUNCH
S         TAD LF212                          /LINE FEED
S         JMS PUNCH
S         TAD AC
S         SZA CLA                            /ZERO ONLY AFTER CONTROL G
S         JMP NWLINE
```

STORE.FT, CONT'D.

```

                GO TO(250,136)MODE
136             READ(1,900) IA
                GO TO(190,200,210) IA
C
C             SABR SUBROUTINE TO GET CHARACTER FROM TTY
C
C SCETCHR, 0
S             CLA CLL
S TTY2,      KSF                /TEST TTY FLAG
S             JMP TTY2
S             KRB                /READ CHARACTER AND CLEAR FLAG
S             TLS                /ECHO CHARACETR
S             DCA \ICCHAR
S             TAD \ICCHAR
S             TAD CIA215        /TEST IF CR
S             SNA CLA
S             JMP CRLF         /YES, CHARACTER WAS CR
S             TAD \ICCHAR
S             TAD CIACC        /TEST IF CONTROL G
S             SZA CLA
S             JMP I GETCHR
S             DCA AG          /YES, CHARACTER WAS CONTROL G
S             JMP CRLF
C
C             SABR SUBROUTINE TO TYPE CHARACTER ON TTY
C
C SPUNCH, 0
S TTY1,      TSF                /SKIP IF TTY FLAG = 1
S             JMP TTY1
S             TLS                /LOAD TTY BUFFER AND PUNCH CHARACTER
S             CLA CLL
S             JMP I PUNCH
SCIA215,7563 /CR 0215 PLUS CIA
SCIA212,7566 /LINE FEED 0212 PLUS CIA
SCR215, 0215 /CR
SLF212, 0212 /LINE FEED
SLINE, 0
S AG, 0
SCIACC, 7571 /CONTROL G PLUS CIA
SCR4040,4040 /SPACE IN A1 FORMAT
SSD2304,2304 /SD IN A2 FORMAT
C
C             OUTPUT DATA IN I5 FORMAT.  FIRST TWO CHARACTERS ARE
C             'IN' = INTEGER FILE
C
C 190          CONTINUE
                DO 195 I=1,NPTS
                IYDATA=YDATA(I)
195           WRITE(4,500) IYDATA
                JMP ~220
C
C             'RD' OUTPUT FILE.  Y IS WRITTEN TO THE OUTPUT DEVICE
C             IN E15.8 FORMAT.200 CONTINUE
C
                WRITE(4,700)(YDATA(I), I=1,NPTS)
                JMP ~220
C
C             'AS' DATA FILE.  Y VALUES WRITTEN AS AN ASCII CHARACTER IN
C             A6 FORMAT.
C
C 210          CONTINUE
                DO 215 I=1,NPTS
215           WRITE(4,800)YDATA(I)
220           WRITE(4,600)
                CALL OCLOSE
250           RETURN
                END
```

FILE NAME: FETCH.FT

SUBROUTINE FETCH(MODE)

FILE NAME: FETCH.FT

SUBROUTINE TO READ A DATA FILE FROM STORAGE DEVICE WRITTEN IN
C.C.E.CO. STANDARD FILE FORMAT. FIRST TWO CHARACTERS
ARE CONTROL CHARACTERS.

; = COMMENT
HD = HEADER (FILE NAME, DATE, YOUR NAME)
IN = INTEGER DATA (I5 FORMAT)
RD = REAL DATA (E15.8 FORMAT)
AS = ASCII DATA (A2 FORMAT)
DK = DATA FOR KINETICS
EF = RETURN TO CALLING PROGRAM
ED = END DATA FILE

THIS PROGRAM WILL OPERATE IN FOUR MODES. THE CALLING PROGRAM
MUST SPECIFY THE MODE OF OPERATION BY PASSING A VARIABLE TO
SUBROUTINE FETCH.FT.

MODE:

- = 1 ASK FOR FILENAME AND OPEN FILE
- = 2 READ DATA UNTIL IT READS AN EF OR ED
- = 3 FETCH ONLY SELECTED POINTS FROM THE DATA FILE
- = 4 FETCH ONLY SELECTED DECAY CURVE

PROGRAMMER: TIMOTHY G. KELLY JAN. 9, 1976
MODIFIED AUC 20, 1976

OPDEF BSW 7002 /BYTE SWAP IN AC
COMMON IADRES, NUMINC, IDATPT, NSCAN, IDELAY, NPTS, ITIME, NAVE, BASE,
ISIGMA, IKINSP, YDATA, TIMPPT, NBASE, ISTART, INCREMENT
DIMENSION YDATA(1024), ICHAR(72), IYNAME(8)

ENTRY POINT

J=0

GO TO(1, 20, 110, 130)MODE

ICOM=-1

1 READ(1, 200)DEVICE

10 FORMAT('INPUT DEVICE: 'A4)

200 READ(1, 300)FNAME

11 FORMAT('ENTER FILE NAME ', A6)

300 CALL IOPEN(DEVICE, FNAME)

READ 2 CONTROL CHARACTERS FROM THE INPUT FILE

20 READ(4, 400)ISWICH,

400 FORMAT(A2)

S TAD \ISWICH

S TAD (6774

/TEST FOR LETTERS 'HD' = HEADER

S SNA CLA

S JMP HEAD

/YES, READ HEADER

S TAD \ISWICH

S TAD (0440

/TEST FOR LETTERS '; ' = COMMENT

S SNA CLA

S JMP \50

/YES, READ COMMENT

S TAD \ISWICH

S TAD (6662

/TEST FOR LETTERS 'IN' = INTEGER FILE

S SNA CLA

S JMP \60

/YES, READ INTEGER DATUM-I5 FORMAT

S TAD \ISWICH

S TAD (5574

/TEST FOR LETTERS 'RD' = REAL DATA FILE

FETCH.FT, CONT'D.

```
S      SNA CLA
S      JMP \70
S      TAD \ISWICH
S      TAD (7655
S      SNA CLA
S      JMP \80
S      TAD \ISWICH
S      TAD (7365
S      SNA CLA
S      JMP \90
S      TAD \ISWICH
S      TAD (7272
S
S      SNA CLA
S      JMP \40
S      TAD \ISWICH
S      TAD (7274
S
S      SNA CLA
S      JMP ENDFIL
```

/YES, READ REAL DATUM-E15.8 FORMAT

/TEST FOR LETTERS 'AS' = ASCII FILE

/YES, READ ASCII DATUM-A6 FORMAT

/TEST FOR LETTERS 'DK' = KINETIC DATA

/TEST FOR LETTERS 'EF' = END
/OF DATA FILE

/RETURN TO CALLING PROGRAM

/TEST FOR LETTERS 'ED' = END OF
/DATA FILE

/YES, RETURN TO CALLING

TIMEDA.FT CONT'D.

S	AND (7077	/STRIP PREVIOUS CLOCK FREQUENCY
S	TAD \N	/ADD CLK FREQ. TO CLK ENABLE WORD
S	DCA CLOCEN	
S	TAD (216	/ADDRESS OF IYDATA IN COMMON -1
S	DCA \IADRES	
S	TAD \NPTS	/SET UP POINTS COUNTER
S	CIA	
S	DCA \IDATPT	
S	TAD \NAVE	/SET UP AVERAGE COUNTER
S	CIA	
S	DCA \NSCAN	
S	TAD \IADRES	/GET ADDRESS POINTER FROM COMMON
S	DCA POINTR	
S	TAD \IDATPT	/GET NUMBER OF DATA POINTS FROM COMMON
S	DCA NUMPTS	
S	TAD \NSCAN	/GET NUMBER OF SCANS FROM COMMON
S	DCA NUMSCA	
S	CMA	
S	CLZE	/CLEARS CLOCK ENABLE REGISTER
S	CLA CLL	
S	TAD \IDELAY	/GET DELAY FROM COMMON
S	CLAB	/AC TO CLOCK BUFFER
S	CLA CLL	
S	ADCL	/CLEAR ALL A/D FLAGS
S	ADLM	/LOAD MULTIPLEXER FROM ACB-11 AND CLEAR AC
S	CLA CLL	
S	TAD ADCEN	/LOAD A/D ENABLE WORD INTO AC
S	ADLE	/LOAD A/D ENABLE REG. AND CLEAR AC
S	TAD CLOCEN	/LOAD CLOCK ENABLE WORD INTO AC
S	CLOE	/SET AC INTO CLOCK ENABLE REGISTER
S	CLA CLL	
S	CLSA	
S	6211	/CHANGE TO DATA FIELD 1
S	FLASH	/FLASH LAMP
S	OVER, CLSK	/TEST FOR OVERFLOW DUE TO SCHIMIT TRIGGER
S	JMP OVER	
S	TAD (7000	
S	TAD XPONTR	
S	DILX	
S	CLA CLL	
S	SGETHDR,ADSK	/SKIP ON A/D DONE
S	JMP GETHDR	
S	ADRB	/READ A/D BUFFER ,CLEAR DONE FLAG
S	ADSE	/SKIP ON A/D ERROR FLAG
S	SKP	
S	JMS ERR	
S	IDCA POINTR	/DEPOSIT DATA IN FIELD 1
S	ISZ NUMPTS	/HAVE I TAKEN ALL THE DATA POINTS?
S	JMP GETHDR	/NO , GETHORI
S	ISZ NUMSCA	
S	CS	
S	HLT	
S	6201	/CHANGE TO DATA FIELD 0
S	TAD \IADRES	/ADDRESS OF DATA IN COMMON-1
S	DCA POINTR	
S	TAD (2216	/ADDRESS OF DOUBLE PRECISSION WORD
S	DCA YPOINT	/IN COMMON-1
S	TAD \IDATPT	
S	DCA NUMPTS	/POINTS COUNTER
S	6211	/CHANGE TO DATA FIELD 1
S	SCONTIN,ITAD POINTR	
S	SMA	/TEST FOR NEGATIVE NUMBER
S	JMP POS	
S	IDCA YPOINT	
S	CMA	
S	IDCA YPOINT	/NEG. POINT MUST BE SIGN EXTENDED
S	JMP TST	
S	SPOS, IDCA YPOINT	
S	IDCA YPOINT	/POSITIVE NUMBER SIGN EXTENDED
S	STST, ISZ NUMPTS	

TIMEDA.FT CONT'D.

```
S      JMP CONTIN
S      6201
        CALL FLOTDB
        CALL CHAIN('EPRMON')
S      HLT
S ADCEN,0200          /A/D ENABLE WORD-EXTERNAL START
S CONVRT,1000
SNUMSCA,0
SCLOCEN,5661        /MOD 01+1MHZ+OVERFLOW START A/D+CLOCK
S      /INHIBIT+EVENT1
S ERR.  0
        WRITE(1,500)
500    FORMAT(1X,'A/D TIMING ERROR')
        CALL EXIT
        END
```

BIBLIOGRAPHY

BIBLIOGRAPHY

A

- [AL68a] R.S. Alger, "Electron Paramagnetic Resonance: Techniques and Applications", Interscience, New York, 1968, p 71.
- [AL68b] R.S. Alger, "Electron Paramagnetic Resonance: Techniques and Applications", Interscience, New York, 1968, p 82.
- [AL68c] R.S. Alger, "Electron Paramagnetic Resonance: Techniques and Applications", Interscience, New York, 1968, pp 106-123.
- [AL68d] R.S. Alger, "Electron Paramagnetic Resonance: Techniques and Applications", Interscience, New York, 1968, p 109.
- [AL68e] R.S. Alger, "Electron Paramagnetic Resonance: Techniques and Applications", Interscience, New York, 1968, p 1520.
- [AL68f] R.S. Alger, "Electron Paramagnetic Resonance: Techniques and Applications", Interscience, New York, 1968, Deprieqx, Laboratory reference 29, p 150.
- [AL68g] R.S. Alger, "Electron Paramagnetic Resonance: Techniques and Applications", Interscience, New York, 1968, p 149.
- [AM72] American Institute of Physics Handbook, Third Ed., McGraw-Hill, 1972, p 5-105.
- [ARGO] Argonne National Laboratory, Batavia, Illinois, Trifunca.
- [AT68a] P.W. Atkins, K.A. McLauchlan, and A.F. Simpson, Chemical Communications 179 (1968).
- [AT68b] P.W. Atkins, K.A. McLauchlan, and A.F. Simpson, Nature 219, 927 (1968).
- [AT68c] P.W. Atkins, K.A. McLauchlan, and A.F. Simpson, Molecular Spectroscopy, 177 (1968).
- [AT70a] P.W. Atkins, K.A. McLauchlan, and A.F. Simpson, Journal Physics E: Scientific Instruments 3, 547 (1970).
- [AT70b] P.W. Atkins, I.C. Buchanan, R.C. Curd, K.A. McLauchlan, and A.F. Simpson, Chemical Communications 513 (1970).

- [AT71] P.W. Atkins, R.C. Curd, K.A. McLauchlan, and A.F. Simpson, *Chemical Physics Letters* 8, 55 (1971).
- [AT73] P.W. Atkins, K.A. McLauchlan, and P.W. Percival, *Molecular Physics* 25, 281 (1973).
- [A105] Design number A-105, Instrument Service, Michigan State University, East Lansing, MI 48824.
- [A109] Design number A-109, Instrument Service, Michigan State University, East Lansing, MI 48824.

B

- [BA64] K. Bar-Eli and T.R. Tuttle, *Journal of Physics* 40, 2508 (1964).
- [BE67] T.J. Bennett, R.C. Smith and T.H. Wilmsbrst, *Chemical Communications* 513 (1967).
- [BE69] T.J. Bennett, R.C. Smith and T.H. Wilmsbrst, *Journal Physics E: Scientific Instruments* 2, 393 (1969).
- [BO39] J.R. Bolton and J.T. Warden, Publication 39, Photochemistry Unit, Chemistry Department, University of W. Ontario, London, Ontario, Canada.
- [BU52] J.H. Burgess and R.M Brown, *Review of Science Instruments* 23, 334 (1952).

C

- [CA59] A. Carrington, R. Dravnieks, and M.C.R. Symons, *Journal Chemistry Society* 1959, 947 (1959).
- [CA66] J.G. Calvert and J.N. Pitts Jr., "Photochemistry", John Wiley and Sons, New York, 1966, p 783.
- [CA75] R. Catterall, and P. Edwards, *Journal Physical Chemistry* 79, 3010 (1975).
- [CA77] R. Catterall, J. Slater and M.O.R. Symons, *Canadian Journal of Chemistry* 55, 1979 (1975).
- [CE77] J.M. Ceraso, P.B. Smith, J.S. Landers and J.L. Dye, *Journal Physical Chemistry* 81, 760 (1977).
- [CHEN] K.M. Chen, Department of Electrical Engineering, Michigan State University, East Lansing, MI 48824, personal communications.

- [CO64] A.R. Cook, L.M. Matarrese and J.S. Wells, Review of Scientific Instruments 35, 114 (1964).
- [COWN] J. Cowen, Physics Department, Michigan State University, East Lansing, MI 48824, measured Q of Micro Now and Varian cavities.
- [CU46] R.L. Cummerow and D. Halliday, Physical Review 70, 433 (1946).
- [C162] CEM 162 Laboratory Manual, Quantitative Analysis, Experiment #6, Department of Chemistry, Michigan State University, East Lansing, MI 48824.

D

- [DA79] M.G. DaGue, Ph.D. Thesis, Michigan State University, East Lansing, MI 48824, 1979, pp 25-37.
- [DEC] Digital Equipment Corporation, Maynard, Mass. 01754.
- [DE64] R. Dewald and J.L. Dye, Journal of Physical Chemistry, 68, 121 (1964).
- [DO57] J.L. Down, J. Lewis, B. Moore and G. Wilkinson, Proceeding of Chemical Society 1957, 209 (1957).
- [DO59] J.L. Down, J. Lewis, B. Moore and G. Wilkinson, Journal Chemical Society 3767 (1959).
- [DY59] J.L. Dye and R.R. Dewald, Journal Physical Chemistry 68, 135 (1964).
- [DY71] J.L. Dye, M.T. Lok, F.J. Tehan, R.B Coolan, N. Papadakis, J.M Caraso, and M.G. Debacker, Ber. Bunsenges Physical Chemistry 75, 659 (1971).
- {DY73} J.L. Dye in "Electrons in Fluids,\", J. Jortner and C.R. Kestner, Ed., Springer-Verlag, W. Berlin, 1973, page 77.

E

- [EL63] J. Eloranta and H. Lischitz, Journal of Chemical Physics 38, 2214 (1963).
- [EN76] C.G. Enke and T.A. Nieman, Analytical Chemistry 48(8), A705 (1976).

F

- [FE57] G. Feher, *Bell System Technical Journal* 36, 447 (1957).
- [FE63] R.W. Fessenden and R.H. Schuler, *Journal of Chemical Physics* 39, 2147 (1963).
- [FE64] R.W. Fessenden, *Journal of Physical Chemistry* 68, 1508 (1964).
- [FE73] R.W. Fessenden, *Journal of Chemical Physics* 58, 2489 (1973).
- [FI67] E.W. Firth and D.J.E. Ingram, *Journal of Scientific Instruments*, 4, 821 (1967).
- [FR76] A. Friedenbergs and H. Levanon, *Chemical Physics Letters* 41, 84 (1976).
- [FR77] A. Friedenbergs and H. Levanon, *Journal of Physical Chemistry* 81, 766 (1977).

G

- [GA70] A. Gaathon and M. Ottolenghi, *Israeli Journal of Chemistry* 8, 165 (1970).
- [GA71] G. Gabor and K. Bar-Eli, *Journal of Physical Chemistry* 75, 286 (1971).
- [GEOS] GEOSYS, A Computer System for the Description and Analysis of Spatial Data, written by R.I. Wittick, Computer Institute for Social Science Research, 1974.
- [GI26] G.E. Gibson and T.E. Phipps, *Journal of American Chemical Society* 48, 312 (1926).
- [GL70] S.H. Glarum and J.H. Marshall, *Journal of Chemical Physics* 52, 5555 (1970).
- [GL73] S.H. Glarum, *Review of Scientific Instruments* 44, 752 (1973).
- [GO71] I.B. Goldberg and A.J. Bard, *Journal of Physical Chemistry* 75, 3281 (1971).
- [GO72] T.E. Gough and F.W. Grossman, *Journal of Magnetic Resonance* 7, 24 (1972).

- [GO74] I.B. Goldberg and A.J. Bard, *Journal of Physical Chemistry* 78, 290 (1974).
- [GO75] I.B. Goldberg, H.R.Crowe, R.S. Carpenter II, *Journal of Magnetic Resonance* 18, 84 (1975).
- [GO76a] I.B. Goldberg, H.R.Crowe, G.S. Wilson, R.S. Glass, *Journal Physical Chemistry* 80, 988 (1976).
- [GO76b] I.B. Goldberg and H.R.Crowe, *Journal Physical Chemistry* 80, 2407 (1976).
- [GO76c] I.B. Goldberg and H.R.Crowe, *Journal Physical Chemistry* 80, 2603 (1976).
- [GO77] I.B. Goldberg, H.R.Crowe and K.O. Christe, *Journal Physical Chemistry* 17, 3189 (1978).
- [GR73] K. Gruber, J. Forrer, e. Aopfi and H.H. Gunthards, *Journal Physics E: Scientific Instruments* 6, 666 (1973).

H

- [HAHN] Controller design B.K. Hahn; Interface design T.G. Kelly, Department of Chemistry, Michigan State University, East Lansing, MI 48824.
- [HA56] C.G. Hatchard and C.A. Parker, *Proceedings of the Royal Society (London)*, A235, 518 (1956).
- [HA62] D. Halliday and R. Resniek, "Physics: Part II", John Wiley and Sons, New York, 1962, p 853.
- [HA70] E.J. Hamilton, Jr., E. Wood, and G.S. Hammond, *Review of Scientific Instruments* 41, 452 (1970).
- [HA72] B.J. Hales and J.R. Bolton, *Journal of the American Chemical Society* 94, 3314 (1972).
- [HEAT] Heath Company, Benton Harbor, MI.
- [HI68] R. Hirasawa, T. Mukaibe, H. Hasegawa, Y. Kanada and T. Maruyama, *Review of Scientific Instruments* 39, 95 (1968).
- [HO69] J.D. Hoeschele, Ph.D. Thesis, Michigan State University, East Lansing, MI 48824 1969.

- [HO72] J.G. Holbrook, T.H. Wilmshurst, and R.R. Simmons, *Journal Physics E: Scientific Instruments* 5, 555 (1972).
- [HO76] F.J. Holler, T.G. Kelly, T.V. Atkinson, C.G. Enke, *American Laboratory* 8, 9 (1976).
- [HO77] R.E. Hoguet, Chief Engineer, Micro-Now Instrument Company, Chicago, Ill, personal communication.
- [HS73] E.S.P. His, L. Fabes, and J.R. Bolton, *Review of Scientific Instruments* 44, 197 (1973).
- [HU68] I. Hurley, T.R. Tuttle, Jr., S.R. Golden, *Journal of Chemical Physics* 48, 2918 (1968).
- [HU70] D. Huppert and K.H. Bar-Eli, *Journal of Physical Chemistry* 74, 3285 (1970).
- [HU74] M. Huisjen and J.S. Hyde, *Review of Scientific Instruments* 45, 669 (1974).
- [HY63] J.S. Hyde, "Principles of EPR Instrumentation", 7th Annual NMR-EPR Varian Workshop, Varian Associates Instrument Division, Palo Alto, CA 1963.

K

- [KL71] J.G. Kloosterboer, L.J. Giling, R.P.H. Rettschnick, J.D.W. VanVoorst, *Chemical Physics Letters* 8, 462 (1971).
- [KL72] J.G. Kloosterboer, P. Jost, O.H. Griffith, "Computers in Chemical and Biochemical Research", Volume 1, C.E. Klopfenstein and C.L. Wilkins, Editors, Academic Press, New York, 1972, p 175.

L

- [LA59] J. Lambe and R. Ager, *Review of Scientific Instruments* 30, 599 (1959).
- [LA76] Jacques Lacoste, Ph.D. Thesis, Universite Des Sciences Et Techniques Du Langnedoc, France, 1976, pp 23-29.
- [LA77] T. Last and C.G. Enke, *Analytical Chemistry* 49, 19 (1977).

[LAST] Interface design by T.A. Last, Department of Chemistry, Michigan State University, East Lansing, MI 48824.

[LO72] M.T. Lok, F.J. Tehan, J.L. Dye, *Journal of Physical Chemistry* 76, 2975 (1972).

M

[MA69] Matalon, S. Golden, M. Ottolenghi, *Journal of Physical Chemistry* 73, 3098 (1969).

[MNOW] Micro-Now Instruments Company, Inc., Chicago, Ill, 60646, Sales literature.

[MULP] Program MULPLT, written by T.V. Atkinson, Department of Chemistry, Michigan State University, East Lansing, MI 48824.

P

[PA53] C.A. Parker, *Proceedings of the Royal Society (London)* A220, 104 (1953).

[PHOT] Photochemical Research Associates, University of W. Ontario, London, Ontario, Canada, James Bolton, Pres.

[PI60] L.H. Piette and W.C. Landgraf, *Journal Chemical Physics* 32, 1107 (1960).

[PIP8] Program PIP8 written by T.V. Atkinson, Department of Chemistry, Michigan State University, East Lansing, MI 48824.

[PO67a] C. Poole, "Electron Spin Resonance, A Comprehensive Treatise on Experimental Techniques", Interscience, New York, 1967, p 259.

[PO67b] C. Poole, "Electron Spin Resonance, A Comprehensive Treatise on Experimental Techniques", Interscience, New York, 1967, p 343.

[PO67c] C. Poole, "Electron Spin Resonance, A Comprehensive Treatise on Experimental Techniques", Interscience, New York, 1967, p 413.

[PO67d] C. Poole, "Electron Spin Resonance, A Comprehensive Treatise on Experimental Techniques", Interscience, New York, 1967, p 321.

S

[SA64] A. Savitzky and J.J.E. Golay, *Analytical Chemistry* 36, 1627 (1964).

- [SA77] F.P.Sargent, Atomic Energy of Canada, Ltd., Whiteshell Nuclear Research Establishment, Pinawa, Manitoba, Canada, personal communication.
- [SE73] T.O. Seim, T.B. Mele, and S. Pyrdz, *Journal of Magnetic Resonance* 9, 175 (1973).
- [SE77] W.A. Seddon, J.W. Fletcher, F.C. Sopchyshyn, and R. Catterall, *Canadian Journal of Chemistry* 55, 3356 (1977).
- [SM64] G.W. Smith, *Journal Applied Physics* 35, 1217 (1964).
- [SM68] B. Smaller, J.R. Remko and E.C. Avery, *Journal of Chemical Physics* 48, 5174 (1968).
- [SM71] B. Smaller, E.C. Avery and J.R. Remko, *Journal of Chemical Physics* 55, 2414 (1971).
- [SM77] G.E. Smith, R.E. Blankenship and M.P. Klein, *Review of Scientific Instruments* 48, 282 (1977).
- [SO68] J. Sohma, t. Komatsu and Y. Kanada, *Japanese Journal of Applied Physics* 7, 298 (1968).
- [ST74] R.L. Stoll, "The Analysis of Eddy Currents", Clarendon Press, Oxford, 1974.

T

- [TE74] F.J. Tehan, B.L. Barnett and J.L. Dye, *Journal of American Chemical Society* 96, 7203 (1974).

V

- [VO63] K.D. Vos and J.L. Dye, *Journal of American Chemical Society* 38, 2033 (1963).

W

- [WA61] H. Wahlquist, *Journal of Chemical Physics* 35, 1708 (1961).
- [WA75] J.K.S. Wan, H.M. Vyas, S.K. Wong and B.B.Adeleke, *Journal of American Chemical Society* 97, 1385 (1975).
- [WA76] J.T. Warden and J.R. Bolton, *Review of Scientific Instruments* 47, 201 (1976).

- [WA77] J.K.S. Wan, Queens University, Hamilton, Ontario, Canada, personal communications.
- [WI68] T.H. Wilmshurst, T.J. Bennett and R.C. Smith, Proceedings of the Royal Society A302, 305 (1968).
- [WE63] W. Weyl, Ann. Physik. 121, 601 (1863).
- [WE72] J.E. Wertz and J.R. Bolton, "Electron Spin Resonance-Elementary Theory and Practical Applications", McGraw-Hill, New York, 1972, p 24.
- [WE72b] J.E. Wertz and J.R. Bolton, "Electron Spin Resonance-Elementary Theory and Practical Applications", McGraw-Hill, New York, 1972, p 451.
- [WE72c] J.E. Wertz and J.R. Bolton, "Electron Spin Resonance-Elementary Theory and Practical Applications", McGraw-Hill, New York, 1972, pp 452-454.
- [WI55] R.P. Winch, "Electricity and Magnetism", Prentice-Hall, 1955, p 506.
- [WO72] S.K. Wong and J.K.S. Wan, Journal of American Chemical Society 94, 7197 (1972).

X

- [XENO] Xenon Corporation, Medford, MA, Manufacturer's literature.

Z

- [ZA45] E. Zavoisky, Journal of Physics USSR 9, 211 (1945).

MICHIGAN STATE UNIVERSITY LIBRARIES



3 1293 02736 3054